ABSTRACT

Title of Dissertation:	RADAR MONITORING OF HYDROLOGY IN MARYLAND'S FORESTED COASTAL PLAIN WETLANDS: IMPLICATIONS FOR PREDICTED CLIMATE CHANGE AND IMPROVED MAPPING
	Megan Weiner Lang, Doctor of Philosophy, 2005
Directed By:	Professor Eric Kasischke, Department of Geography

Wetlands provide important services to society but Mid-Atlantic wetlands are at high risk for loss, with forested wetlands being especially vulnerable. Hydrology (flooding and soil moisture) controls wetland function and extent but it may be altered due to changes in climate and anthropogenic influence. Wetland hydrology must better understood in order to predict and mitigate the impact of these changes. Broad-scale forested wetland hydrology is difficult to monitor using ground-based and traditional remote sensing methods. C-band synthetic aperture radar (SAR) data could improve the capability to monitor forested wetland hydrology but the abilities and limitations of these data need further investigation. This study examined: 1) the link between climate and wetland hydrology; 2) the ability of ENVISAT SAR (C-HH and C-VV) data to monitor inundation and soil moisture in forested wetlands; 3) limitations inherent to C-band data (incidence angle, polarization, and phenology) when monitoring forested wetland hydrology; and 4) the accuracy of forested wetland maps produced using SAR data. The study was primarily conducted near the Patuxent River in Maryland but the influence of

incidence angle was considered along the Roanoke River in North Carolina. This study showed: 1) climate was highly correlated with wetland inundation; 2) significant differences in C-VV and C-HH backscatter existed between forested areas of varying hydrology (uplands and wetlands) throughout the year; 3) C-HH backscatter was better correlated to hydrology than C-VV backscatter; 4) correlations were stronger during the leaf-off season; 5) the difference in backscatter between flooded and non-flooded areas did not sharply decline with incidence angle, as predicted; and 6) maps produced using SAR data had relatively high accuracy levels. Based on these findings, I concluded that hydrology is influenced by climate at the study site, and C-HH data should be able to monitor changes in hydrology throughout the year. Larger incidence angles should be explored when using C-HH data to monitor forested wetland hydrology, and C-band SAR has the potential to increase the ability to map forested wetlands throughout the year. The methods developed have the potential to fill the need of managers for increased hydrologic information and improved forested wetland maps.

RADAR MONITORING OF HYDROLOGY IN MARYLAND'S FORESTED
COASTAL PLAIN WETLANDS: IMPLICATIONS FOR PREDICTED CLIMATE
CHANGE AND IMPROVED MAPPING

By

Megan Weiner Lang

Dissertation submitted to the Faculty of the Graduate School of the
University of Maryland, College Park, in partial fulfillment
of the requirements for the degree of
Doctor of Philosophy
2005

Advisory Committee:
Professor Eric Kasischke, Chair
Associate Professor Andrew Baldwin
Professor Michael Kearney
Professor Stephen Prince
Associate Professor Philip Townsend

Dedication

This manuscript is dedicated to family and friends who supported me through the dissertation process. To my close friends, whose kindness and companionship mean so much. To my local family, the Cassees, the Kanfers, and the Styles who welcomed me in, provided me with many happy holidays, and supported me during life's milestones. To my long-distance family, the Alfassas, Langs, and Weiners who gave me their love, provided me with roots, and encouraged me to succeed. To my loving parents, Dr. David and Hillary Weiner who sat with me while I prepared elementary school science projects and took me on nature walks. A special debt of gratitude goes to my husband, Steven Lang, for his support, understanding, and patience but most of all, for his love.

Acknowledgements

Table of Contents

List of Tables

List of Figures

Chapter 1: Introduction

1.1 Opening

Prior to the 1960s, the biologic, aesthetic, and economic values of wetlands were largely overlooked, resulting in the loss of over half the wetlands in the conterminous United States to deforestation, agriculture, settlement, and a range of other human activities (Dahl and Johnson 1991). Although the value of wetlands has not always been appreciated, these ecosystems have long provided important goods and services to human society (Williams 1996). Wetlands in the Chesapeake Bay Watershed are especially vital as they help to maintain water quality and aquatic habitat in one of the largest and most productive estuarine ecosystem in the U.S. (Tiner 1987; Chesapeake Bay Program 1998).

Wetlands are often viewed as transitional lands between terrestrial and open water ecosystems. Situated at this hydrologic edge, small changes in the hydrologic regime can cause large changes in ecosystem characteristics (Mitsch and Gosselink 2000). Anthropogenic impacts, long-term cycles of drought and flood, and seasonal patterns of evapotranspiration work at a variety of spatial and temporal scales to influence the existence and functions of wetlands.

Broad-scale wetland hydrology at all temporal frequencies has been difficult to study with conventional ground-based methods because the number of hydrologic gauges is limited and the surface topography that influences the formation of wetlands is often subtle and difficult to map. Models of climate change predict not only rising temperatures (Moore et al. 1997; Fisher 2000), but increasingly variable amounts of precipitation for the Chesapeake Bay region (Mid-Atlantic Regional Assessment Team 2000). Greater

amounts of impervious surface also raise the area's susceptibility to impacts from

climatic extremes (Moore et al. 1997; Mid-Atlantic Regional Assessment Team 2000).

Important factors controlling the hydrologic conditions of wetlands are likely to continue

to change in the future (Najjar et al. 2000; Neff et al. 2000; Rogers and McCarty 2000).

In order to understand and forecast these changes, new approaches are needed to

systematically monitor and assess hydrologic conditions.

Remotely sensed data provide a unique means to study and monitor wetland hydrology.

Traditionally, optical imagery has been used to map wetlands but this approach is problematic

because cloud cover limits collection, and the presence of foliage precludes viewing of the

ground surface in forested wetlands (Tiner 1999). For this reason forested wetlands, especially

ephemeral forested wetlands, have been difficult to map and monitor.

Imaging radar systems have been used to obtain information on the spatial and temporal

patterns of flooding and soil moisture in forested wetlands (Hess et al. 1995; Wang et al. 1995;

Kasischke and Bourgeau-Chavez 1997; Townsend and Walsh 1998; Weiner et al. 2001;

Townsend 2001; Townsend 2002). Imaging radars have the unique capability to monitor

changes in the status of key hydrologic characteristics of wetlands (e.g., patterns of flooding

and variations in soil moisture) throughout the year and with greater frequency, in part due to

the ability of synthetic aperture radar (SAR) to collect images regardless of solar illumination

and cloud cover.

1.2 Research Goals and Hypotheses

I used C-band (5.6 cm wavelength) synthetic aperture radar (SAR) to study forested

wetland hydropattern, or the temporal and spatial dynamics of inundation and saturation,

in the Coastal Plain of Maryland. Unlike longer wavelength L-band (~24 cm wavelength) SAR sensors, C-band SARs have been in operation since the early 1990s, have accumulated an extensive record of historic imagery, and are likely to continue collecting data in the future; thus, they offer the best available opportunity for long-term, remote monitoring of wetland hydrology. The goals of this study were to better understand how variations in climate influence the hydrologic condition of forested wetlands in the Coastal Plain of Maryland and to improve the capability to map and monitor these ecosystems through the use of spaceborne imaging radars.

To meet the first goal of improving our understanding of how variations in climate influence the hydrologic condition of forested wetlands in the Coastal Plain of Maryland, two sets of hypotheses were developed. The first set guided research to define the sensitivity of C-band SAR to forested wetland hydrology, while the second set explored the limitations of using C-band SAR to monitor wetlands.

A. The Sensitivity of SAR to Wetland Hydrology

Hypothesis A1: In the Coastal Plain of Maryland, variations in precipitation, evapotranspiration, and stream discharge cause predictable changes in forested wetland hydropattern that can be measured using SAR.

Hypothesis A1a: Changing levels of inundation will affect the radar backscatter signature in forested wetlands, with increases in backscatter when forests are inundated and decreases in backscatter when they are not.

Hypothesis A1b: Radar backscatter will be positively related to soil moisture, with higher soil moisture resulting in higher radar backscatter.

B. Limitations on Using SAR to Monitor Forested Wetland Hydrology

Hypothesis B1: Differences in the character of the SAR sensor (system parameters) will influence the ability of spaceborne SARs to monitor hydrologic conditions in forested wetlands.

Hypothesis B1a: At smaller incidence angles, microwave energy from C-band SARs will be more sensitive to inundation under forest canopies than at larger incidence angles.

Hypothesis B1b: Relative to C-VV, microwave energy from C-HH SARs will be more sensitive to hydrologic variations under tree canopies.

Hypothesis B2: Variations in plant phenology will influence the ability of spaceborne SARs to monitor the hydrologic condition of forested wetlands

Hypothesis B2a: Microwave energy from C-HH and C-VV SARs will be more sensitive to changes in hydrology during times of low canopy closure.

Hypothesis B2b: Because of its greater ability to penetrate the forest canopy, microwave energy from C-HH SARs will be sensitive to variations in hydrology over a longer time period than microwave energy from C-VV SARs.

C. Mapping Forested Wetlands with SAR and Optical Data

To meet the second goal of improving capabilities to map and monitor forested wetlands, the following hypothesis was addressed:

Hypothesis C1: At intermediate spatial scales (30m), image processing approaches that use C-band SAR data are better able to differentiate forested wetlands from forested uplands than approaches that use optical data.

1.3 Research Approach

SAR, optical, and ancillary data were used to address the research goals. The first portion of this research used ENVISAT data and concurrent ground measurements to better understand forested wetland hydropattern in the Mid-Atlantic U.S. The approach to this portion of the study was two-fold. First, the study characterized the relationship between SAR backscatter, ground parameters, and climate and then evaluated the limitations of certain parameters (incidence angle, polarization, and canopy closure). The majority of the field measurements were collected near Laurel, Maryland at the Patuxent Wildlife Research Center. Consisting of 5,160 ha of upland and wetland forest adjacent to the Patuxent River, the Research Center is one of the largest relatively undisturbed tracts of land in the Washington, D.C./Baltimore metropolitan area. Ideally, all portions

of this study would have been conducted at the Patuxent study site, but due to sensor

conflicts, a multi-incidence angle data set could not be acquired there. Instead, the effect

of incidence angle on the ability of C-band SAR to detect flooding was addressed using a

multi-incidence angle Radarsat SAR data set provided by Dr. Philip Townsend. This

imagery was collected over the lower Roanoke River in northeastern North Carolina.

This floodplain ecosystem is one of the most expansive, largely undisturbed areas of

bottomland forest in the eastern U.S.

The second portion of this study was a natural extension of the first and aimed to

improve forested wetland mapping capabilities. It used historic Landsat ETM+ and ERS-

1/2 in addition to recently acquired ENVISAT ASAR data collected over the Patuxent

study site, although it encompassed a larger area. The methodology included decision

tree analysis and the use of an error matrix to assess the quality of resultant maps which

were evaluated using hydrologic ground data and National Wetlands Inventory data.

1.4 Dissertation Organization

This dissertation is organized into seven chapters (including this introduction). The

research is presented as a set of stand-alone manuscripts (Chapter 3 to 6) that will be

submitted to journals for peer-review. The second chapter summarizes previous research

pertinent to this study and provides other necessary background material. The next four

chapters include: 3) Controls on Hydropattern in a Mid-Atlantic Floodplain Wetland, 4)

Using C-band Synthetic Aperture Radar to Monitor Forested Wetland Hydrology in

Maryland's Coastal Plain, 5) Influence of Incidence Angle on the Ability of C-band

Synthetic Aperture Radar to Monitor Inundation in the Floodplain of the Roanoke River,

North Carolina, and 6) Assessment of C-band Synthetic Aperture Radar Imagery for

Mapping Coastal Plain Forested Wetlands in the Mid-Atlantic Region, U.S.A. The final

chapter (7) summarizes the major conclusions and discusses the significance of the

research.

Chapter 2: Background

2.1 Forested Wetlands in the Coastal Plain of Maryland

Wetland ecosystems in the Coastal Plain of Maryland provide many benefits to society and are undergoing hydrologic and other changes that will alter both their function and distribution. Most of Maryland's wetlands are found inland, and the vast majority of these are swamps or forested wetlands located in floodplains, between drainage systems in broad flats, and in upland depressions (Tiner and Burke 1996). The importance of these wetlands is underlined by the fact that surrounding upland areas are densely populated and these populations are rapidly expanding. Therefore, the need for wetland functions, such as nutrient reduction, is increasing while wetland area is simultaneously being reduced through development. The Mid-Atlantic/New England region has a higher population density than any other area in North America and its population is expected to increase at the same time that scientists are forecasting changes in climate (Moore et al. 1997). Temperatures in the Mid-Atlantic region have already increased over the past century and many Global Circulation Models (GCMs) predict an increase in the rate of temperature rise (Moore et al.1997; Fisher 2000; Mid-Atlantic Regional Assessment Team 2000; Nichols 2003). In addition, precipitation is expected to experience increased variability (Mid-Atlantic Regional Assessment Team 2000; Nichols 2003) in the future. Anthropogenic impacts along with changes in precipitation and increases in evapotranspiration due to higher temperatures will alter the water balance of the region's fresh water ecosystems, including wetlands (Moore et al.1997).

In the Mid-Atlantic region, natural hydrologic patterns in non-tidal wetlands occur at a variety of temporal scales. Seasonal variations in evapotranspiration, inter-annual cycles of drought and flood, and long-term shifts in climate work in concert to modify wetland hydrology. At finer temporal scales, seasonal changes in climate and transpiration cause annual cycles in soil moisture and inundation. During years of normal precipitation, most wetlands are flooded for a relatively short time, usually in the late winter or early spring after snowmelt and before leaf-out. As temperature increases during the growing season, so does evaporation and transpiration, lowering levels of wetland inundation and soil moisture, and by mid-summer, the flooding often recedes. However, come late fall and winter, the water table usually rises as temperatures cool down and trees lose their leaves. At an intermediate time scale, inter-annual deviations from average climate conditions modify seasonal hydrologic patterns. Periods of less than or greater than average precipitation alter the area of wetland that becomes saturated and/or inundated (National Research Council 1995; Tiner; 1999; Mitsch and Gosselink 2000). During years of low precipitation, standing water is not present in many locations where it is normally found and soil moisture drops. In contrast, when precipitation is higher than normal, the area that is saturated and/or inundated increases (Mitsch and Gosselink 2000) (Chapter 3). Models predict that periods of drought and/or flood will become more common during this century (Mid-Atlantic Regional Assessment Team 2000).

Fluctuations in the areal extent, duration, and frequency of wetland flooding and saturation are called wetland hydropattern or hydroperiod (National Research Council 1995; Mitsch and Gosselink 2000). Wetland hydropattern results from all transfers of

water into and out of the ecosystem and can be expressed as a water budget (National Research Council 1995; Mitsch and Gosselink 2000) (see Chapter 3).

Although numerous factors interact to influence wetlands, water level is the single most important force in the formation and functioning of a wetland (Nestler and Long 1997; Mitsch and Gosselink 2000). Hydrologic conditions control important abiotic factors, which in turn influence soil properties and vegetation composition (Mitsch and Gosselink 2000). Wetland vegetation and soils are therefore unique and they interact to serve a variety of functions valued by humans, such as pollution reduction and flood control (Whitehead and Thompson 1993; Richardson 1994; Hruby et al. 1995; Whigham 1996; Poor 1999; Woodward and Wui 2001). Information on hydropattern can be used to infer what types of functions may be served by a wetland (Nestler and Long 1997; Cole and Brooks 2000; Mitsch and Gosselink 2000). Primary productivity, and therefore the production of organic matter, is enhanced by a rapidly fluctuating hydropattern (Mitsch and Ewel 1979; Brown 1981; Mitsch and Gosselink 2000). However, if the intensity of over-land flow is too high, organic matter may be flushed from the system. Since wetlands are situated at a hydrologic edge, small changes in hydrologic regime can cause substantial changes in ecosystem characteristics and function (Mitsch and Gosselink 2000).

Current literature states that the hydrological sciences are limited by a lack of data (Engman 1996; Conly and Van der Kamp 2001; Mendoza et al. 2003; Price 2005), especially long-term data at broad spatial scales, and suggests studies be designed to better comprehend the relationship between climate change and freshwater ecosystems, such as forested wetlands (Moore et al. 1997). The research carried out for this

dissertation used synthetic aperture radar (SAR) data to add to this knowledge base. It focused primarily on Maryland's Coastal Plain forested wetlands since these are the type of wetland most commonly found in the Coastal Plain of the Chesapeake Bay Watershed. Forested wetlands are also the type of wetland most likely to be lost in the future (U.S. Fish and Wildlife Service 2002), and they have been historically difficult to map and monitor. Many forested wetlands, especially those with ephemeral expression of surface hydrology, are not regulated by the government or even mapped by the National Wetland Inventory (Tiner and Burke 1996).

2.2 Monitoring Wetland Hydrology Using Imaging Radar

Synthetic aperture radar (SAR) sensors have different operating parameters, including wavelength, polarization, and incidence angle. Microwave wavelengths commonly used for remote sensing include: X-band (2.4 – 3.8), C-band (3.9 – 7.5 cm), L-band (15 – 30 cm), and P-band (30 – 100 cm) (Jensen 2000). Electromagnetic energy transmitted from the SAR sensor towards the surface of the Earth is composed of an electric and a magnetic component. These two components travel, at the speed of light (3×10^8 m s^{-1}), orthogonal to one another. The orientation of the electric component of electromagnetic energy (perpendicular to the direction of travel) determines the polarization of that energy. In operational, spaceborne SAR systems, the energy is either transmitted or received horizontally (H) or vertically (V), relative to the surface of the Earth (Figure 2.1). SAR bands are often described by their wavelength (e.g. X, C, L or P) and polarization (e.g. HH = horizontally transmitted and received and VV = vertically transmitted and received). The energy from SARs is also transmitted and received at
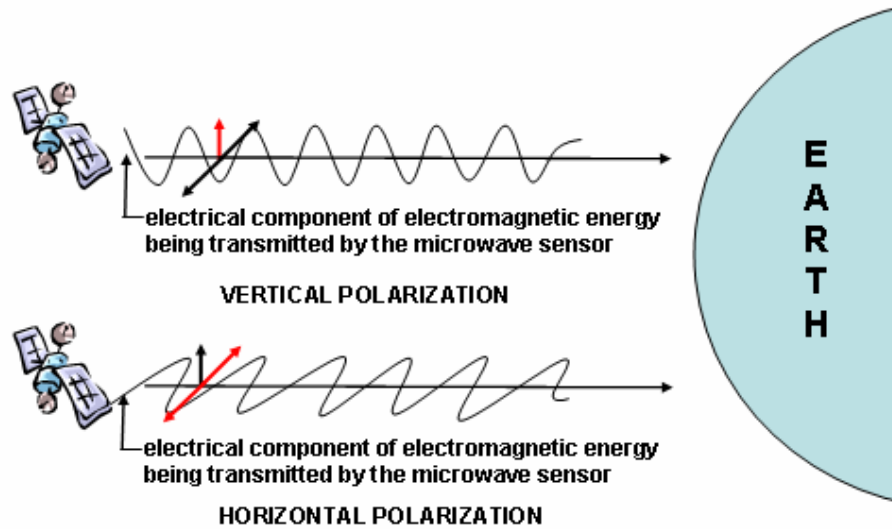
Figure 2.1: Polarization of incident electromagnetic energy where the same principal applies to returned energy. Polarization refers to the orientation of the electrical component of the energy, perpendicular to the direction of travel. Microwave energy is often transmitted and received with a vertical (V) or horizontal (H) polarization (adapted from Jensen 2000).

different angles relative to the earth's surface. These incidence angles are measured

relative to an imaginary line perpendicular to the surface of the Earth (Figure 2.2), with

smaller angles being closer to perpendicular to the terrain and larger angles being closer

to parallel.

It is primarily the wavelength, polarization, and incidence angle of the microwave

energy in combination with certain key characteristics of Earth's surface (dielectric

property, size/roughness, and structure) that determine the amount of energy reflected in

the direction of the sensor (energy returned to the sensor). The dielectric property of most

natural materials is determined by its water content. Typically, the higher the water

content, the higher the dielectric constant (a measure of the aptitude of a substance to

conduct electrical energy) of the material and therefore the greater the amount of incident
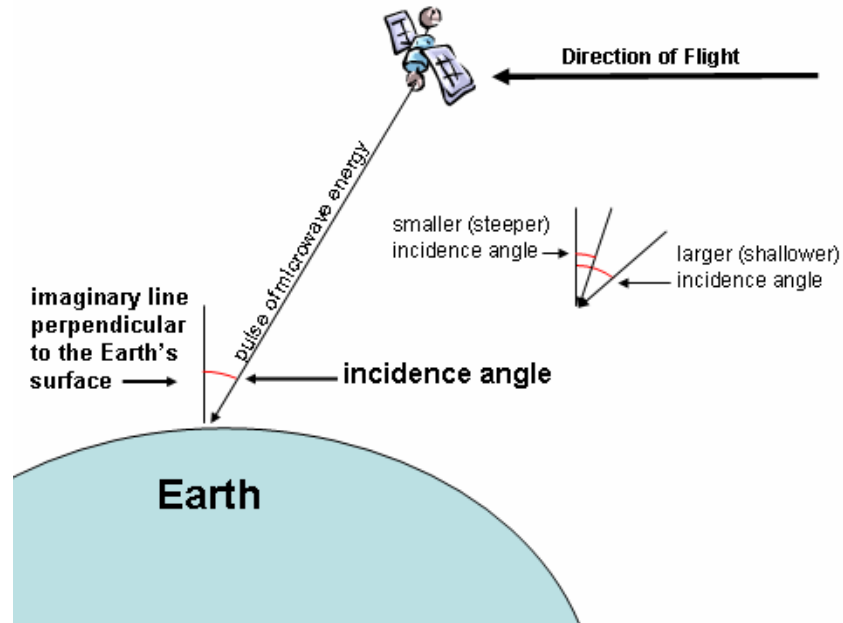
Figure 2.2: Incidence angle of energy transmitted from a SAR sensor. Incidence angle is the angle between an imaginary line perpendicular to the surface of the Earth and the transmitted pulse of electromagnetic energy. Smaller angles are closer to nadir and larger angles are more parallel with the surface of the Earth (adapted from Jensen 2000).

energy returned from the material (Jensen 2000). This energy is usually measured as radar backscatter. The energy, as a fraction of incident energy from the sensor, is described as the backscatter coefficient ($\sigma°$) once it is normalized by pixel area. The backscatter coefficient is usually expressed in logarithmic (decibel [dB]) units since it can vary over several orders of magnitude (Raney 1998).

When monitoring hydrology in forested ecosystems, imaging radars have many advantages over sensors that operate in the visible and infrared portions of the electromagnetic spectrum (Smith 1997). Microwave energy is sensitive to variations in soil moisture and inundation, and is only partially attenuated by vegetation canopies, especially in areas of lower biomass (relative to tropical forests) such as the temperate forests of the eastern U.S. (Townsend and Walsh 1998; Townsend 2001; Townsend 2002). The sensitivity of microwave energy to water, due to its high dielectric constant

and its ability to penetrate forest canopies, makes SAR ideal for the detection of hydrologic features below forest canopies (Hall 1996; Kasischke et al. 1997; Kasischke and Bourgeau-Chavez 1997; Rao et al. 1999;). Radar sensors can also collect data regardless of solar illumination and cloud cover. Not being restricted by clouds is especially important when collecting data during rainy periods, when wetlands are often easier to discriminate (Federal Geographic Data Committee 1992; Kasischke and Bourgeau-Chavez 1997; Kasischke et al. 1997). Hypothesis C1 for this dissertation (to compare the relative utility of C-band SAR data versus optical data for mapping wetlands) was designed to further evaluate the abilities of SAR and optical data when documenting hydrology through forest canopies as it is the ability to sense hydrology that allows the mapping of wetlands.

Although the capability of SAR for wetland research is promising, the technology is relatively new compared to optical sensors, and further research is required to develop this capability. Seasat, launched in 1978, was one of the first imaging radars to be used to study wetlands. Researchers found that the L-HH microwave energy transmitted by Seasat was particularly sensitive to inundation below forest canopies due to the increase in backscatter caused by double-bounce scattering between tree trunks and the flooded surface (Krohn et al. 1983; Hess et al. 1990; Pope et al. 1997). In addition to Seasat, the ability of L-HH SAR to map inundation in forested wetlands has been well documented with a variety of other sensors including AIRSAR, SIR-C, and JERS-1 (Ormsby et al. 1985; Hess et al. 1995; Wilen and Smith 1996; Townsend and Walsh 1998).

The use of SAR for forested wetland monitoring was further advanced using data collected by several sensors in the 1990's. The launch of ERS-1 (C-VV) in 1991 and the

subsequent launches of ERS-2 in 1994 and ENVISAT (C-VV, C-HH, C-HV, and C-VH) in 2002 have provided the capability for continuous C-VV monitoring of wetlands for over a decade. Additional coverage of wetlands has been provided by JERS-1 (L-HH) (1992-1998) and RADARSAT (C-HH) (1995 to present). These systems offer enhanced data quality (digital rather than analog) and the temporal frequency required to study dynamic processes such as wetland hydropattern (Kasischke et al. 1997).

After the successful launch of ERS-1/2 and RADARSAT, C-band data were increasingly available and wetland studies using this shorter wavelength data were initiated. Researchers found that although C-HH band radar data were not as well suited for forested wetland studies as those from L-HH SARs, they could be used to monitor inundation patterns, especially in areas of lower biomass (Townsend and Walsh 1998; Townsend 2000; Costa 2004). C-VV data from the ERS systems (for which the longest continuous record of SAR observations exist) have primarily been used to study herbaceous vegetation (e.g., Kasischke et al. 2003), but have also been successful in detecting inundation under forest canopies during the leaf-off period (Kasischke et al. 1997; Townsend 2002).

Although SIR-C/X-SAR(deployed onboard NASA's Space Shuttle) only collected data during the spring and fall of 1994, it provided new details regarding the advantages and limitations of spaceborne multi-wavelength (X, C, and L bands), polarimetric SAR (Hall 1996). The SIR-C/X-SAR data set provided information regarding backscatter phase as well as magnitude (Evans et al. 1997), which led to the ability to detect finer details of vegetation structure and therefore improved the accuracy of wetland classifications from space (Pope et al. 1994; Hess et al. 1995; Hall 1996; Smith 1997;

Bourgeau-Chavez et al. 2001). Although SIR-C/X-SAR was the only fully polarimetric SAR to be flown in space, a new earth orbiting sensor, ENVISAT ASAR, does have multiple polarizations, an advance over prior satellite-borne SARs.

While past research has documented the potential of SAR for the monitoring of forested wetland hydropattern, further studies are necessary to fully develop this capability. Although researchers have established the ability of C-band SAR to differentiate between inundated and non-inundated forests in relatively large floodplain systems with continuous patterns of inundation, such as the Amazon and Roanoke River floodplains, no studies have tested this ability in smaller floodplains where flooding may be discontinuous. Thus the ability of C-band SAR to determine if varying amounts of inundation can be detected, at relatively low levels (< 50 or 60% percent of the total area), is not known. In addition, the relatively new dual polarization ASAR imagery allows the direct comparison of the abilities of C-HH and C-VV SAR data to detect flooding and soil moisture throughout the year. Furthermore, the relationship between SAR backscatter, hydrology, and variations associated with climate change and/or variability has not been investigated. Establishing this relationship would provide scientists and regulators a synoptic method for predicting the effect of changing climate on forested wetlands.

2.3 Limitations of Using SAR Data to Monitor Wetland Hydrology

The limitations of C-band SAR data for monitoring hydrology under forest canopies include the variation of canopy transmissivity with different incidence angles, the effect of polarization on backscatter from forested areas, and the limited transmittance of

16

microwave energy through the canopy as governed by plant structure and microwave wavelength. Hypotheses B1 and B2 address the impact of these parameters on the ability to detect soil moisture and inundation under forest canopies.

The effects of SAR parameters (incidence angle and polarization) on the ability of microwaves to penetrate the forest canopy are investigated with Hypothesis B1. According to previous research, the ability of microwave energy from C-band SAR sensors to penetrate the forest canopy and detect changes in hydrology is greater at small incidence angles (Hess et al. 1990; Brown and Manore 1995; Wang et al.1995; Bourgeau-Chavez et al. 2001). Microwave energy at these incidence angles penetrates the canopy more directly, and thus reduces the interaction of the SAR signal with the canopy. Addressing Hypothesis B1a will allow the investigation of the relationship between incidence angle and the ability to detect hydrologic features below the forest canopy. It is intended to define the range of incidence angles that can be used for this purpose and thus the frequency that SAR images can be collected over a site as the wider the range of incidence angles that are acceptable, the shorter the satellite repeat time. Polarization also affects the way in which microwave radiation interacts with the surface of the Earth. Microwave energy that is both vertically transmitted and received (VV) does not pass as readily through forests as horizontally transmitted and received (HH) microwave energy (Hess et al. 1995; Wang et al. 1995). It is important to understand the varying limitations of VV and HH polarized data because the archives containing these polarizations differ in duration and availability (see Chapter 4). Hypothesis B2b seeks to better define the varying abilities of HH and VV polarizations under a variety of vegetation phenological conditions.

The relationship between the size of individual structures (leaves and branches), the orientation of those structures, and total volume of material in the canopy and microwave wavelength determines the degree to which SAR can penetrate forest canopies (Wang et al. 1995). Seasonal variation in leaf area and hence canopy closure occurs in most forested wetlands in the Coastal Plain of Maryland as their canopies are dominated by deciduous tree species. Temporal variations in canopy closure as well as variations in tree density and canopy diameter interact to attenuate the SAR signal as it passes through the canopy (Wang et al. 1995). The denser the tree canopies and the higher the canopy closure, the more the microwave energy should be attenuated as it passes through the canopy. Hypothesis B2 was designed to address the effects of variations in leaf area. Hypothesis B2a tests whether or not C-band microwave energy is less sensitive to surface hydrologic changes during the leaf-on period (approximately mid-April through early November) in the Mid-Atlantic region and seeks to better quantify the time period for which C-band SAR can monitor variations in hydrology.

2.4 Improved Wetland Mapping Using SAR Data

While the principal focus of this research was on using SAR to assess hydrologic conditions in forested wetlands, it also provided an opportunity to address a critical issue, the need for improved forested wetland mapping. Traditional methods for mapping and monitoring wetlands rely primarily on optical data derived mostly from aerial photographic systems but also from VIS/IR satellite sensors. Due to the interference of the canopy, this methodology is problematic when mapping forested wetlands, especially those that do not remain inundated year round. When using optical data, deciduous

18

forested wetlands are best mapped during the spring before leaf-out (National Research Council 1995; Tiner 1999). However, it can be difficult to collect optical imagery at this time due to persistent cloud cover (Federal Geographic Data Committee 1992). When aerial photos are obtained over wetlands, they are usually collected infrequently, due to high costs and other limitations; but they are assumed to be representative of wetland environments although wetland hydrology varies throughout the year. New methods must be developed to obtain a more complete picture of these ecosystems. This is especially important because forested wetlands comprise over half of all U.S. wetlands (Welsch et al.1995).

The hypothesis associated with Goal 2 of this proposal was designed to provide the link between the ability of SAR to detect patterns of saturation and inundation and the usefulness of SAR data in mapping wetlands. It builds on the knowledge gained during the initial investigations of C-band SAR sensitivity to hydrologic parameters. If it can be confirmed that variations in saturation and inundation cause predictable changes in SAR backscatter throughout the year, then it follows that SAR can be used to monitor the time for which an area is saturated or inundated. This duration and timing of condition is the most important characteristic that is used to determine if an area is a wetland.

Chapter 3: Controls on Hydropattern in a Mid-Atlantic Floodplain Wetland

3.1 Introduction

Wetlands in the Mid-Atlantic Coastal Plain serve numerous valuable functions, yet many have been lost and the future of existing wetlands is threatened. Due to the high density of wetlands found in the Mid-Atlantic Coastal Plain, the U.S. Fish and Wildlife Service (FWS) has determined the region is at high risk for wetland loss due to land clearing and construction activity driven by population increases. Forested wetlands are especially vulnerable due to their frequent ephemeral hydrology and inadequate legal protection (Tiner and Burke 1996; U.S. Fish and Wildlife Service 2002).

Because wetland hydrology influences wetland distribution and function (see Chapter 2), additional models and/or analytical approaches are needed to provide managers with the capability to predict how future changes in climate combined with changes in land use and land cover will affect wetland hydrology. This information must be modeled because of the difficulty in directly obtaining reliable and accurate information on patterns of wetland inundation over large spatial scales (see Chapters 2 and 6).

Models have been developed to predict wetland hydrology, and include quantitative, mathematical models and simpler, often conceptual models. Both types of hydrologic models are often based on water budgets and linked to processes describing wetland functions (Cronk and Mitsch 1994; Winter and Rosenberry 1998; Moustafa 1999; Liao et al. 2001; Burke et al. 2003; Baber et al. 2004). While complex mathematical models can be more accurate and detailed, they usually require inputs that are difficult to obtain. Because of this, their use is typically confined to research instead of regulation and

broad-scale management (National Research Council 1995). In 1995, the National

Research Council emphasized the importance of assessing wetland hydrology without

obtaining site specific details, which is often difficult. While simple conceptual models

can be less precise, by relying on simplifying assumptions they allow environmental

managers to make relatively quick decisions regarding wetland hydrology without site

specific details. To use these conceptual models, the validity of their simplifying

assumptions and other limitations need to be identified and evaluated (Bolster and Saiers

2002).

The goal of the study presented in this chapter was to better understand the influence

of climate and stream flow on the hydrologic status of a forested floodplain wetland in

the Coastal Plain of Maryland. A simple, conceptual water budget model of riparian

wetland flooding was used to meet this goal at different spatial scales and within different

areas of the floodplain. The ability of this model to predict wetland flooding was assessed

using multiple-linear regressions based on detailed, multi-temporal measurements of

wetland hydrology, basic site descriptions, and climate data. As a result of this analysis,

issues concerning the simplifying assumptions of the model and ways to improve similar

models were identified. The assessment approach developed during this study can be

used by resource managers to evaluate wetland hydrology in similar systems and to

improve models of wetland hydrology.

3.2 Background

Although numerous factors interact to influence wetlands, hydrology is the single

most important force in their formation and functioning (Bedford 1996; Mitsch and

Gosselink 2000). Wetland ecosystems in the Coastal Plain of Maryland are currently

undergoing hydrologic changes. Future climate change (Moore et. al. 1997; Mid-Atlantic

Regional Assessment Team 2000; Conly and Van der Kamp, 2001; Price 2005) and

human land use activities (Moore et al. 1997) are likely to further alter the water balance

in the region's fresh water ecosystems, including wetlands (see Chapter 2).

Wetland hydrology is often described with respect to wetland hydropattern – the

fluctuation in the area, duration, and frequency of wetland flooding and soil saturation.

Wetland hydropattern results from complex and often small topographic variations in

floodplain geomorphology, the type of soils present, and transfers of water into and out of

the ecosystem. These transfers can be summarized in a water budget, with inflows

coming from precipitation, surface water inflows (such as over bank flow from a river),

and influx of groundwater and outflows including evapotranspiration, surface water

outflows (such as water flowing out of a wetland after stream levels decrease), and the

flow of groundwater out of the system. Increases in inflows relative to outflows will

increase inundation while decreases in inflows relative to outflows will lessen inundation

(Mitsch and Gosselink 2000).

Simple water budget models are often used to characterize wetland hydropattern

and/or how it is altered in response to changes in inputs or outputs (Kadlec 1993; Walton

et al. 1996; Lent et al. 1997; Brooks 2004; Krasnostein and Oldham 2004; Zhang and

Mitsch 2005). These models use fairly straightforward methods and simplifying

assumptions, and are often based on empirical relationships established from field

observations. Although they can be less accurate than other models, these simplified

models do not require detailed, site-specific information that is often difficult to obtain by

resource managers. The necessity for this site-specific information is often cited as a

major limitation to gathering hydrologic information necessary to make ecosystem

management decisions (Cole and Brooks 2000; Price 2005). While these simpler

approaches are limited by a number of environmental factors which are not fully

accounted for, the information they provide can be more readily supplied to

environmental managers. These simpler water budget models often form the basis for

more complex mathematical models, which can be, but are not always, more accurate

(Townsend and Foster 2002).

Complex mathematical models of hydropattern have been developed for a variety of

different wetlands (Richardson and McCarthy 1994; Skaggs et al. 1994; Konyha 1995;

Stewart et al. 1998; Johnson et al. 1999; Bradley 2002; Kirk et al. 2004; Trepel and

Kluge 2004). For example, DRAINMOD is a computer simulation model that can predict

soil moisture, evapotranspiration, drainage, water table depth, and surface runoff for a

prescribed set of soil qualities, climate conditions, vegetative cover, and other site

conditions. It has been used to determine whether or not an area qualifies as a wetland

(Skaggs et al. 1994) and to gauge the effects of different land development activities on

the water storage and release patterns in peatlands (Richardson and McCarthy 1994).

These models usually require detailed site-specific information (e.g. soil profiles,

hydraulic conductivity of soil layers, relative humidity, short-wave radiation, wind speed,

etc.) which is difficult to acquire for large areas.

This study is part of a larger research initiative designed to determine whether information derived from C-band synthetic aperture radar (SAR) data can be used to monitor forested wetland hydrology (see chapters 4 and 5). The ground data collected in this study are being used to evaluate the effectiveness and limitations of C-band SAR data in detecting hydropattern in forested wetlands. The detailed measurements of inundation required to validate the radar data also provide the opportunity to examine the factors that control inundation in wetlands located in Mid-Atlantic floodplains.

A simple, conceptual water budget model of wetland hydropattern was used to guide this investigation regarding the influence of climate and stream flow on inundation in a Mid-Atlantic forested floodplain wetland. Multi-temporal measurements of percent area inundation were collected during 2003 and 2004 in 16 field plots, including wetter (backwater) and drier (levee) areas of the Patuxent River floodplain. The ground measurements were used as the dependent variable in a multiple regression analysis to test the validity and limitations of the water budget model. The relationship between inundation and the independent variables used in the model (stream discharge, precipitation, and temperature as a proxy for evapotranspiration) was examined at three spatial scales: fine (individual plot), intermediate (sections of the floodplain), and coarse (entire floodplain). At the fine spatial scale, the influence of time on the relationship between plot flooding and discharge and precipitation was determined in different areas of the floodplain. Once the optimal time periods (3, 5, 10, or 15 days) for aggregation (the time period of discharge and precipitation that was best correlated with area flooded) were determined for the individual plots, the relationship between flooding and the independent variables was considered over the entire floodplain (coarse spatial scale). To

increase the correlation between area flooded and the independent variables, the relationship between flooding and the independent variables was examined at an intermediate spatial scale where plots were placed into three groups (backwater, levee, and road-influenced) based on floodplain geomorphology and hydrologic connectivity determined by the presence of a road. Lastly, the influence of elevation was examined at the intermediate and coarse spatial scales by adding it as an independent variable to the analysis.

3.3.1 Study Area

The study area was located at the Patuxent Wildlife Research Center (PWRC), (76.8° W latitude and 39.1° N longitude) within Maryland's Coastal Plain Physiographic Province (Figure 3.1). The PWRC lies midway between Washington, D.C. and Baltimore, Maryland and contains 5,160 hectares of upland and wetland forests, nearly all having been cultivated at one time. The region's climate is temperate (average temperature 12° C) and has high summer humidity. The 108 cm of annual precipitation is evenly distributed throughout the year (Hotchkiss and Stewart 1979).

The study focused on upland and wetland areas surrounding the 182 km long Patuxent River, a tributary of the Chesapeake Bay. The Patuxent River is spanned by two dams, with the closest being the Howard T. Duckett Dam (~8 km upstream from PWRC). Within the boundaries of the PWRC, the floodplain is 0.40 to 0.81 km wide and bordered by upland terraces (Hotchkiss and Stewart 1979). The braided river channel is surrounded by levees that gradually decrease in elevation into backwater areas adjacent to the uplands on either side of the floodplain. Most of the Patuxent River floodplain is

inundated for only part of the year, with some backwater areas remaining flooded for

much of the year.

Patuxent River Study Site
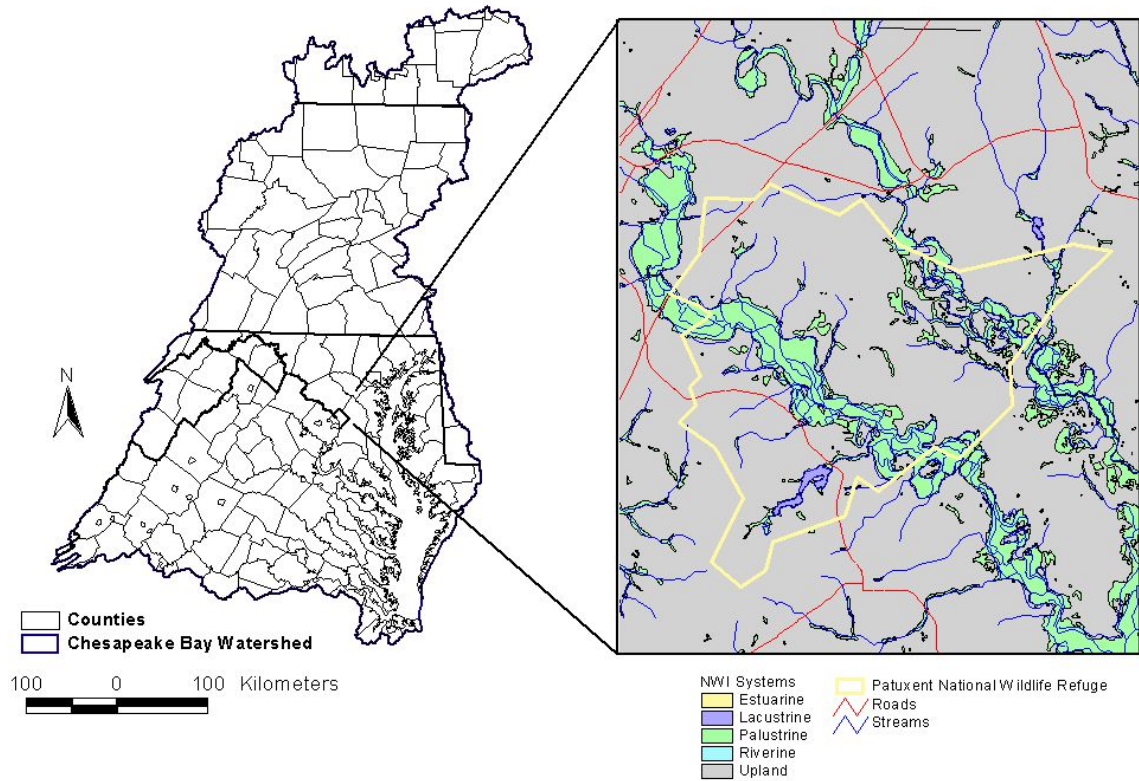
Figure 3.1: Location of the study area within the Chesapeake Bay watershed. A U.S. Fish and Wildlife Service National Wetland Inventory (NWI) map overlaid with roads and the boundary of the Patuxent Wildlife Research Center can be seen to the right. The majority of wetlands in the PWRC are palustrine or generally, inland wetlands not directly associated with lakes or stream channels (low water depth < 2 m) (Cowardin et al. 1979).

3.3.2 Conceptual Model of Wetland Hydropattern

Three hypotheses were developed to investigate the influence of climate and stream

flow on hydrology: 1) increases in stream discharge will result in greater flooding; 2)

greater amounts of precipitation will cause increases in flooding; and 3) higher

26

temperatures will result in decreases in flooding due to increased evapotranspiration.

These hypotheses represent the components of a simple, conceptual water budget model

of wetland inundation, where change in area flooded per unit time (dA/dt) can be

described as:

$$dA/dt \; = \; D + P - ET$$

where:

D = stream discharge, P = precipitation, and ET = evapotranspiration.

The model is composed of easily quantifiable and commonly available water balance

inputs and outputs (see section 3.2), the importance of which are modified by site

location (geomorphology and elevation). Stream discharge and precipitation are the two

major inputs and temperature, as a proxy for evapotranspiration, is the major output. The

use of commonly available parameters, instead of time-sensitive, site-specific

information, allows this model to estimate past levels of inundation using historic

hydrometeorologic variables (assuming similar geomorphology). The model was

simplified by assuming the influence of ground water, which is difficult to quantify, was

absent from the study area. Anthropogenic impacts on inundation were not considered

because the study site was located in a relatively undisturbed area.

Methods for computing evapotranspiration, such as Penman (1948) and Priestley-

Taylor (Stewart and Rouse 1976), are available but are often complicated by variations in

vegetation type, soil drainage, and micro-climate, which in turn require detailed

measurements (e.g. change in heat stored in the water body, net solar radiation, and

atmospheric pressure at the site) (Drexler et al. 2004; Pyke 2004; Rosenberry et al. 2004).

For this reason, average monthly temperature was used as a proxy for evapotranspiration, since warmer temperatures tend to increase both evaporation and transpiration, it is easily obtained, and estimates of evapotranspiration often rely strictly on temperature (Rosenberry et al. 2004). Rosenberry et al. (2004) compared several different methods for obtaining evapotranspiration and found a method that relying exclusively on temperature (Mather 1978) performed well. The Mather (1978) method was found to be relatively unbiased and produced results within 20% of actual evapotranspiration 75% of the time. This method performed just as well or better than two other methods that required measurements of solar radiation or vapor pressure and empirically derived constants (Rosenberry et al. 2004).

3.3.3 Field Measurements

Inundation levels were measured in sixteen 200 x 200 m (4 ha) plots (Figure 3.2). Eight plots were located in backwater sites and eight in forests that experience less inundation for a total of 16 plots. The plots with less inundation were usually found close to the levees on either side of the stream and are therefore referred to as levee sites. Although plots were originally divided into backwater and levee sites, a third group was created during the analysis stage for plots with inundation levels affected by a dirt road. Plots were selected in areas of relatively homogeneous forest cover and expected hydrology based on examination of aerial photographs and maps of wetland type (FWS National Wetland Inventory [NWI]). Final selections were made after a preliminary field reconnaissance was undertaken to ensure homogeneity of forest cover as well as geomorphology which could influence hydrology. Corner points of each plot were

located using a differentially-corrected global positioning system (GPS), and entered into a geographic information system (GIS) to identify the plot locations on an aerial photograph.
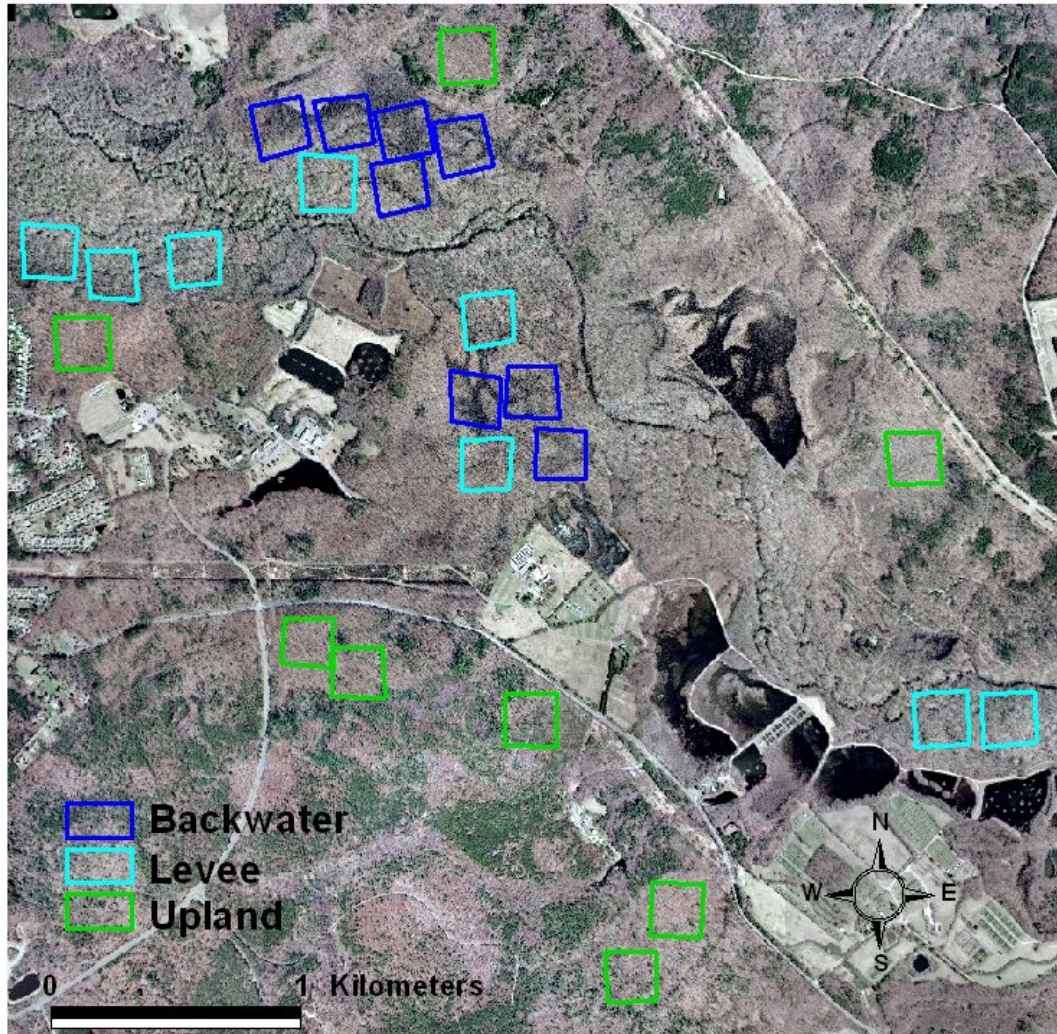
Figure 3.2: Aerial photograph of study site with the locations of the ground data collection plots. The image was taken during the leaf-off season (United States Geological Survey 2003).

Measurements of percent area inundated were collected at monthly intervals within each plot from May of 2003 until November of 2004 by dividing each into 64 equal sub-sections (each 25 x 25 m), and visually estimating percent inundation (i.e. percent of the area of each 25 x 25 m plot subsection that was flooded) using a Daubenmire cover class

approach (where 1 = 1-5% inundation, 2 = 6-15%, 3 = 16-25%, 4 = 26-50%, 5 = 51-75%, 6 = 76-95%, and 7 = 96-100%) (Daubenmire 1968). All 64 measurements were averaged to provide monthly area inundated estimates for each site.

When field collection was complete, the inundation values for each plot were averaged over all dates so plot inundation could be compared between plots. Upon reviewing the results, it was found one of the levee sites (L1) was wetter than anticipated and this site was reclassified as a backwater site for future analysis (Table 3.1).

Plot	% Inundation	SE	Class
B1	25.5	4	Natural Wetland
B2	25.2	4.1	Natural Wetland
B3	37.6	5.2	Natural Wetland
B4	33.6	5.7	Natural Wetland
B5	28.1	8.4	Natural Wetland
B7	16.6	2.3	Road Influenced
B8	22.8	2.6	Road Influenced
B9	21.6	3.2	Road Influenced
L1	20.1	1.9	Natural Levee
L2	16.4	4.1	Natural Levee
L3	6.4	3.1	Natural Levee
L4	9.7	4.6	Natural Levee
L5	1.5	0.2	Road Influenced
L8	8.7	1.3	Road Influenced
L9	6.8	1.7	Natural Levee
L10	5.5	2.1	Natural Levee
Natural Wetland	28.4	2.6	N/A
Natural Levee	9	2	N/A
Road-Influenced	14.2	4	N/A

Table 3.1: Average percent area inundated and standard error of inundation (SE) for all individual plots and classes. Names of the ground data collection plots are on the left. Plots starting with B were originally designated as backwater plots and those beginning with L were designated as levee plots (hydrology intermediate to the backwater plots and upland sites). Note that although L1 was originally designated as a levee site, it was re-assigned as a backwater site due to its high level of inundation and that the road-influenced group contains both backwater and levee sites.

3.3.4 Model Components

Stream discharge data were provided by the United States Geological Survey's

National Water Information System (NWIS). The NWIS provides current and historic

information concerning ground water, surface water, and water quality from areas across

the United States, Guam, and Puerto Rico (U.S. Geological Survey 2005). Stream

discharge was obtained at USGS station 01592500 along the Patuxent River near Laurel,

Maryland, about 8 km upstream from the study site. Precipitation and temperature data

were acquired from the National Oceanic and Atmospheric Administration's (NOAA)

National Climatic Data Center (NCDC). The climate station (180700) used for this study

was located in Beltsville, Maryland (about 10 km from the study site).

3.3.5 Data Analyses

The statistical analyses were conducted using SAS 9.0 (SAS Institute Inc). A step

wise linear regression model was used to analyze the relationships between the dependent

and independent variables. All models were considered significant at the 0.05 level (alpha

= 0.05) and a 0.15 level was used as the criterion for inclusion into all stepwise regression

models. A t-test was used to test the hypothesis that there were significant differences in

inundation between backwater and levee plots.

Stream discharge and precipitation were averaged for different periods of time (3, 5,

10, and 15-day periods) relative to the date inundation was measured in the field and

multiple regression (MaxR) was used to determine which period of time was best

correlated with inundation for each plot based upon the highest correlation coefficient

obtained. The 3, 5, 10, and 15 day averages were selected because shorter time intervals

may not give the floodplain wetlands a long enough time to respond to changes in stream

discharge or runoff caused by precipitation and/or they might overemphasize the

responsiveness of floodplain inundation to relatively brief spikes in discharge or

precipitation. Longer intervals were not chosen because the increase in inundation in

response to such events can be transient. Townsend and Foster (2002) found discharge

averaged over periods between 10 and 20 days had the highest correlations with water

levels in the Roanoke River floodplain. However, the Roanoke River floodplain is much

larger than the floodplain examined in this study so longer periods of time were not

examined.

Once the best correlated time periods of discharge and precipitation were determined

for each study plot, these measurements and average monthly temperature were used in

stepwise linear regressions with the inundation measurements collected for each plot.

Average monthly temperature was used instead of temperature averaged over a shorter

time period because temperature affects evapotranspiration, and therefore inundation,

more slowly and over longer periods of time.

Based on the results for the individual plots, ten day discharge, five day precipitation,

and monthly temperature were regressed against inundation for all plots. This multiple

regression was repeated for groups of plots (natural backwater plots, natural levee plots,

and road-influenced plots) divided according to geomorphology and reduced connectivity

as result of the presence of a dirt road.

Regressions were repeated for the entire floodplain as well as the three groups using sub-meter, lidar-derived elevation data (Blair et al. 1999) in addition to the other independent variables.

3.4 Results

There were significant differences in average inundation levels between the backwater and levee plots (t-Test, t = 8.81, $p = < 0.0001$), with the backwater plots having a greater percent of area inundated (28.4%, standard error = 2.6), on average, than the levee plots (9%, standard error = 2.0) (Table 3.1).

The level of inundation in the different plots was best correlated with different time periods of discharge and precipitation (Table 3.2). Inundation in the backwater plots was generally more correlated with 10 day discharge, and was not significantly correlated with precipitation at any time scale. Inundation in the levee plots was better correlated with discharge averaged over a shorter time period than inundation in backwater plots, but results varied for precipitation. Inundation at some levee plots was correlated with precipitation while inundation in other plots was not. Inundation in road-influenced plots was not significantly correlated with discharge but was, on average, correlated with precipitation summed over a 5 day period.

When inundation in individual plots was regressed against temperature, stream discharge, and/or precipitation, multiple-linear correlation values (r^2) ranged from a low of 0.41 (*p = 0.0413*) to a high of 0.96 (*p = < 0 .0001*), with all but two greater than or equal to 0.65 (Table 3.3). Inundation in all non-road influenced backwater and levee plots was significantly correlated with discharge, while inundation in road-influenced plots

Plot	D3	D5	D10	D15	D N/A	P3	P5	P10	P15	P N/A
B1			0.42							x
B2			0.66							x
B3			0.5							x
B4				0.75						x
B5		0.88								x
B7					x		0.43			
B8					x	0.12				
B9					x			0.07		
L1		0.26								x
L2	0.89									x
L3	0.87									x
L4	0.09						0.7			
L5					x		0.48			
L8					x		0.47			
L9			0.81					0.15		
L10	0.94									x
All			0.19					0.01		

Table 3.2: Correlation coefficients (r^2) between inundation levels and time period of discharge (D) and precipitation (P) in days that correspond with the number of aggregated daily measurements. Only values for the highest correlations with inundation are shown. All correlations are significant at $p < 0.05$. Otherwise discharge or precipitation is marked (x) as not applicable.

was not. Inundation in backwater plots was not correlated with precipitation, while inundation in all road-influenced plots was. Inundation in these road impacted plots was always correlated with temperature. However, inundation in levee plots was never correlated with temperature, while inundation in some backwater plots was. Flooding in the road-influenced plots with lower levels of inundation was better correlated with precipitation, while flooding in the plots with higher levels of inundation was better correlated with temperature. Inundation in all backwater and levee plots, excluding L1, was more correlated with discharge than with precipitation or temperature.

It was found that grouping the plots according to floodplain geomorphology (backwater versus levee) and connectivity (road-influenced versus natural plots) greatly increased r^2 values, especially for the non road-influenced plots (Table 3.4).

Plot	N	r^2	F	p	Discharge Prt r^2	F	p	SE	Coef	Temperature Prt r^2	F	p	SE	Coef	Precipitation Prt r^2	F	p	SE	Coef
B1	14	0.65	10	0.0033	0.42	9	0.0128	0.02	0.06	0.23	7	0.0218	0.17	-0.45	----	----	----	----	----
B2	15	0.66	26	0.0002	0.66	26	0.0002	0.01	0.07	----	----	----	----	----	----	----	----	----	----
B3	15	0.68	13	0.0011	0.50	13	0.0030	0.02	0.09	0.17	6	0.0261	0.25	-0.64	----	----	----	----	----
B4	11	0.75	26	0.0006	0.75	26	0.0006	0.03	0.14	----	----	----	----	----	----	----	----	----	----
B5	11	0.92	46	<.0001	0.88	65	<.0001	0.01	0.10	0.04	4	0.0755	0.17	-0.20	----	----	----	----	----
L1	16	0.66	14	0.0005	0.26	11	0.0057	0.01	0.04	0.41	10	0.0059	0.10	-0.33	----	----	----	----	----
L2	15	0.89	131	<.0001	0.89	131	<.0001	0.01	0.07	----	----	----	----	----	----	----	----	----	----
L3	17	0.90	64	<.0001	0.87	111	<.0001	0.01	0.05	----	----	----	----	----	0.02	3	0.0980	1.66	2.93
L4	17	0.79	23	<.0001	0.09	5	0.0416	0.01	0.03	----	----	----	----	----	0.70	30	0.0001	3.84	8.97
L9	19	0.96	112	<.0001	0.81	43	<.0001	0.00	0.02	----	----	----	----	----	0.15	35	0.0002	0.38	2.25
L10	18	0.94	193	<.0001	0.94	193	<.0001	0.00	0.03	----	----	----	----	----	----	----	----	----	----
B7	15	0.68	14	0.0006	----	----	----	----	----	0.25	5	0.0505	0.10	-0.44	0.43	17	0.0011	1.37	5.69
B8	16	0.41	4	0.0413	----	----	----	----	----	0.29	5	0.0366	0.16	-0.68	0.12	2	0.1472	2.17	3.89
B9	16	0.65	13	0.0006	----	----	----	----	----	0.58	20	0.0004	0.15	-0.76	0.07	3	0.1046	1.44	2.50
B5	12	0.63	10	0.0027	----	----	----	----	----	0.14	5	0.0516	0.01	-0.03	0.48	12	0.0040	0.21	0.92
B8	14	0.79	24	<.0001	----	----	----	----	----	0.31	19	0.0008	0.05	-0.22	0.47	13	0.0033	0.67	4.29

Table 3.3: Results from multiple linear stepwise regressions performed for each ground data plot using inundation as the dependent variable and discharge, temperature, and precipitation as the independent variables. The partial r^2, F, p, standard error, and regression coefficient for each independent variable are included in the table. Dashes were used to signify variables excluded from the model because they were not significant at the 0.15 level.

Plot	N	r^2	F	p	Discharge Prt r^2	F	p	SE	Coef	Temperature Prt r^2	F	p	SE	Coef	Precipitation Prt r^2	F	p	SE	Coef
Nat Backwater	83	0.59	38	<.0001	0.50	79	<.0001	0.01	0.06	0.06	10	0.0023	0.11	-0.46	0.04	7	0.0089	2.52	6.75
Nat Levee	78	0.62	62	<.0001	0.57	101	<.0001	0.01	0.04	----	----	----	----	----	0.05	10	0.0020	1.35	4.32
Road Influenced	79	0.21	10	0.0001	----	----	----	----	----	0.12	10	<.0001	0.09	-0.37	0.09	9	0.0041	1.21	3.58
All	240	0.23	24	<.0001	0.19	56	<.0001	0.01	0.03	0.03	10	0.0015	0.08	-0.27	0.01	3	0.1047	1.53	2.49

Table 3.4: Results from multiple linear stepwise regressions performed for each ground data plot class using inundation as the dependent variable and discharge, temperature, and precipitation as the independent variables. The partial r^2, F, p, standard error, and regression coefficient for each independent variable are included in the table. Dashes were used to signify variables that were excluded from the model when they were not significant at the 0.15 level.

When regressing inundation with average monthly temperature, 10 day discharge and 5 day precipitation, r^2 values ranged from 0.23 ($p = < 0.0001$) for all groups together to 0.59 ($p = < 0.0001$), 0.62 ($p = < 0.0001$), and 0.21 ($p = 0 .0001$) for the backwater, levee, and road-influenced groups respectively. From the correlation of inundation in these groups with discharge, precipitation, and temperature, it is evident that flooding in levee plots is most correlated with discharge, followed by that in natural backwater plots, and finally flooding in road-influenced plots. The reverse is true for temperature.

Elevation was found to be significantly correlated to inundation when all plots were analyzed together, as well as when each group was analyzed separately (Table 3.5). Including elevation as an additional independent variable resulted in a slight increase in the r^2 of all plots together from 0.23 to 0.27 ($p = < 0.0001$), the backwater group from 0.59 to 0.64 ($p = < 0.0001$), the levee group from 0.62 to 0.68 ($p = < 0.0001$), and dramatically in the road-influenced group from 0.21 to 0.60 ($p = < 0.0001$).

3.5 Discussion and Summary

This study supports the finding by Cole and Brooks (2000) that flooding in mainstem floodplain wetlands is controlled primarily by stream discharge. The influence of stream discharge can be lessened and that of precipitation and evapotranspiration increased according to placement of the wetland within the floodplain (geomorphology) and human influence (roads).

Although the flooding in backwater and levee plots were greatly correlated to stream discharge, flood waters remained in backwater plots for longer periods of time.

The water in the levee plots to either side of the stream was more transient, flowing into and out of areas of lower elevation (channels) serving as conduits. For this reason, inundation in levee plots was better correlated with stream discharge averaged over shorter time intervals. This supports the finding of Roberts et al. (2000) that low-lying floodplain areas experience a greater duration of flooding than areas of higher elevation.

		Natural Backwater	Natural Levee	Road Influenced	All
All Variables	N	83	78	79	240
	r^2	0.64	0.68	0.60	0.27
	F	35	53	37	28
	p	<.0001	<.0001	<.0001	<.0001
Discharge	Prt r^2	0.50	0.57	----	0.19
	F	79	101	----	56
	p	<.0001	<.0001	----	<.0001
	SE	0.010	0.006	----	0.005
	Coef	0.06	0.04	----	0.04
Temperature	Prt r^2	0.06	----	0.13	0.04
	F	10	----	19	12
	p	0.0023	----	<.0001	0.0007
	SE	0.103	----	0.064	0.066
	Coef	-0.45	----	-0.38	-0.22
Precipitation	Prt r^2	0.04	0.05	0.09	----
	F	9	10	18	----
	p	0.0037	0.002	<.0001	----
	SE	2.370	1.283	0.865	----
	Coef	7.09	5.54	3.62	----
Elevation	Prt r^2	0.05	0.06	0.38	0.04
	F	9	15	47	12
	p	0.0028	0.0003	<.0001	0.0006
	SE	0.966	0.295	0.474	0.375
	Coef	-3.24	1.13	-4.05	-1.37

Table 3.5: Results from multiple linear stepwise regressions performed for each ground data plot class using inundation as the dependent variable and discharge, temperature, precipitation and elevation as the independent variables. The F, probability of F (Pr > F) or P, and the partial r^2 for each independent variable is included in the table. Dashes were used to signify variables that were excluded from the model when they were not significant at the 0.15 level.

The results of this study support the view that not only different locations within the floodplain but also different levels of stream connectivity led to varying inundation

origins and residence times. At the study site, stream connectivity seemed to be lessened by road construction and, therefore, the initial assumption of no anthropogenic impact was not valid. Although road-influenced plots are still connected to the stream through culverts, these passageways can be blocked by debris and are often targeted by beavers. Even when water is flowing freely through the culverts, the volume of water moving into and out of the road-influenced sites appears smaller than that flowing to and from the non-road influenced sites. For these reasons, flooding in the road-influenced plots was not significantly correlated with river discharge.

The significant statistical correlations support the hypothesis that precipitation has a much greater influence on inundation in road-influenced plots, relative to inundation in non-road influenced plots. Perhaps because the influence of stream discharge is reduced in road-influenced plots, the link between precipitation and inundation in these areas is more important than in the natural backwater and levee plots. Since the water in road-impacted plots was not significantly correlated with stream discharge, these plots were hydrologically less variable, usually experiencing less inundation than the natural backwater sites during flood events. This reduction in inundation variability has been noted in constructed wetlands (Cole and Brooks 2000).

Plots containing large areas of still water, especially those less influenced by stream discharge, were most correlated with temperature whereas inundation in natural levee plots was not significantly correlated with temperature. It is hypothesized this is due to the rapid movement of water through these systems, leaving less time for this water to be evaporated or transpired.

Although the inundation in all natural backwater areas was correlated with stream discharge, while inundation in road influenced sites was not, it should be noted that natural backwater plots can also be more or less connected to the stream channel. This can occur, as for plot L1, when water travels a greater distance to reach the site. Although the flooding in L1 was correlated with stream discharge, it was much less correlated than were any other natural backwater sites. However, flooding in L1 was not correlated with precipitation as it was in the road impacted sites. Flooding in L1 was better correlated with temperature than flooding in other natural backwater sites. It is therefore hypothesized that it was more difficult for water to reach L1, but once it did, the water remained there for extended periods of time. Already having high levels of flooding, inundation in L1 was less correlated with varying amounts of precipitation.

Although the inclusion of elevation as an independent variable greatly increased the correlations once plots were grouped, its addition to regressions before grouping only increases r^2 by 0.04. The most substantial increase in r^2 (an increase of 0.39) occurred for the road-influenced group. This was probably partially due to the close proximity of the road-influenced plots to one another, making relative changes in elevation more important.

Although much is known about the flow of water in river channels, less is known about patterns of water flow and residence time in the floodplains (Mertes et al. 1995; Hupp 2000; Dollar 2002). Many of this study's findings were intuitive, but they are rarely documented due to the large amount of ground data needed to do so. These findings included: 1) the increased residence time of flood waters in backwater areas as compared to areas of the floodplain closer to the stream channel and its associated levees, 2) the

strong relationship between floodplain inundation and stream discharge, 3) the ability of roads to restrict water flow and therefore greatly decrease the correlation between stream discharge and inundation, 4) the stronger relationship between precipitation and increases in flooding in areas not affected by stream discharge, 5) the higher correlation between evapotranspiration and the reduction in flooding in areas with longer hydrologic residence times, and 6) the higher amounts of water found in areas of the floodplain with lower elevations.

While the hypotheses and simplifying assumptions in this research were logical, they did not prove to be true in all circumstances. For example, one hypothesis stated higher levels of stream discharge would result in greater flooding, but this did not occur in all plots. This was the direct result of one of the simplifying assumptions of not accounting for anthropogenic impacts in the model. Increases in discharge were positively correlated with inundation in backwater plots were not influenced by roads, but backwater plots separated from streams by a single lane dirt road underlain with culverts were not significantly correlated with discharge. Temperature, and therefore evapotranspiration, was significantly correlated with flooding only in geomorphic conditions that encouraged the longer-term storage of water. Precipitation was not significantly correlated with flooding in plots strongly affected by discharge, especially in areas able to store larger volumes of water.

The conditionality of these simple, intuitive hypotheses underlines the importance of scale. Although at a broad scale all of these statements are probably true, at a finer scale small variations in landscape position and roads negated even the most basic hypotheses.

Simple water budget models are not constrained by detailed site-specific information and their accuracy will vary not only between sites but also at different scales. Nevertheless it can be concluded that the correlation between inundation and stream discharge, precipitation, and temperature can be greatly improved by dividing floodplain areas into groups based on geomorphology and connectivity, since these factors have a large effect on the movement of water. Although connectivity in this study was related to the presence of a road, connectivity can also be related to distance of the plot from a stream or, more accurately, the distance water travels from the stream to the plot through drainage systems. These divisions can be made using aerial photography or high spatial resolution optical satellite imagery, and categorization may be improved with maps of roads and topography.

Some of the spatial variability in the correlation between flooding and the independent model variables could be attributed to variations in the influence of ground water due to factors such as differences in soils and geomorphology. However, the inclusion of groundwater into the water balance model would significantly increase the complexity of the model and similar studies have found discharge, precipitation, and evapotranspiration are the dominant controls on flooding in most wetland environments (Roberts et al. 2000).

Similar to most models of wetland hydrology, the model described in this study is most helpful to those examining floodplain inundation in similar systems (Cole and Brooks 2000) However, some generalizations can be made to improve the characterization of floodplain hydropattern elsewhere. A large amount of variability in floodplain inundation was explained using readily available information. The grouping of

floodplain areas into backwater and levee areas, as well as road impacted and non-road impacted areas, dramatically raised the predictability of hydropattern. Although human impacted streams are often characterized as "flashy," being subject to more abrupt increases and decreases in water levels, even relatively small anthropogenic modifications between the stream and backwater wetlands can cause a large decrease in the variability of wetland flooding. Further investigation is needed to determine whether the cumulative impact of society is to increase flood variability due to "flashier" stream flow or to decrease variability due to the impact of roads and other barriers and the prevalence of constructed wetlands. Finally, the high spatial resolution (< 1m) elevation data was of limited use for the prediction of inundation in portions of the floodplain extending over a few kilometers, even though the study site was in an area of relatively low topographic variability (the Coastal Plain). Even in the Coastal Plain, elevation must be measured relative to the stream bank, because it is the height of the stream bank relative to the height of the water in the channel that determines whether or not water is allowed to flow into the floodplain. This is complicated in smaller streams, especially when the spatial resolution of topographic information is limited.

3.6 Conclusions

Hydrological studies have been limited by a lack of data (Engman 1996; Cole and Brooks 2000; Price 2005). Many studies have been undertaken to provide that information but most are based on site specific components which are of only marginal benefit at other sites and many have been undertaken at a fine scale (Cole and Brooks 2000). The relationships established through this research, although originally intended to

validate remotely sensed data, could be used to improve the quality of hydrologic models in a wide range of wetland environments and at multiple scales. This is especially true because the independent variables (stream discharge, precipitation, and temperature) that were correlated with inundation are readily available, often on the internet.

Chapter 4: Using C-Band Synthetic Aperture Radar Data to Monitor Forested Wetland Hydrology in Maryland's Coastal Plain

4.1 Introduction

Wetlands in the Chesapeake Bay watershed are important as they help to maintain water quality and aquatic habitat in one of the nation's largest and most productive estuarine ecosystems (Tiner 1987; Chesapeake Bay Program 1998). The U.S. Fish and Wildlife Service (FWS) has determined that this region is at high risk for wetland loss, especially the region's forested wetlands (U.S. Fish and Wildlife Service 2002). Small changes in wetland hydrology can cause large changes in wetland functions and extent (Mitsch and Gosselink 2000). Anthropogenic impacts, long-term cycles of drought and flood, and seasonal patterns of climate and plant physiology work in concert to modify wetland hydrology. Predicted climate change will further affect hydrology in the Mid-Atlantic region, placing an even greater importance on the ability to systematically monitor and assess current wetland hydrology and predict future changes.

Broad-scale forested wetland hydrology has been difficult to study at all temporal frequencies using conventional ground-based and traditional remote sensing methods. Forested wetland hydrology is particularly difficult to assess using more traditional optical imagery (e.g. aerial photography), because cloud cover limits its collection and the presence of foliage precludes viewing of the ground surface (Tiner 1999).

Imaging radars have the unique capability to monitor changes in the status of key hydrologic characteristics of wetlands (e.g., patterns of flooding and variations in soil

moisture) throughout the year and with greater frequency in part due to the ability of SAR to collect images regardless of solar illumination and cloud cover. Most studies have used L-band (~ 24 cm wavelengths) radars to detect hydrology (inundation and soil moisture) below forest canopies. Although L-band data are best for this application (Hess et al. 1995; Wang et al. 1995), C-band data can also be used to detect forested wetland hydrology (Townsend and Walsh 1998). Currently, there are no L-band satellite sensors in operation and the L-band historic record is very limited. On the other hand, there are three C-band satellites currently in operation and C-band data archives date back to 1991.

The goal of this study was to more clearly define the abilities and limitations of spaceborne C-band SAR data for monitoring hydrology in a small riparian wetland, something that has not been done before. To achieve this goal, I established the effects of variations in % inundation and soil moisture, different polarizations (HH and VV), and leaf on versus leaf-off conditions on C-band SAR backscatter. The test site was located along the Patuxent River in Maryland where different levels of inundation and soil moisture were monitored in the field throughout the year.

4.2 Background

4.2.1 Forested Wetlands in the Mid-Atlantic Coastal Plain

The majority of wetlands in the Mid-Atlantic U.S. are forested and most of these are found in the Coastal Plain, including many in floodplains (Tiner and Burke 1996). These wetlands provide many functions that society values, but their existence and functioning is threatened by the alteration of their hydrology (see Chapters 2 and 3).

Changes in Mid-Atlantic climate are anticipated (Mid-Atlantic Regional Assessment Team 2000) that could further alter the water balance in this region's fresh water ecosystems, including wetlands (see Chapter 2). These factors emphasize the need to document current wetland hydrology and develop approaches to forecast future patterns of flooding and soil saturation under modified climate and human modified environmental conditions.

Wetlands are defined by their hydrology (inundation and soil saturation for a certain period of time) which is usually dynamic, with flooding or soil saturation persisting for only a portion of the year. In the Mid-Atlantic region, non-tidal, riparian wetlands follow natural hydrologic patterns at a variety of temporal scales. Seasonal variations in plant and weather-driven evapotranspiration, inter-annual cycles of weather-driven drought and flood, and long-term shifts in climate work to modify wetland hydrology (see Chapter 2). In addition to these temporal variations, riparian wetland hydrology is spatially variable as a result of fluvial geomorphology and soil characteristics. Together these spatial and temporal variations in hydrology create wetland hydropattern - fluctuations in the area, duration, and frequency of wetland flooding and soil saturation. Wetland hydropattern is the single most important factor in the formation and functioning of a wetland and small changes in water regime can cause large changes in wetland location and function (see Chapter 2) (Mitsch and Gosselink 2000).

The relationship between climate and hydropattern at the study site was described in Chapter 3 where patterns of flooding and soil moisture at the site were found to be strongly correlated with stream discharge, precipitation, and evapotranspiration (as indicated by average monthly temperature) and a simple water budget model was

developed to estimate wetland flooding based on those three parameters. High levels of evapotranspiration (brought on by the warm summer months) and normal rainfall were found to lead to reductions in flooding while lower levels of evapotranspiration and above normal precipitation were found to lead to large expanses of flooded forest. The study also showed that a single lane, dirt road lessened the influence of stream discharge on inundation. Finally, this research found that hydropattern could be predicted, fairly accurately, at the moderate, floodplain spatial scale required for the use of SAR data.

4.2.2 Monitoring Forested Wetlands Using C-band SAR

When monitoring hydrology in forested ecosystems, imaging radars have certain advantages over sensors that operate in the visible and infrared portions of the electromagnetic spectrum (see Chapter 2) (Smith 1997). The sensitivity of microwave energy to flooding and soil moisture, and its low attenuation by foliage (e.g., ability to penetrate forest canopies) makes radar ideal for the detection of hydrologic features below moderately dense, deciduous forest canopies (Hall 1996; Kasischke and Bourgeau-Chavez 1997; Rao et al. 1999; Kasischke et al. 2003). Imaging radar systems can also collect data independently of cloud cover and solar illumination (Federal Geographic Data Committee 1992; Kasischke and Bourgeau-Chavez 1997; Kasischke et al. 1997). This is important because the Wetlands Subcommittee of the Federal Geographic Data Committee (Federal Geographic Data Committee 1992) found that the difficulty of acquiring cloud-free imagery during the optimal time period was a key obstacle to mapping wetlands with optical satellite data. In many areas of the US, this optimal period

may only last two to three weeks, between snow/ice melt and the beginning of the leaf-on period.

Although the capability of SAR data for wetlands monitoring is promising, the technology is relatively new compared to optical sensors, and further research is required. L-HH band data have proven to be particularly well suited for monitoring hydrology below the forest canopy (see Chapter 2) (Krohn et al. 1983; Ormsby et al. 1985; Hess et al. 1990; Hess et al. 1995; Pope et al. 1997; Townsend and Walsh 1998). However, no L-band satellite sensors are currently in operation and the historic archive of L-band imagery is limited to the years when JERS was in operation (1992 - 1998).

The ability of C-band SAR data to map flooding under forest canopies was initially thought to be limited (Hess et al. 1995; Wang et al. 1995) but researchers found that although C-HH band radar is not as well suited for forested wetland studies as L-HH SAR, it could be used to map the extent of flooding in temperate and even tropical forests (Townsend and Walsh 1998; Townsend 2000; Costa 2004). C-VV data have primarily been used to study flooding in wetlands dominated by herbaceous vegetation (e.g., Morrissey et al. 1994; Kasischke et al. 2003), but have also been successful in detecting inundation under forest canopies during the leaf-off period (Kasischke et al. 1997; Townsend 2000). The rationale for studying the capability of C-HH and C-VV SAR to monitor forested wetland hydrology comes from the fact that C-band imagery represents the longest continuous historic record of SAR imagery (dating from 1991).

Although SIR-C/X-SAR was the only fully polarimetric SAR to be flown in space, a new earth-orbiting sensor, ENVISAT ASAR, does have dual polarizations, an advancement over prior satellite-borne SARs. The dual polarization ENVISAT SAR data

48

allow for the simultaneous study of both C-HH and C-VV SAR. While past research has documented the potential of C-band SAR for monitoring forested wetland hydroperiod (Townsend and Walsh 1998; Townsend 2000; Costa 2004), further studies are necessary to fully develop this capability, as discussed below.

4.2.3 Limitations on Using SAR Data to Monitor Wetland Hydrology

Like any remote sensing system, C-band SARs do have limitations. The limitations of C-band SAR data for the monitoring of hydrology under forest canopies include the limited transmittance (penetration) of microwave energy through the canopy as governed by the combination of plant structure and microwave wavelength/polarization. These limitations can be explained using a simple model of microwave backscatter coefficient, which also clarifies why the *in situ* measurements gathered in this study were needed to interpret the total backscatter coefficient received at the sensor. This model can be used to understand what happens to the transmitted microwave energy as it is attenuated and reflected from different elements that comprise the scattering surface, resulting in the microwave energy that is eventually detected by the imaging radar. With this model, forests can be conceptualized as having three layers: The canopy layer, the trunk layer and the ground layer (Kasischke and Bourgeau-Chavez 1997; Townsend 2002), with the total backscatter coefficient from a forest (σ^o) being:

$$\sigma^o = \sigma^o_c + \tau^2_c \, \tau^2_t \, (\sigma^o_t + \sigma^o_s + \sigma^o_d + \sigma^o_m)$$

where

σ^o_c = backscatter coefficient of the crown layer of branches and foliage,

τ_c = transmissivity of the crown layer,

τ_t = transmissivity of the trunk layer,

σ^o_t = backscatter coefficient from the trunk layer,

σ^o_s = backscatter coefficient from the surface layer,

σ^o_d = double-bounce between the trunks and the surface layers, and

σ^o_m = multi-path scattering between the ground and canopy layers.

Due to the size (usually 5 - 6 cm) of the microwave wavelength in relation to smaller woody branches and foliage found in forests, C-band SAR backscatter coefficient is most influenced by scattering caused by the crown layer (σ^o_c). The size of individual structures (leaves and branches), the orientation of those structures, and total volume of material in the canopy combine with microwave wavelength to determine the degree to which SAR can penetrate forest canopies. Thus, backscatter coefficient from and transmission (τ_c) by the canopy will be related to the amount of canopy foliage, which in turn, is related to tree type, tree size, and stand density. Because most forested wetlands in the Coastal Plain of Maryland are dominated by deciduous tree species, seasonal variations in canopy closure will also affect canopy scattering and transmission (Wang et al. 1995). Although the orientation, size, and shape of leaves can affect scattering and transmissivity of the canopy layer, these factors were assumed to be constant for this study as all plots were selected in areas of broad-leaved, deciduous forest that had similar canopy structure.

The polarization of the transmitted electromagnetic energy also affects microwave transmission through the forest. Microwave energy that is both vertically transmitted and received (VV) does not pass as readily through forests as compared to horizontally transmitted and received (HH) microwave energy because vertically oriented structures (such as tree trunks) interact more with vertically polarized energy. Tree trunks decrease transmissivity (τ_t) by increasing attenuation and scattering at the trunk layer. For this reason, HH polarized microwave energy is better able to pass through the trunk layer and interact with the ground surface, where hydrologic conditions, such as inundation and soil moisture, affect scattering and reflection (Hess et al. 1995; Wang et al. 1995). It is important to understand the varying limitations of VV and HH polarized data because the data available with these polarizations differ in start and end dates and availability. The combination of ERS-1 (launched in July 1991), ERS-2 (launched in April 1995), and the newly launched ENVISAT (launched in March 2002) provide 15 years of continuous C-VV coverage while RADARSAT (launched in November 1995) and ENVISAT provide ten years of C-HH imagery. Even if the ERS/ENVISAT C-VV data are of limited utility during the growing season, they would still be useful for studies of fall/winter hydrological conditions (when leaf-off conditions increase canopy transmission), which may help to understand longer-term hydrologic patterns.

After the microwave energy is transmitted through the canopy and trunk layers, it can interact with the surface layer. In flooded forests, double-bounce and multi-path scattering can have large effects on backscatter coefficient assuming the transmissivity of the crown and trunk layers are high enough. Flooding under the forest canopy will greatly increase double-bounce and multi-path scattering (σ^o_d and σ^o_m, respectively), as well as

eliminate surface scattering. Because of the high intensity backscatter that flooding

causes, inundated forests are depicted as being very bright on radar images. With non-

flooded forests, while increases in soil moisture should increase the surface backscatter

coefficient (σ^o_s) and likely result in small increases in double-bounce and multi-path

scattering, the increases would not be as large compared to flooded forest backscatter.

For a more detailed explanation of microwave scattering from vegetated surfaces see

Dobson et al. (1995), Wang et al. (1995), and Kasischke et al. (2003).

4.3 Methods

This study analyzed the use of C-HH and C-VV SAR data collected by ENVISAT

ASAR to detect varying levels of flooding and soil moisture during the leaf-off and the

leaf-on seasons. I hypothesized that increases in flooding would result in higher

backscatter coefficient, and that in the non-flooded areas, increases in soil moisture

would result in higher backscatter coefficient. In addition, I hypothesized that these basic

relationships would be modified by differences in season (leaf-on and leaf-off) and

polarization (HH and VV) of the microwave energy. Differences in backscatter

coefficients between areas of varying inundation and soil moisture were expected to be

most pronounced during the leaf-off period when imaged by C-HH polarized SAR.

Statistical analyses [ANOVA and Tukey's studentized range (HSD)] were used to test the

hypothesis that backscatter coefficients collected during different seasons and from sites

of varying inundation and soil moisture (backwater, levee, and upland forests) varied

significantly. Regression analyses were then used to analyze the relationship between

backscatter coefficient and inundation, soil moisture, and other *in situ* measurements that could influence backscatter.

To evaluate the ability of the SAR data to monitor hydrology, field data were collected in backwater, levee, and upland plots from spring of 2003 through winter of 2004. Percent area flooded and soil moisture data were collected because they have been shown to influence radar backscatter in previous studies (see section 4.2.3). Stand density and canopy closure (relative leaf density) measurements were collected to establish the conditions under which C-VV and C-HH SAR data can be used to monitor flooding and because they have also been shown to influence backscatter (see section 4.2.3).

4.3.1 Study Area

The study area was located at the Patuxent Wildlife Research Center (PWRC), within Maryland's Coastal Plain Physiographic Province (see Chapter 3), focusing on upland and wetland areas surrounding the 182 km long Patuxent River. Within the boundaries of the PWRC, the Paxtuxent River floodplain varies from 0.40 to 0.81 km in width and is bordered by areas of upland terrace (Hotchkiss and Stewart 1979). There are levees adjacent to each side of the braided river channel that gradually decrease in elevation into backwater areas towards the uplands on either side of the floodplain. While most of the Patuxent River floodplain is inundated for only part of the year, some backwater areas remain flooded for much of the year. The timing of inundation is controlled by annual variations in evapotranspiration, precipitation, and the amount of water coming from upstream dams (see Chapter 3).

I established 24 plots (200 by 200 m, 4 ha) in the PWRC for measurement of surface characteristics and variations in SAR backscatter coefficient. Eight plots each were located in upland, backwater, and levee forests. The plots were placed in areas of relatively homogeneous forest and expected hydrology (see Chapter 3).

4.3.2 Field Measurements

Hydrologic data (inundation and soil moisture) were collected approximately once per month from April of 2003 through December of 2004. Inundation was visually estimated in each plot (see Chapter 3). Upon reviewing the results, it was found that one of the levee sites (L1) was wetter than anticipated and this site was reclassified as a backwater site. Soil moisture (volumetric water content) was measured at eight locations distributed evenly within each plot using a time-domain reflectometer (Hydrosense ® meter, Campbell Scientific, Inc.) with an accuracy of +/- 3% volumetric water content. Five measurements were taken at each of the 8 locations, one at the center and one at a random distance in each of the four cardinal directions. These 40 measurements from each plot were then averaged for comparison with the SAR data.

Forest structure was measured to help explain variations in backscatter coefficient between plots. Relative basal area (a combination of tree diameter and density) of the canopy trees was collected from each plot using a 2 factor prism and the Bitterlich method (Shiver and Borders 1996). Basal area was observed at 9 areas, spread evenly throughout each plot, and then averaged. Percent canopy cover was measured at multiple times throughout the year (more frequently during the spring and fall) using digital hemispherical photos of the canopy (see Figure 6.1). These measurements were collected

54

at 2 backwater, 2 levee, and 2 upland sites. Photographs were taken at eight locations, spread evenly throughout each plot. Photos were standardized by tripod height and orientation, and analyzed with HemiView software (Vieglais and Rich 1997). Tree height, derived by the Vegetation Canopy Lidar (VCL) Science Team using data from the Laser Vegetation Imaging Sensor (LVIS) collected in October of 1999, was also used in the analysis (Blair et al. 1999). The LVIS data have a horizontal spatial resolution of 25 m, a vertical resolution of ~ 30 cm, and a geo-locational accuracy that is usually < 1 m (Dubayah et al. 2000; Drake et al. 2002).

4.3.3 Synthetic Aperture Radar Data

ENVISAT ASAR (C-HH and C-VV; average incidence angle of ~23°) data were obtained from the European Space Agency (ESA). The ascending and descending ASAR images were acquired approximately once per month from July 2003 to November 2004 (Table 4.1). The ASAR data were delivered in precision image (PRI) format and were multi-looked, calibrated (corrected for antenna elevation gain and range spreading loss), and geocoded (geolocated and resampled to map projection) by ESA. Multi-looking is done in the early stages of SAR data processing and involves the averaging of different sub-images. It is one way to reduce speckle (or the salt and pepper appearance of most SAR imagery) at the expense of spatial resolution (Raney 1998). The georegisteration was later modified in the image headers to ensure spatial agreement among the data. This was necessary because although the data were geocoded, this information was not accurate at the spatial resolution needed for this study. The SAR image intensity values

Orbit	Date
Ascending	7/15/2003
Descending	10/2/2003
Ascending	10/28/2003
Ascending	12/2/2003
Descending	3/25/2004
Ascending	4/20/2004
Descending	4/29/2004
Ascending	5/25/2004
Descending	6/3/2004
Ascending	6/29/2004
Descending	7/8/2004
Ascending	10/12/2004
Descending	10/21/2004
Descending	11/25/2004

Table 4.1: Orbits and dates for all of the ENVISAT ASAR acquisitions used in the analysis.

extracted from all test sites were converted to dB (see Chapter 2) and averaged within

each ground data collection plot. Each 4 ha ground data collection plot represents over

100 independent samples of backscatter coefficient. Therefore each value of average plot

backscatter coefficient has a total uncertainty of 1.0 dB, 0.5 dB from ASAR absolute

calibration error (European Space Agency ASAR Science Team 2004) and 0.5 from

image fading error (Ulaby et al. 1982).

4.3.4 Analysis Procedures

The statistical analyses were conducted using SAS 9.0 (SAS Institute, Inc). All

regression models were considered significant at the 0.05 level (alpha = 0.05) and a 0.15

level was used as the criterion for inclusion into all stepwise regression models.

Differences in basal area, canopy height, percent area inundated, and soil moisture

between the backwater, levee, and upland plots were analyzed using an analysis of

variance (ANOVA) and a Tukey's studentized range test (HSD).

Variations in backscatter coefficients (C-HH and C-VV) between different plot locations (backwater, levee, and upland) were analyzed as a function of time of data collection (leaf-off versus leaf-on conditions). A 3-way ANOVA was used to test the hypothesis that there were significant differences in C-HH and C-VV backscatter coefficient between plot types during leaf-off and leaf-on seasons and a Tukey's studentized range (HSD) test was used to compare least square means of C-HH and C-VV backscatter coefficients between backwater, levee, and upland plots during different seasons.

Variation in backscatter coefficients (C-HH and C-VV) between backwater, levee, and upland plots without flooding was examined during the leaf-on season using a 2-way ANOVA to isolate the influence of soil moisture on backscatter coefficient and to test the hypothesis that soil moisture causes significant variations in backscatter coefficient between plot types. A Tukey's studentized range (HSD) test was used to compare least square means of C-HH and C-VV backscatter coefficients between backwater, levee, and upland plots without flooding during the leaf-on period. This analysis was limited to leaf-on data since no backwater or levee plots were without inundation during the leaf-off period.

Sources of backscatter coefficient variation between plot locations (backwater and levee) were explored using linear regression analysis. First, simple linear regression was used to examine the relationship between C-HH and C-VV backscatter coefficients and inundation in backwater and levee plots during leaf-off and leaf-on seasons. A stepwise, multiple linear regression approach was then used to test the hypothesis that variations in inundation and tree stand characteristics influence backscatter coefficient and to analyze

differences in this relationship as a function of season and polarization in backwater and levee plots. C-HH and C-VV backscatter coefficients were regressed against inundation, canopy closure, basal area, and canopy height.

The relationship of C-HH and C-VV backscatter coefficients to soil moisture was examined separately from the analyses including inundation because the two variables were found to be closely related (e.g., areas with higher levels of inundation often have higher soil moisture). This analysis was designed to test the hypothesis that variations in soil moisture influence radar backscatter. First, backscatter coefficients were averaged within the backwater, levee, and upland plots when no flooding was present. To equalize ground conditions between backwater and levee sites with 0 percent flooding and upland sites which always have 0 percent flooding, only the upland backscatter coefficients from days in which most backwater and levee sites had 0 percent flooding were used in the analysis. Stepwise multiple linear regression was then used to test the hypothesis that variations in soil moisture, canopy closure, basal area, and canopy height influence backscatter coefficient and to analyze the difference in these relationships as a function of polarization and season. A similar set of regressions were run on the same data set using inundation instead of soil moisture for comparison with the first analysis (backscatter coefficient regressed against soil moisture, canopy closure, basal area, and canopy height during the entire year, leaf-off and leaf-on seasons for C-HH and C-VV data). Note that this data set did not include as many samples as the first regression using only inundation data since soil moisture data were not collected as many times as inundation data.

Finally, simple linear regression was used to examine the relationship between C-HH and C-VV backscatter coefficients and hydrology (inundation and soil moisture) in

the backwater, levee, and upland plots during the leaf-off and leaf-on seasons. Backscatter coefficients were regressed against inundation. By including the upland sites (with much lower soil moisture) in this analysis the influence of soil moisture could be more fully examined.

4.4 Results

There were significant differences in average basal area (ANOVA, $F = 6.4$, $p < 0.007$) and height (ANOVA, $F = 5.1$, $p < 0.02$) between the backwater, levee, and upland plots, with trees in upland plots being slightly shorter and having a lower basal area than those in levee or backwater plots (Table 4.2). As expected, average inundation was significantly different between the three plot locations (ANOVA, $F = 55.0$, $p < 0.0001$). Soil moisture was also found to vary significantly between plot locations (ANOVA, $F = 34.6$, $p < 0.0001$).

	Plot Location		
	Backwater	**Levee**	**Upland**
Inundation (%)	26.6	9.5	0
Soil Moisture (%)	59	47	24
Basal Area (m2 ha -1)	38.0 a	37.1 a	31.8
Canopy Height	27.5 bc	28.1 b	25.8 c

Table 4.2: Summary of average inundation, basal area, and tree height as a function of plot location. The letters denote those groups where significant differences were not found between plot locations (Tukey's studentized range [HSD] test, $p < 0.05$).

Overall, the 3-way ANOVA model including polarization, season (leaf-on and leaf-off), and plot location (backwater, levee, and upland) was found to be significant (ANOVA, $F = 107.2$, $p < 0.0001$), explaining 66% of the variability in backscatter coefficient ($r^2 = 0.66$). Significant differences between backscatter coefficients were

found between the two polarizations – HH and VV (ANOVA, F = 28.0, $p < 0.0001$),

backwater, levee, and upland plots (ANOVA, F = 166.4, $p < 0.0001$) and the different

seasons (ANOVA, C-HH F = 650.2, $p < 0.0001$). Significant interaction factors were

found between polarization and season (ANOVA, F = 54.0, $p < 0.0001$), polarization and

plot location (ANOVA, F = 13.3, $p < 0.0001$), and season and plot location (ANOVA, F

= 6.4, $p = 0.0018$). Significant differences were also found when comparing the least

square means of backscatter coefficients between different polarizations, seasons, and

plot types (Table 4.3). Significant differences in the least square means of the C-HH

backscatter coefficients were found between all plot locations during the leaf-off season.

Significant differences between the least square means of C-HH backscatter coefficients

during the leaf-on period and C-VV backscatter coefficient during the entire year were

found between the upland and the backwater or levee plots but not between the backwater

and the levee plots. Backscatter coefficients were generally higher during the leaf-off

season with greater differences in C-HH backscatter coefficients between plot locations

as opposed to the C-VV backscatter coefficients (Figure 4.1).

Overall, the 2-way ANOVA model including polarization and plot location

(backwater, levee, and upland) and examining backscatter coefficients in the non-

inundated plots during the leaf-on period was found to be significant (ANOVA, F = 23.6,

$p < 0.0001$). The 2-way ANOVA model explained 55% of the variability in backscatter

coefficient ($r^2 = 0.55$). Significant differences in backscatter coefficient were found

between the two polarizations – HH and VV (ANOVA, F = 71.5, $p < 0.0001$) and

backwater, levee, and upland sites (ANOVA, F = 22.9, $p < 0.0001$). The interaction

factor between polarization and plot type was found to not be significant (ANOVA,

Polarization	Season	Plot Location	Mean
HH	off	B	-4.93
HH	off	L	-5.78 ab
HH	off	U	-7.26 cdef
HH	on	B	-7.66 cgm
HH	on	L	-7.99 gh
HH	on	U	-9.06
VV	off	B	-5.61 bi
VV	off	L	-6.02 ai
VV	off	U	-6.76 djk
VV	on	B	-7.00 fkl
VV	on	L	-7.18 ejl
VV	on	U	-7.93 hm

Table 4.3: Summary of average C-HH and C-VV backscatter coefficients in the different plot locations (B=backwater, L=levee, and U=upland) during the leaf-off and the leaf-on seasons. The letters denote where significant differences were not found between plot locations (Tukey's studentized range [HSD] test, $p < 0.05$).
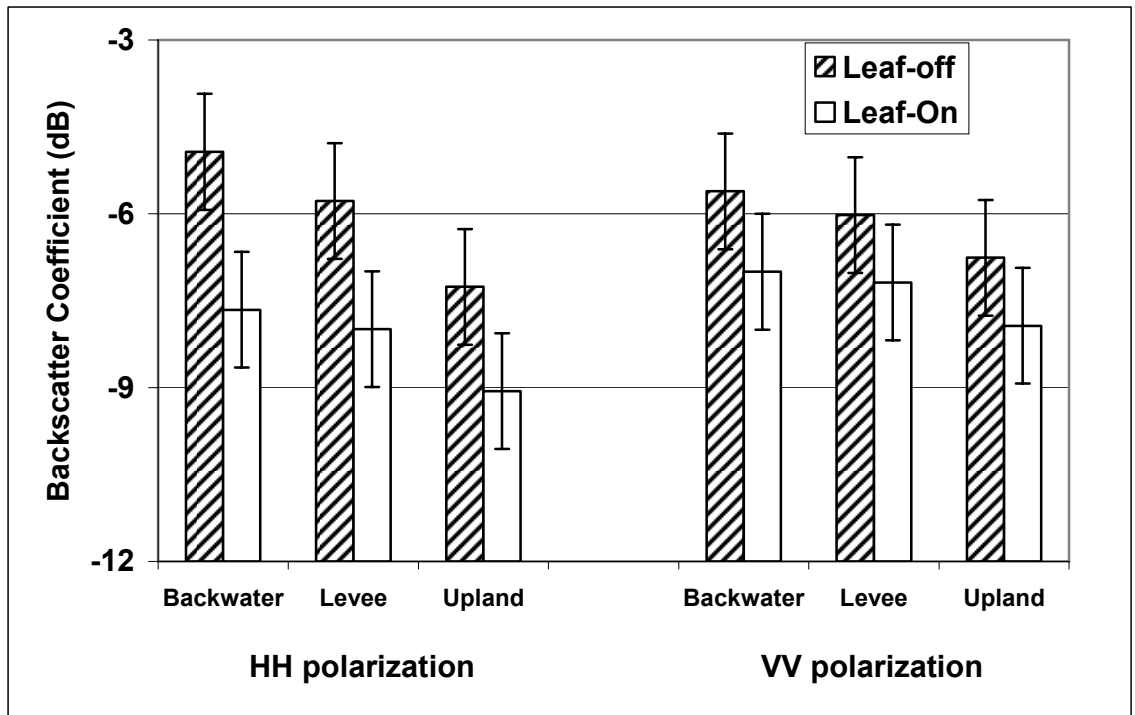
Figure 4.1: Mean C-HH and C-VV backscatter coefficients for backwater, levee and upland plots during the leaf-off and leaf-on seasons. Error bars depict total uncertainty based on radar fading and absolute calibration errors.

F = 0.2, *p = 0.8631*). Significant differences were found when comparing least square

means of backscatter coefficients between different polarizations and between upland and

backwater or levee plots but not between backwater and levee plots (Tukey's studentized

range [HSD] test, *p < 0.1132*, Table 4.4). C-VV backscatter coefficients were higher than

C-HH backscatter coefficients in the respective plot locations although there was a

slightly greater difference in C-HH backscatter coefficients between the backwater and

upland plots (C-HH = 1.04, C-VV = 0.88) (Figure 4.2). The relationship between these

differences in backscatter coefficient and *in situ* measurements was later examined using

linear regression.

Polarization	Season	Plot Location	Mean
HH	on	B	-8.06ac
HH	on	L	-8.39ab
HH	on	U	-9.1
VV	on	B	-7.11d
VV	on	L	-7.38d
VV	on	U	-7.99bc

Table 4.4: Summary of average C-HH and C-VV backscatter coefficients in the different plot locations (B=backwater, L=levee, and U=upland) during the leaf-on season (when plots were not flooded). The letters denote those groups where significant differences between plot types were not found (Tukey's studentized range [HSD] test, *p < 0.05*).

A positive linear relationship existed between inundation and backscatter

coefficient (Figures 4.3 and 4.4). The regression equation of C-HH radar backscatter

coefficient as function of inundation shows that during the leaf–off period, there was a

2.5 dB increase in backscatter coefficient as inundation increased from 0 to ~ 60%.

During the leaf-on season there was a ~ 1.5 dB increase in backscatter coefficient with

plots ranging from 0 to ~ 50% inundation. The regression equation of C-VV radar

backscatter coefficient as function of inundation shows that during the leaf–off period,
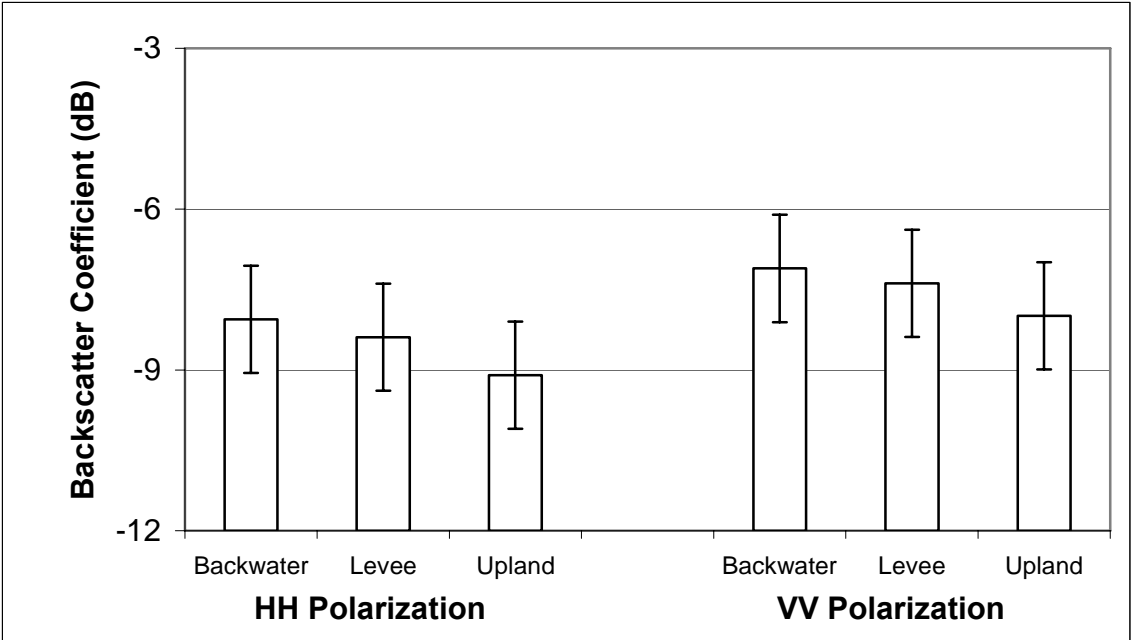
Figure 4.2: Mean C-HH and C-VV backscatter coefficients for backwater, levee and upland plots without flooding during the leaf-on season. Error bars depict total uncertainty based on radar fading and absolute calibration errors.
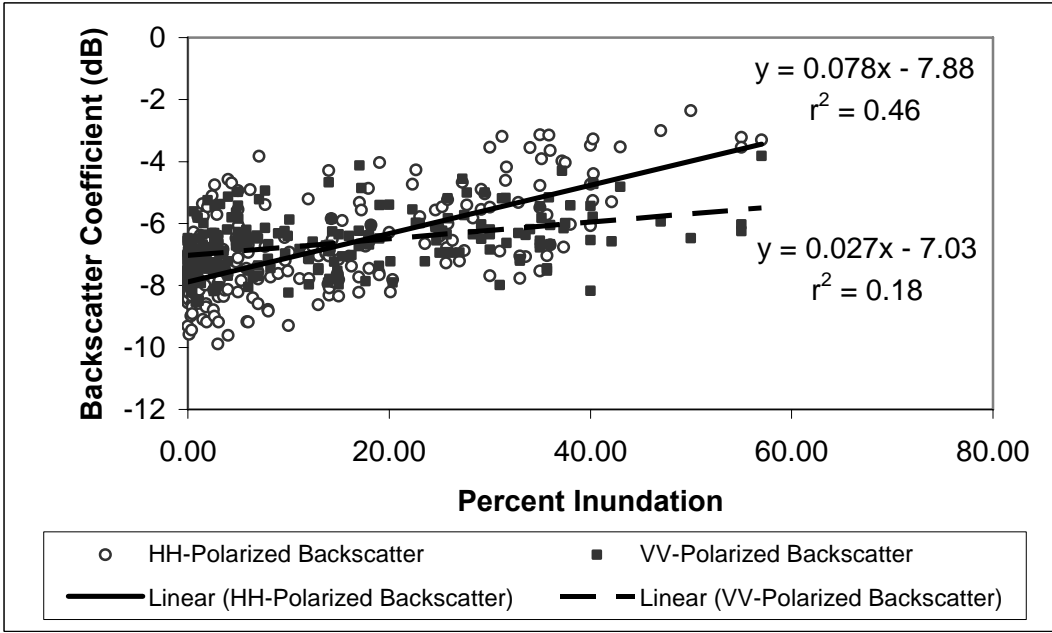
Figure 4.3: Regression of C-HH and C-VV backscatter coefficients in the backwater and levee plots against percent area inundated during all times of the year. Top equation and r^2 value corresponds to C-HH backscatter coefficient and the lower one with C-VV (significant at the < 0.0001 level). Total uncertainty in both data sets is 1 dB.
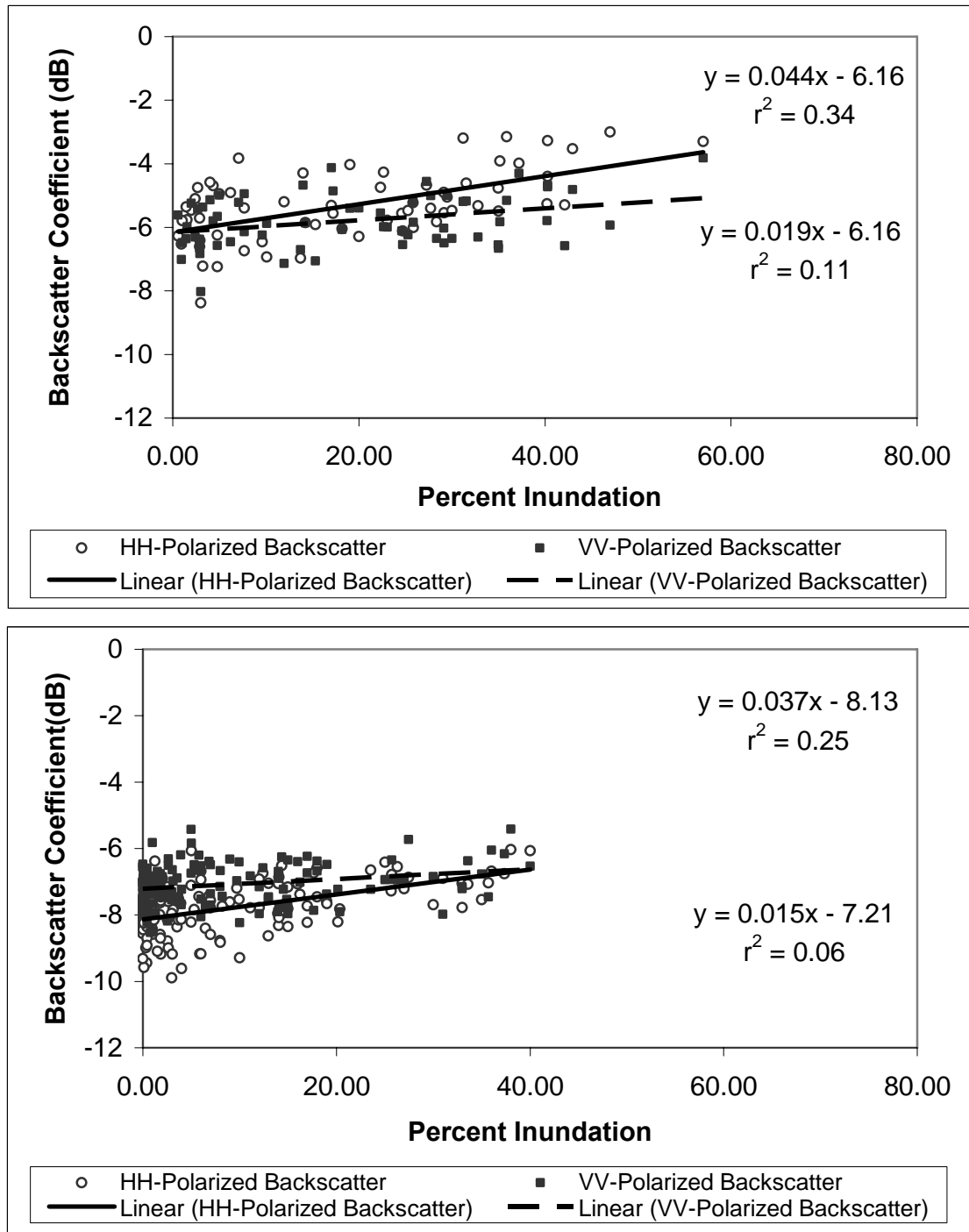
Figure 4.4: Regressions of C-HH and C-VV backscatter coefficients in backwater and levee plots against percent area inundated during leaf-off (top) and leaf-on (bottom) seasons. Top equation and r^2 values within both charts correspond with C-HH backscatter coefficient and the bottom with C-VV. All C-HH correlations are significant at the < 0.0001 level while C-VV correlations are significant at the 0.0024 level during the leaf-on season and the 0.0071 level during the leaf-off season. Total uncertainty in both data sets is 1 dB.

there was a ~1.0 dB increase in backscatter coefficient as inundation increased from 0% to ~ 60% and during the leaf-on season, this increase in backscatter coefficient was reduced to ~ 0.75 dB with plots ranging from 0 to ~ 50% inundation.

Over the entire year, the stepwise multiple linear regression between backscatter coefficient (C-HH and C-VV) and area inundated, canopy closure, basal area, and canopy height showed degree of canopy closure explained most variation in both polarizations, followed inundation and then tree height (Table 4.5). During the entire year, the influence of canopy closure, inundation, and canopy height explained 69% of variation in C-HH backscatter coefficient, but only 40% of variation in C-VV backscatter coefficient. Inundation and canopy height were positively correlated with backscatter coefficient while canopy closure was either positively or negatively correlated. Basal area was not significantly correlated with backscatter coefficient and was excluded from all regression models. Inundation explained a larger percent of variation in C-HH backscatter coefficient, as compared to C-VV. Total explanation of variation in radar backscatter coefficient was greater during the leaf-off as compared to the leaf-on period (Table 4.5).

On average, 70% of the variability in soil moisture was explained by inundation during the leaf-off period while 50% was explained during the leaf-on season ($p < 0.0001$). When areas without flooding were examined, C-HH and C-VV backscatter coefficients were found to be highest in backwater plots followed by levee and then upland plots. C-HH backscatter coefficients were -8.01, -8.39, and -9.10 and C-VV backscatter coefficients were -7.11, -7.38, and -8.00 for backwater, levee, and upland plots respectively. All of these values were collected during the drier, leaf-on season. Soil moisture was found to be significantly related to C-HH and C-VV backscatter

65

		Season and Polarization					
		Both HH	Both VV	Lf-Off HH	Lf-Off VV	Lf-On HH	Lf-On VV
All Variables	N	122	122	64	64	142	142
	r^2	0.69	0.40	0.34	0.39	0.27	0.11
	F	164	49	32	20	26	8
	p	<.0001	<.0001	<.0001	<.0001	<.0001	0.0004
Inundation	Prt r^2	0.22	0.06	0.34	0.10	0.25	0.06
	F	154.41	19.81	31.69	10.18	46.97	9.57
	p	<.0001	<.0001	<.0001	0.0022	<.0001	0.0024
	SE	0.005	0.004	0.008	0.006	0.005	0.005
	Coef	0.06	0.02	0.04	0.02	0.04	0.02
Canopy Closure	Prt r^2	0.47	0.34	-----	0.29	0.02	-----
	F	195	111	-----	25	4	-----
	p	<.0001	<.0001	-----	<.0001	0.0546	-----
	SE	0.477	0.367	-----	1.634	2.740	-----
	Coef	6.04	3.22	-----	-8.64	-5.31	-----
Canopy Height	Prt r^2	0.004	0.01	-----	-----	-----	0.04
	F	3	4	-----	-----	-----	6
	p	0.087	0.0377	-----	-----	-----	0.0127
	SE	0.040	0.031	-----	-----	-----	0.032
	Coef	0.07	0.06	-----	-----	-----	0.08

Table 4.5: Results from stepwise multiple linear regression using backscatter coefficient as the dependent variable and average percent area inundated, forest canopy closure, and canopy height as the independent variables. Although basal area was used as an input (independent variable), it was not significantly correlated with backscatter coefficient and it was therefore removed from the model. Analyses were conducted with HH and VV polarized C-band SAR data during the entire year (both), the leaf-off (lf-off), and leaf-on (lf-on) seasons. Dashes signify variables that were excluded from the model because they were not significant at the 0.15 level.

coefficients at all times of the year (Table 4.6), explaining more of the variability than

canopy closure, canopy height, or basal area. C-HH backscatter coefficients were better

correlated with soil moisture than C-VV backscatter coefficients. C-HH backscatter

coefficients were better correlated with soil moisture during the leaf-off season while C-

VV backscatter coefficients were better correlated with soil moisture during the leaf-on

season. Although inundation was better correlated to C-HH backscatter coefficients than

soil moisture over the entire year, soil moisture was better correlated to backscatter

coefficients at all other times and polarizations (Tables 4.6 and 4.7).

		Season and Polarization					
		Both HH	Both VV	Lf-Off HH	Lf-Off VV	Lf-On HH	Lf-On VV
All Variables	N	144	144	48	48	88	88
	r^2	0.67	0.46	0.73	0.51	0.55	0.39
	F	97	30	39	24	105	27
	p	<.0001	<.0001	<.0001	<.0001	<.0001	<.0001
Soil Moisture	Prt r^2	0.37	0.25	0.58	0.24	0.55	0.36
	F	84	48	64	15	105	48
	p	<.0001	<.0001	<.0001	0.0004	<.0001	<.0001
	SE	0.0053	0.0048	0.0079	0.0069	0.0046	0.0047
	Coef	0.051	0.024	0.059	0.038	0.047	0.026
Canopy Closure	Prt r^2	0.30	0.18	0.10	0.27	----	----
	F	126	45	15	25	----	----
	p	<.0001	<.0001	0.0004	<.0001	----	----
	SE	0.6042	0.5250	1.9873	1.9984	----	----
	Coef	6.863	3.680	-7.324	-9.989	----	----
Basal Area	Prt r^2	0.01	0.01	0.04	----	----	----
	F	3	3	7	----	----	----
	p	0.0763	0.1124	0.0112	----	----	----
	SE	0.0170	0.0156	0.0298	----	----	----
	Coef	0.030	0.025	0.079	----	----	----
Canopy Height	Prt r^2	----	0.02	----	----	----	0.03
	F	----	5	----	----	----	4
	p	----	0.0253	----	----	----	0.0401
	SE	----	0.0532	----	----	----	0.0511
	Coef	----	0.025	----	----	----	0.106

Table 4.6: Results from a stepwise multiple linear regression using backscatter coefficient as the dependent variable and average soil moisture, forest canopy closure, tree basal area, and canopy height as the independent variables. Analyses were conducted with HH and VV polarized C-band SAR data during the entire year (both), the leaf-off (lf-off), and leaf-on (lf-on) seasons. Dashes signify variables that were excluded from the model because they were not significant at the 0.15 level. Only a portion of the field plot sites and imagery dates were used in this analysis because soil moisture was not collected as frequently as inundation. However, the inundation analysis in table 4.7 used the same reduced data set that was used for this soil moisture analysis so they can be directly compared.

A positive linear relationship existed between hydrology, as indicated by inundation, and backscatter coefficient (Figure 4.5). Including upland plots in the analysis and thus increasing the influence of soil moisture (due to the relatively low soil moisture of upland plots) raised the correlation between backscatter coefficient and hydrology, as indicated by inundation. The regression equation of C-HH radar backscatter coefficient as

		Season and Polarization					
		Both HH	Both VV	Lf-Off HH	Lf-Off VV	Lf-On HH	Lf-On VV
All Variables	N	144	144	48	48	88	99
	r^2	0.69	0.47	0.65	0.48	0.49	0.35
	F	79	30	20	10	27	23
	p	<.0001	<.0001	<.0001	<.0001	<.0001	<.0001
Inundation	Prt r^2	0.42	0.23	0.50	0.21	0.39	0.19
	F	101	42	46	12	54	20
	p	<.0001	<.0001	<.0001	0.001	<.0001	<.0001
	SE	0.006	0.005	0.009	0.008	0.008	0.007
	Coef	0.062	0.028	0.047	0.022	0.058	0.034
Canopy Closure	Prt r^2	0.23	0.15	0.03	0.18	----	----
	F	92	33	3	13	----	----
	p	<.0001	<.0001	0.0797	0.0008	----	----
	SE	0.599	0.531	2.238	2.086	----	----
	Coef	6.259	3.418	-4.270	-8.022	----	----
Basal Area	Prt r^2	0.01	0.01	0.10	0.03	0.02	----
	F	5	3	11	2	3	----
	p	0.0293	0.0693	0.0015	0.0324	0.1142	----
	SE	0.017	0.015	0.035	0.033	0.017	----
	Coef	0.038	0.028	0.094	0.049	0.027	----
Canopy Height	Prt r^2	0.04	0.08	0.02	0.06	0.09	0.16
	F	16	20	3	5	15	22
	p	0.0001	<.0001	0.1057	0.0324	0.0002	<.0001
	SE	0.057	0.051	0.099	0.093	0.060	0.048
	Coef	0.155	0.169	0.164	0.144	0.164	0.223

Table 4.7: Results from a stepwise multiple linear regression using backscatter coefficient as the dependent variable and average percent inundation, canopy closure, tree basal area, and canopy height as the independent variables. Analyses were conducted with HH and VV polarized C-band data during the entire year (both), the leaf-off (lf-off), and leaf-on (lf-on) seasons. Dashes signify variables that were excluded from the model because they were not significant at the 0.15 level. Only a portion of the field plot sites and imagery dates were used in this analysis (see Table 4.6).

a function of inundation shows that during the leaf–off period there was a ~ 4.0 dB increase in backscatter coefficient intensity as inundation increased from 0 to ~ 60% and a ~ 2.5 dB increase in backscatter coefficient during the leaf-on season as inundation increased from 0 to 50 percent. The regression equation of C-VV radar backscatter coefficient as a function of inundation shows that during the leaf–off period there was a ~ 2.0 dB increase in backscatter coefficient and a ~ 1.0 dB increase in backscatter coefficient during the leaf-on season as inundation increased from 0 to 50%.
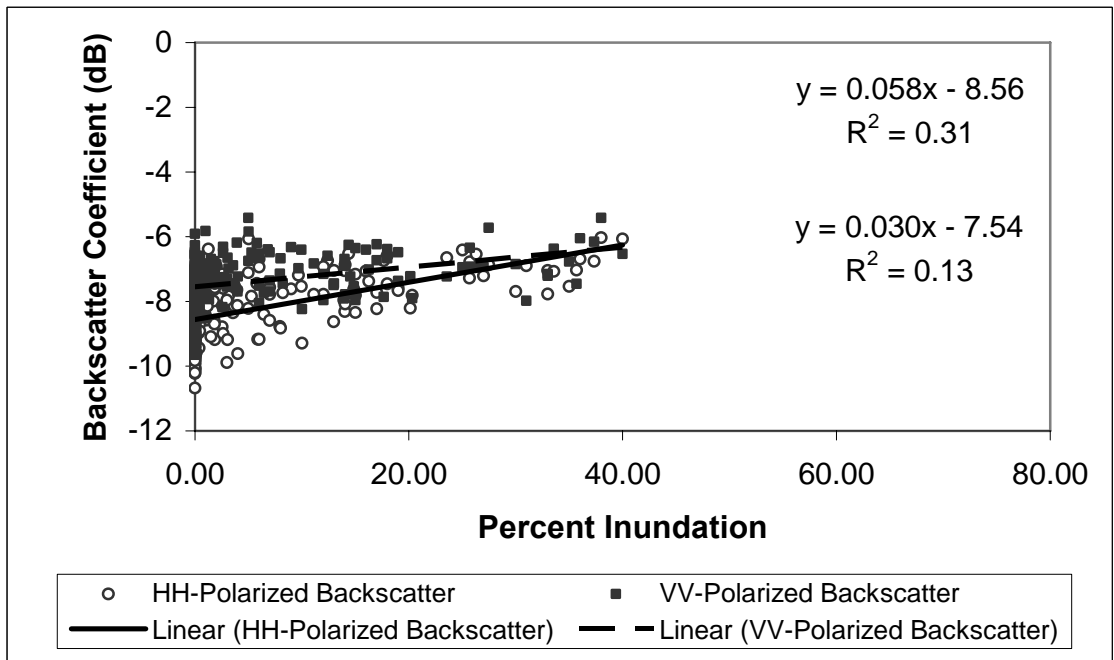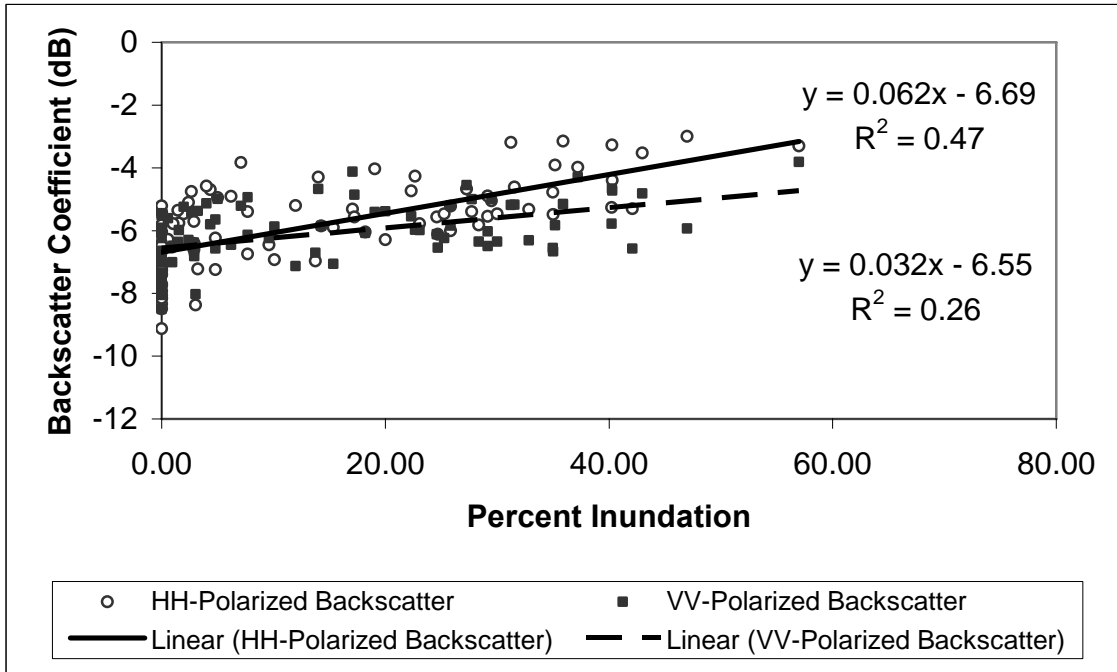
Figure 4.5: Regressions of C-HH and C-VV backscatter coefficients in the backwater, levee, and upland plots against percent area inundated during the leaf-off (top) and leaf-on (bottom) seasons. Top equation and r^2 values within both charts correspond with C-HH backscatter coefficients and the bottom with C-VV. All are significant at the < 0.0001 level.

4.5 Discussion

Significant differences in inundation and soil moisture support the hypothesis that variation in hydrology between sites resulted in differences in backscatter coefficient between backwater, levee, and upland plots. The results support the hypothesis that both polarizations of SAR backscatter coefficient are significantly different between wetlands (backwater and levee) and uplands during all times of the year.

Polarization (C-HH and C-VV), season (leaf-on and leaf-off), and plot location (backwater, levee, and upland) explain the majority of the variation in ASAR backscatter coefficients when all plot types and times of the year are considered. The significant interaction between polarization and season is most likely due to the larger increase in C-HH backscatter coefficients (as compared to C-VV) during the leaf-off season as compared to the leaf-on season. This may have partly been due to the lower attenuation of C-HH (relative to C-VV) microwave energy as it passed through the trunk layer, leaving more C-HH energy to interact with higher levels of soil moisture and/or inundation often present during the leaf-off season. The significant interaction between polarization and plot location may be due to greater differences in C-HH backscatter coefficients between different plot locations as compared to C-VV energy. This again, may have been caused by lower attenuation of C-HH microwave energy (compared to C-VV) as it passed through the trunk layer leaving more energy to be scattered at the ground layer. The significant interaction between season and plot location was likely a product of decreased attenuation of C-band microwave energy in the canopy layer during the leaf-off season (as compared to the leaf-on) resulting in increased transmittance of energy to the ground layer. At the ground layer, the presence of inundation and, to a

lesser degree, higher levels of soil moisture (often present during the leaf-off season when evapotranspiration is lower) can increase surface, multi-, and double-bounce backscattering. In this way, total backscatter coefficient is increased, as well as the difference in backscatter coefficients between plot locations due to varying amounts of inundation and levels of soil moisture.

Stepwise multiple linear regressions using hydrology and tree stand characteristics were used to further explore variations observed between backscatter coefficient measurements at different plot locations (Table 4.5 – 4.7). As expected, C-HH SAR backscatter coefficients were better correlated to inundation than C-VV SAR backscatter coefficients, and correlations between backscatter coefficient and inundation were stronger during the leaf-off season. Not surprisingly, canopy closure is better correlated to C-HH and C-VV backscatter coefficients when the entire year is considered.

Given a total uncertainty of 1 db for the ASAR data, the ~ 2.5 dB range in C-HH backscatter coefficients between 0 and less than 60 % inundation should allow for monitoring of percent inundation under forest canopies during the leaf-off period. Correlation between C-HH backscatter coefficient and inundation during the leaf-on period resulting in a ~ 1.5 dB variation in backscatter coefficient makes detection of inundation using C-HH SAR data during the leaf-on season less certain. It is unlikely that C-VV SAR data can be used to detect variations in flooding during either season.

Correlation of backscatter coefficient with polarization and plot location explained the majority of variability in backscatter coefficients when only non-flooded sites were considered during the leaf-on season. Both polarizations of C-band data could be used to differentiate between uplands and wetlands but not between different types of wetlands

71

(backwater and levee). It is hypothesized that the 1.1 dB difference in C-HH backscatter coefficients and 0.9 dB difference in C-VV backscatter coefficients between backwater and upland sites during the leaf-on season in sites that were not flooded was primarily due to higher levels of soil moisture in backwater (60% volumetric water content) relative to the upland (17% volumetric water content) sites during that time. Given the higher correlation between backscatter coefficient and soil moisture during the leaf-off season, differences in backscatter coefficients should increase during this time of year.

The fact that soil moisture was significantly and positively correlated with both polarizations of backscatter coefficient was not surprising. What was unexpected was the high level of soil moisture correlation with backscatter coefficient, exceeding the correlation of inundation and backscatter coefficient during both leaf-off and leaf-on seasons. This indicates that the strong correlation of backscatter coefficient with soil moisture, combined with those between backscatter coefficient and inundation resulted in significant differences in backscatter coefficient between backwater, levee, and upland ecosystems, allowing for the differentiation of hydropattern. Furthermore, it is thought that this combination of the correlations of backscatter coefficient with inundation and soil moisture, although collinear, resulted in the ability of C-band SAR to detect variations in hydropattern (inundation and soil moisture) during both leaf-off and leaf-on periods.

Although it is hypothesized that the influence of soil moisture on backscatter coefficient may be lower than regression analyses suggest (due to collinearity between soil moisture and inundation), the relationship between soil moisture and backscatter coefficient was not entirely due to collinearity. Differences in backscatter coefficient between upland and wetland areas

were also found when inundation was not present. Most studies using C-band SAR data to detect soil moisture were conducted in areas with no vegetation or only herbaceous vegetation (Dubois et al. 1995; Wickel et al. 2001; Oldak et al. 2003; Sahebi et al. 2003; Wang et al. 2004), but a few have been conducted in forested areas. French et al. (1996) found that C-band SAR data can detect variations in soil moisture in recently burned boreal forest sites (< 4 years after burn) but not after vegetation is more established. A study by Grover et al. (1999) determined that differences in soil moisture due to rainfall in tropical forests do not significantly affect C-band backscatter coefficient.

However, the differences in soil moisture due to rainfall are often much smaller than those caused by groundwater. For example, the study conducted by Grover et al. (1999) assumed a 10% variation in volumetric water content (vwc). However, a 53% difference in vwc was found between wetland and upland sites at the PWRC when no flooding was present. Even though surface water was not present at that time, it is likely that the capillary fringe (the near saturated area that exists between the vadose [unsaturated] and the saturated soil zones) may have been at or near the soil surface. According to a study (Wang et al. 1998) that modeled the sensitivity of SAR data to ground surface parameters in a temperate pine forest, one can expect an increase of 0.9 to 2.3 dB for C-HH data and 0.7 to 2.3 dB for C-VV data when soil moisture varies from 11.6 to 43.8 % vwc (in forests similar to those at the PWRC). The results of this study support those of Wang et al. (1998). I found a difference of 1.1 dB using C-HH and 0.9 dB using C-VV data when soils ranged from 17 to 60% vwc. It is probable that previous ground-based studies did not find variation in C-band backscatter coefficient because rainfall caused a smaller variation in soil moisture than ground water caused at the PWRC site.

Although the relationship between canopy height and backscatter coefficient was weak (r^2 at or below 0.05), this may be partially due to the fact that the forests considered in this study were of similar height (1.8 m standard deviation; Table 4.2). The positive nature of basal area's relationship with backscatter coefficient may be due, in part, to the increase in trunk area available for double-bounce and multi-bounce scattering in moist and flooded forests with larger basal area. Although basal area can also influence the transmissivity of the trunk layer, this effect is thought to be not as important when compared to the influence of basal area on double-bounce and multi-bounce scattering (Townsend 2000). Townsend (2000) also noted that greater heights to lowest branch increased double-bounce scattering and this may explain the positive relationship between canopy height and backscatter coefficient given that taller trees tend to have longer distances between the ground and their first branches.

The analyses indicate that differences in forest structure in different plot locations may have contributed to variations in backscatter coefficient. Specifically, differences in basal area between plot locations may have contributed to variations in backscatter coefficients between wetland (backwater and levee) and upland plots while differences in canopy height may have contributed to variations in backscatter coefficient between levee and backwater and upland plots.

Since stand characteristics (e.g. basal area and tree height) can also influence backscatter coefficient, this information is needed to attribute variations in backscatter coefficient to differences in soil moisture and inundation instead of differences in vegetation structure. Predictions of wetland hydrology can therefore be improved by picking relatively homogeneous forest stands, controlling for variation in canopy closure.

4.6 Conclusions

This research supports the findings of Townsend (2000) who found that C-band SAR data can be used to identify areas of 100% flooding within forests. However, this research was conducted in an area with much smaller expanses of flooded forest compared to Townsend's study. It was conducted in wetlands that experienced a range of inundation levels within a much smaller area. I found that C-HH SAR could be used not only to identify flooded versus non-flooded areas during the leaf-off season but also to distinguish different levels of flooding, even when forests were less than 60% inundated.

The significant differences in backscatter coefficients found between forested areas with varying hydropatterns (inundation and soil moisture) and the relatively large range in backscatter coefficient between areas of different hydropatterns support the conclusion that C-band SAR data can be used to map hydropattern within forested areas, even during the leaf-on season. The ability to distinguish varying levels of flooding and soil moisture beneath forest canopies, even during the leaf-on period, should allow the continuous monitoring of forested wetland hydropattern, a parameter that has been difficult to assess in the past. This capability makes the detection of variations in hydropattern due to changes in climate or anthropogenic influence possible. The ability to monitor hydrology through time could be used to develop more realistic maps of forested wetlands, in which forested wetlands are represented as dynamic systems, flooded and/or saturated for varying amounts of time and with variable boundaries of flood extent. Improved maps of wetland hydropattern could also help to improve the definition of threshold circumstances necessary for wetland formation. Establishing the link between hydrology and a synoptic, continuous way of measuring it gives both scientists and regulators a

unique tool for predicting the effect of climate changes, monitoring the health and

functioning, and mapping forested wetlands at local to global scales.

Chapter 5: Influence of Incidence Angle on the Ability of C-band Synthetic Aperture Radar to Monitor Inundation in the Floodplain of the Roanoke River, North Carolina

5.1 Introduction

Wetland hydropattern, or spatial and temporal variations in inundation and saturation, is the single most important factor in the formation and functioning of a wetland. Small changes in water regime can cause large changes in wetland characteristics and functions (Townsend and Walsh 1998; Mitsch and Gosselink 2000). Although the importance of hydropattern is widely understood, knowledge is still lacking (Hess et al. 1990) due to the large amount of resources needed to accurately collect ground-based information, the inability to use optical remote sensing methods during much of the year, and the difficulty of modeling hydrology in floodplains with subtle and detailed topography due to the lack of high spatial resolution digital elevation models (Townsend and Walsh 1998).

Imaging radars are emerging as a viable alternative to demanding *in situ* data collection and temporally limited optical data for monitoring inundation in wetland ecosystems (Krohn et al. 1983; Ormsby et al. 1985; Imhoff et al. 1987; Hess et al. 1990; Hess et al. 1995; Wang et al. 1995; Townsend and Walsh 1998; Kasischke et al. 2003; Bourgeau-Chavez 2005). However, the capability of SAR for this purpose has not been fully explored and important questions still remain regarding sensor and environmental conditions that may limit the ability of SAR data to detect flooding beneath forest canopies. Incidence angle (the angle between the radar signal and an imaginary line perpendicular to the Earth's surface) can affect the ability of SAR data to monitor

flooding (see Chapter 2). Although the incidence angle effect has been modeled (Enheta and Elachi 1982; Richards et al. 1987) and some studies have been conducted, direct evidence of this effect is still limited. The goal of this research was to investigate the influence of incidence angle on the ability of C-HH SAR to detect flooding under forest canopies. To achieve this goal, I analyzed Radarsat C-HH SAR data in a study region where these data have already been used to map flooded forests (Townsend 2002).

5.2 Background

The capability of SAR for forested wetlands research is promising because of the sensitivity of microwave energy to the presence or absence of standing water (due to its high dielectric constant) and its ability to penetrate forest canopies (even during the leaf-on period) (Hall 1996; Kasischke et al. 1997; Kasischke and Bourgeau-Chavez 1997; Rao et al. 1999) (see Chapter 4). Because the technology is relatively new compared to optical remote sensing, research has been ongoing to fully develop the capabilities of imaging radars.

Synthetic aperture radars (SARs) are active sensors, using different wavelengths of microwave radiation and often transmitting and receiving that energy in different planes relative to the direction that the energy is traveling (see Chapters 2 and 4). Although a number of past studies have used L-band (15.0 – 30.0 cm wavelengths) SAR data to study flooding beneath forest canopies, no L-band satellite sensors are currently in operation. This has led researchers to assess the use of C-band (4.0 – 7.5 cm wavelengths) SAR data to study forested wetland hydrology. As more studies concluded

that C-HH could be used to detect flooding accurately beneath the forest canopy under certain conditions, the need to fully define the limitations of these data increased.

Radar energy is typically transmitted at angles incident to the surface of the Earth (see Chapter 2) ranging from ~ 10 to ~ 65 degrees, where small angles (closer to nadir) are considered steep incidence angles and larger angles are termed shallow. Many studies concluded that smaller incidence angles were preferable for distinguishing flooded from non-flooded forests (Richards et al. 1987; Ford and Casey 1988; Hess et al. 1990; Wang et al.1995; Bourgeau-Chavez et al. 2001; Toyra et al. 2001). Others have not shown incidence angle to affect the ability of SAR data to detect flooding beneath vegetation (Ormsby et al. 1985; Imhoff et al. 1986. Hess et al. (1990) concluded that the role of incidence angle on the ability of SAR to detect flooding beneath forest canopies should be further explored.

For hydrologic studies in forested wetlands, a simple model of backscatter coefficient can be employed to explain the sources of microwave backscatter measured at the sensor. With this model, forests are conceptualized as having three layers: The canopy layer, the trunk layer, and the ground layer (Kasischke and Bourgeau-Chavez 1997; Townsend 2002), with total backscatter coefficient from a forest (σ^o) being:

$$\sigma^o = \sigma^o_c + \tau^2_c \, \tau^2_t \, (\sigma^o_t + \sigma^o_s + \sigma^o_d + \sigma^o_m)$$

where

σ^o_c = backscatter coefficient of the crown layer of branches and foliage,
τ_c = transmissivity of the crown layer,
τ_t = transmissivity of the trunk layer,
σ^o_t = backscatter coefficient from the trunk layer,

σ^o_s = backscatter coefficient from the ground surface layer,

σ^o_d = double-bounce between the trunks and the ground surface layers, and

σ^o_m = multi-path scattering between the ground surface and canopy layers.

Due to the size (usually 5-6 cm) of the microwave wavelength in relation to smaller woody branches and foliage, C-band total SAR backscatter coefficient is mostly influenced by scattering caused by the crown layer (σ^o_c). However, in flooded forests double-bounce scattering (σ^o_d) and multi-path scattering (σ^o_m) between the ground and trunk layers can have a large effect on the total backscatter coefficient when the transmissivity of the crown (τ_c) and trunk (τ_t) layers is high (because of low stand density or the absence of foliage). Flooding under the forest canopy not only greatly increases double-bounce and multi-path scattering but it also eliminates surface scattering (σ^o_s). Because of the large increases in total backscatter coefficient that flooding causes, inundated forests often have a total backscatter coefficient (σ^o) that is much higher that non-flooded forests. Dry soil absorbs microwave energy leading to lower direct scattering as well as decreased multi-path scattering. In non-flooded forests, increases in soil moisture raise the surface backscatter coefficient and multi-path scattering. However, the increase in double-bounce and multi-path scattering that flooding causes is much higher than the increase caused by higher soil moisture levels. Increases in canopy foliage (LAI) during the warmer months will decrease the transmissivity of the crown layer (τ_c), and thus decrease the amount of microwave energy reaching the forest floor. Thus, an increase in foliage should reduce the effectiveness of the radar to detect flooded forests. For a more detailed explanation of microwave scattering from forests see Dobson et al. (1995) and Wang et al. (1995).

The impact of different incidence angles on backscatter coefficient varies according to forest structure (basal area, canopy height, canopy depth, and branching characteristics) and characteristics of the ground layer, including surface roughness, soil moisture, and the presence/absence of standing water (Hess et al. 1990; Rauste 1990). Just as certain substances are often said to have a spectral signature (reflectance as a function of wavelength) when using optical sensors, forests have distinct angular signatures (backscatter coefficient as a function of incidence angle) when imaged at multiple incidence angles (Rauste 1990). When backscatter coefficient is plotted as a function of incidence angle, certain trends (peaks and valleys) in the backscatter coefficient become apparent and these trends can be related to properties (mostly structure and the presence of water) on the ground. Microwave energy transmitted by SARs operating at larger (shallower) incidence angles are expected to interact more with the canopy layer, thus decreasing transmissivity in the crown layer (τ_c) but increasing the ability of the radar to estimate the characteristics (e.g., biomass and canopy closure) of this layer (Sun and Simonett 1988; Rauste 1990; Magagi et al. 2002). On the other hand, microwave energy transmitted at smaller (steeper) incidence angles has a shorter path length through the canopy, increasing transmissivity in the crown layer (τ_c), and therefore leaving more energy to interact with the trunk and ground layers.

Backscatter coefficient is expected to vary with incidence angle in flooded and non-flooded forests and under leaf-on and leaf-off conditions. The increase in path length with larger incidence angles should generally increase attenuation and therefore decrease backscatter coefficient originating from the ground surface (Sun and Simonett 1988; Hess et al. 1990; Rauste 1990; Magagi et al. 2002). Backscatter coefficient in flooded and non-

flooded sites should decrease with increasing incidence angle due to decreased transmissivity in the crown and trunk layers; however, it is hypothesized that the decrease should be greater for flooded sites due to increased attenuation of multi-path and double-bounce scattering. Therefore, while I expect backscatter coefficient to decrease with incidence angle in both flooded and non-flooded forests, I expect the decreases in backscatter coefficient to be greater for flooded forests. As a consequence, the difference in backscatter coefficient between flooded and non-flooded forests should decrease with increasing incidence angle.

In leaf-off forests, greater transmissivity in the canopy layer should lead to higher backscatter coefficient, relative to leaf-on forests, when forests are flooded (Hess et al. 1990). In floodplain environments, this may also be true for non-flooded forests since soil moisture is often high. It is hypothesized that the greater canopy transmissivity during the leaf-off season will increase the difference between flooded and non-flooded sites as more energy should be able to penetrate the crown layer and interact with the ground, flooded or not. Figure 5.1 presents a simple representation of how backscatter coefficient should respond to increasing incidence angle, based on the simple model presented above.

5.3 Methods

The effect of incidence angle on the ability of C-HH SAR data to detect flooding was examined in three forest types found within the study region: Open tupelo-cypress (<50% canopy cover), tupelo-cypress, and deciduous bottomland hardwood forests during both the winter (leaf-off) and summer (leaf-on). Backscatter coefficient was also examined in

82

upland deciduous and pine forests for comparison with the floodplain forests. A flood

simulation model (Townsend and Foster 2003), derived from river stage and radar

backscatter coefficient values, was used to distinguish areas of flooding from non-flooded

areas. A digital map of vegetation cover was then used to isolate forest types in flooded

and non-flooded areas within Radarsat SAR data with incidence angles from 20° to 49°.

Average radar backscatter coefficient ($\sigma°$) measurements from each forest type were

compared in flooded and non-flooded areas using the multi-incidence angle data.
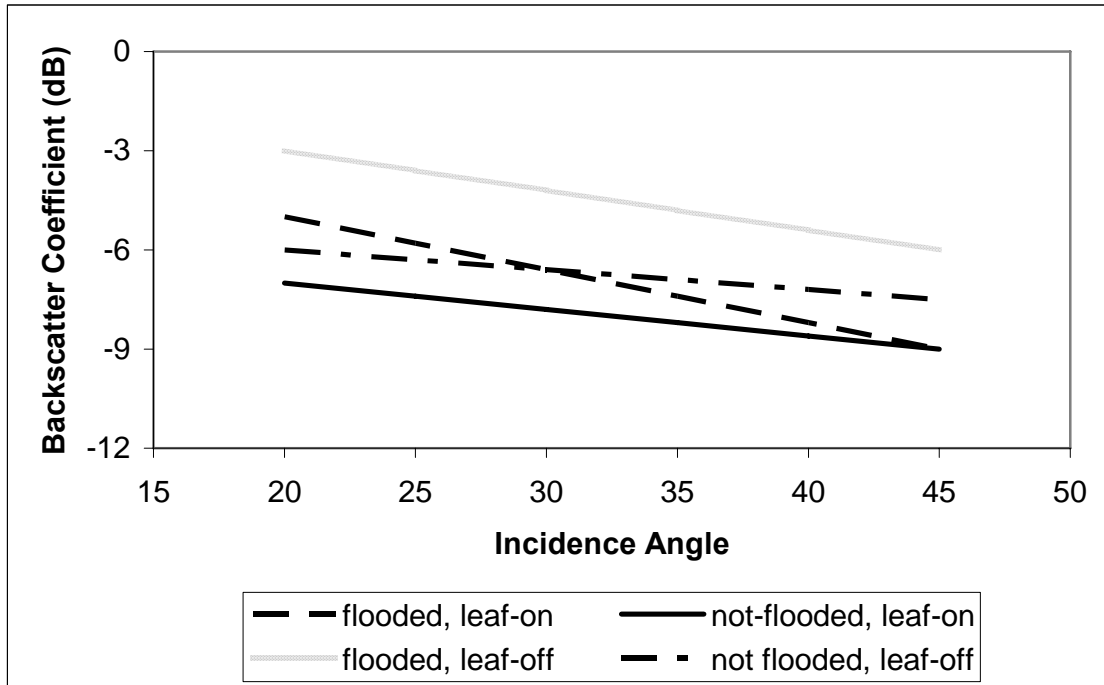
Figure 5.1: Theoretical chart of backscatter coefficient as a function of incidence angle for flooded and non-flooded forests during the leaf-on and leaf-off seasons according to initial hypotheses based on prior research.

5.3.1 Study Area

The study area was located in northeastern North Carolina, including the lower

Roanoke and the much smaller Cashie Rivers, and covered some of the most expansive

and pristine forested wetlands on the East Coast of the U.S. (Figure 5.2). The Roanoke River originates in the Blue Ridge Mountains of Virginia and flows 209 km through the Blue Ridge, Piedmont, and Coastal Plain Physiographic Provinces before emptying into the Atlantic Ocean. The river's floodplain covers approximately 61,000 ha and varies in width between less than 5 and 10 km. The study area has a humid subtropical climate with lingering, humid summers and mild winters (average annual temperature of 15.5° C). Annual precipitation averages 120 cm, and usually exceeds evapotranspiration, with the most rain occurring during the summer.
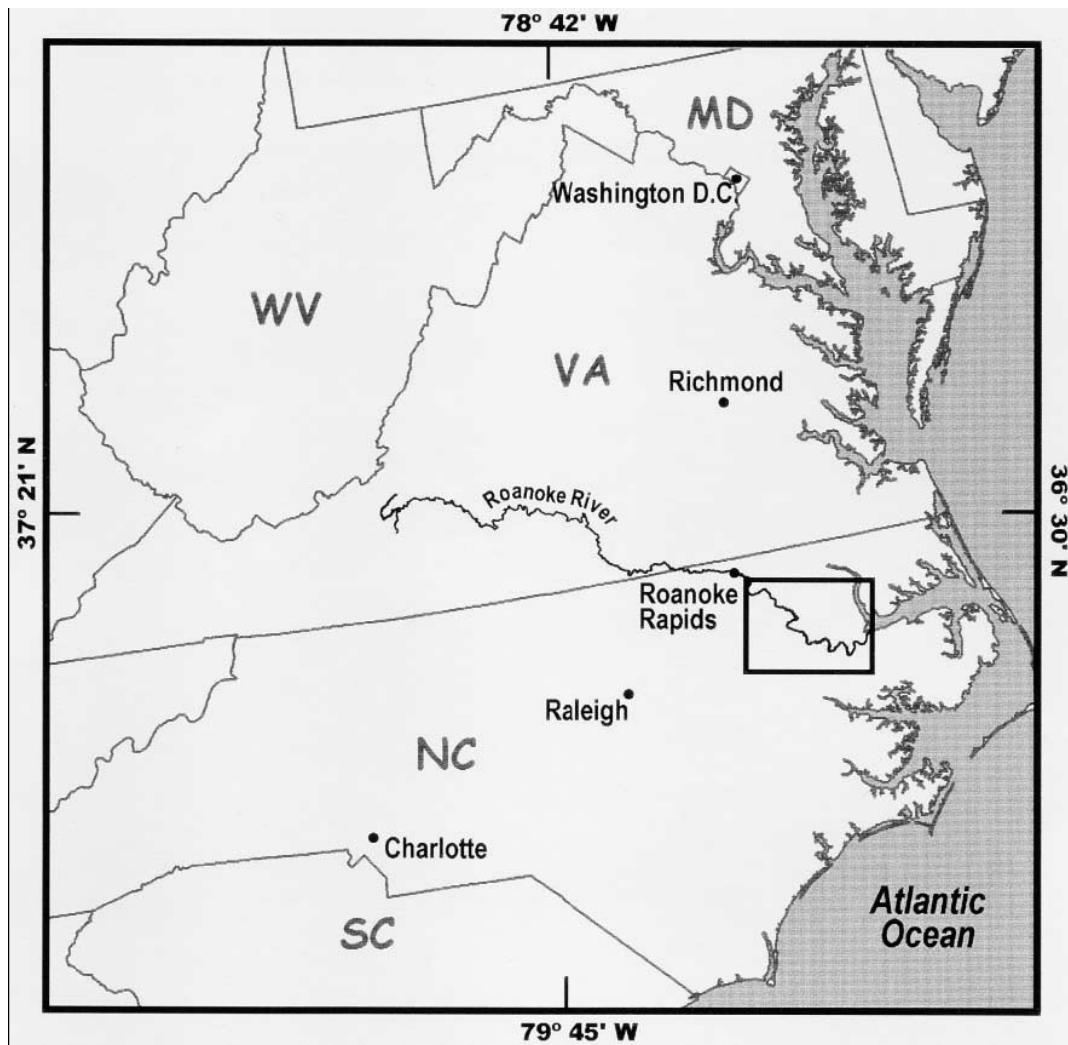
Figure 5.2: The Roanoke River Study Site, North Carolina, U.S.A. The study focused on the floodplain of the lower Roanoke River (shown inside box).

The area around the Roanoke River can be divided into two general geomorphic settings: Floodplain and upland. Within the floodplain, small changes in elevation lead to large differences in hydropattern. The meandering river channel is surrounded by depositional levees that decrease in elevation into backwater areas towards the terraces and uplands on either side of the floodplain. Higher areas are often traversed by intermittent stream channels that serve as conduits into and out of the backwater areas. Much of the floodplain is inundated at one point during the year and the backwater areas can remain flooded for longer periods. As a result, tupelo-cypress (*Nyssa aquatica - Taxodium distichum*) forests dominate in the backwater areas while a mixture of deciduous floodplain species are found in the drier areas. Although cypress trees used to be more dominant in the tupelo-cypress forests, their numbers have been reduced by selective logging and they now represent less than 30% of the canopy trees in tupelo-cypress forests (Townsend 2002). The dominant trees in the mixed deciduous bottomland hardwood forests include: Red maple (*Acer rubrum*), green ash (*Fraxinus pennsylvanica*), sweet gum (*Liquidambar styraciflua*), oaks (*Quercus michauxii, Quercus lyrata, Quercus phellos,* and *Quercus laurifolia*), American elm (*Ulmus americana*), box elder (*Acer negundo*), and sugarberry (*Celtis laevigata*). The duration of flooding and subtlety of variations in elevation generally increases down-stream. The timing of inundation is mainly controlled by variations in evapotranspiration, precipitation, soil texture and organic matter content, antecedent conditions, and the amount of water released from upstream dams (Townsend and Foster 2003).

5.3.2 Data and Analysis

Data from eleven standard beam Radarsat (C-HH) images collected in 2000 were analyzed, five from the leaf-on (Figure 5.3) and six from the leaf-off (Figure 5.4) periods.
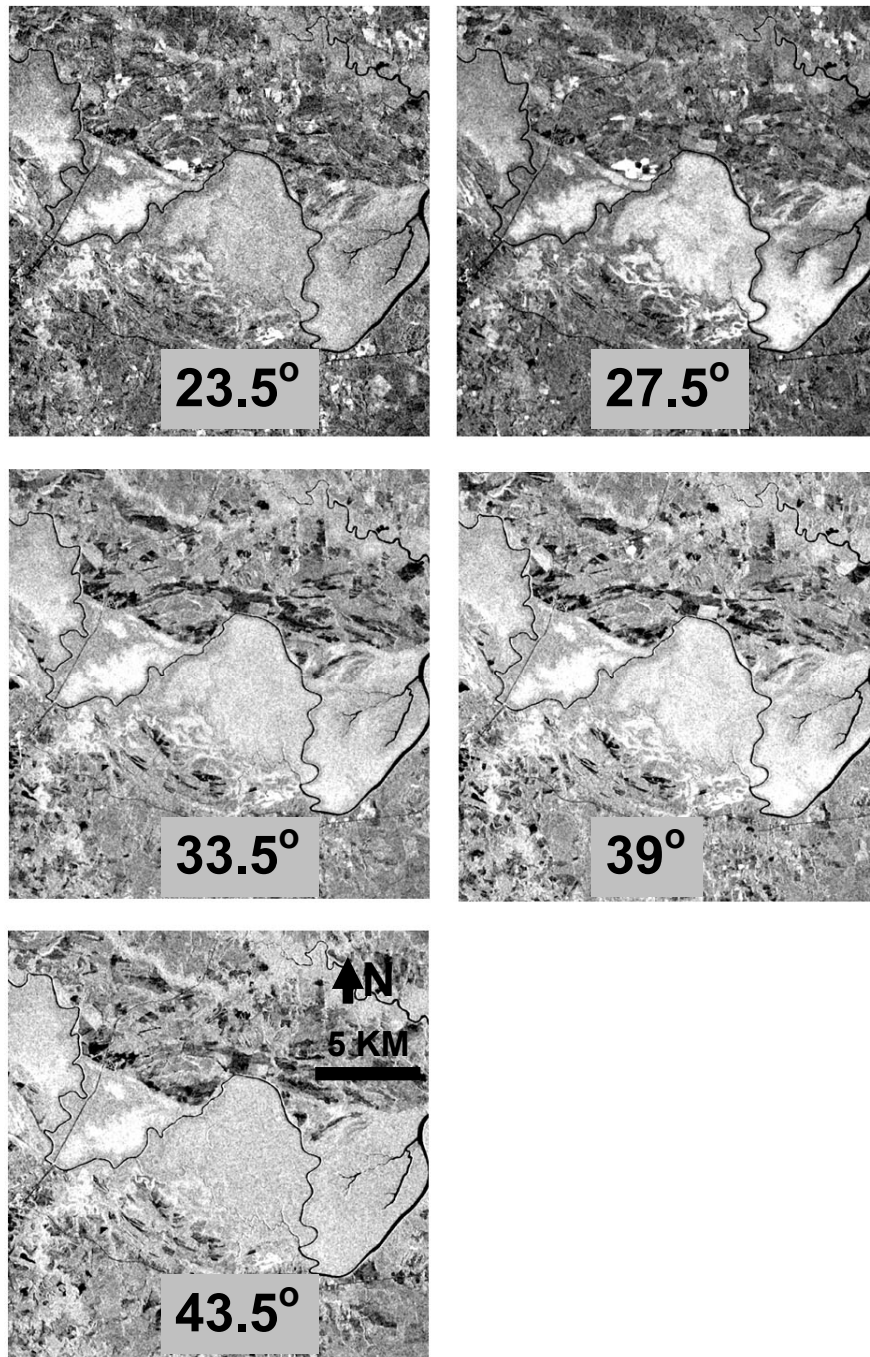
Figure 5.3: A portion of the leaf-on Radarsat images in order of increasing incidence angle. All images are from December of 2000 and were collected during a period of similar river discharge.
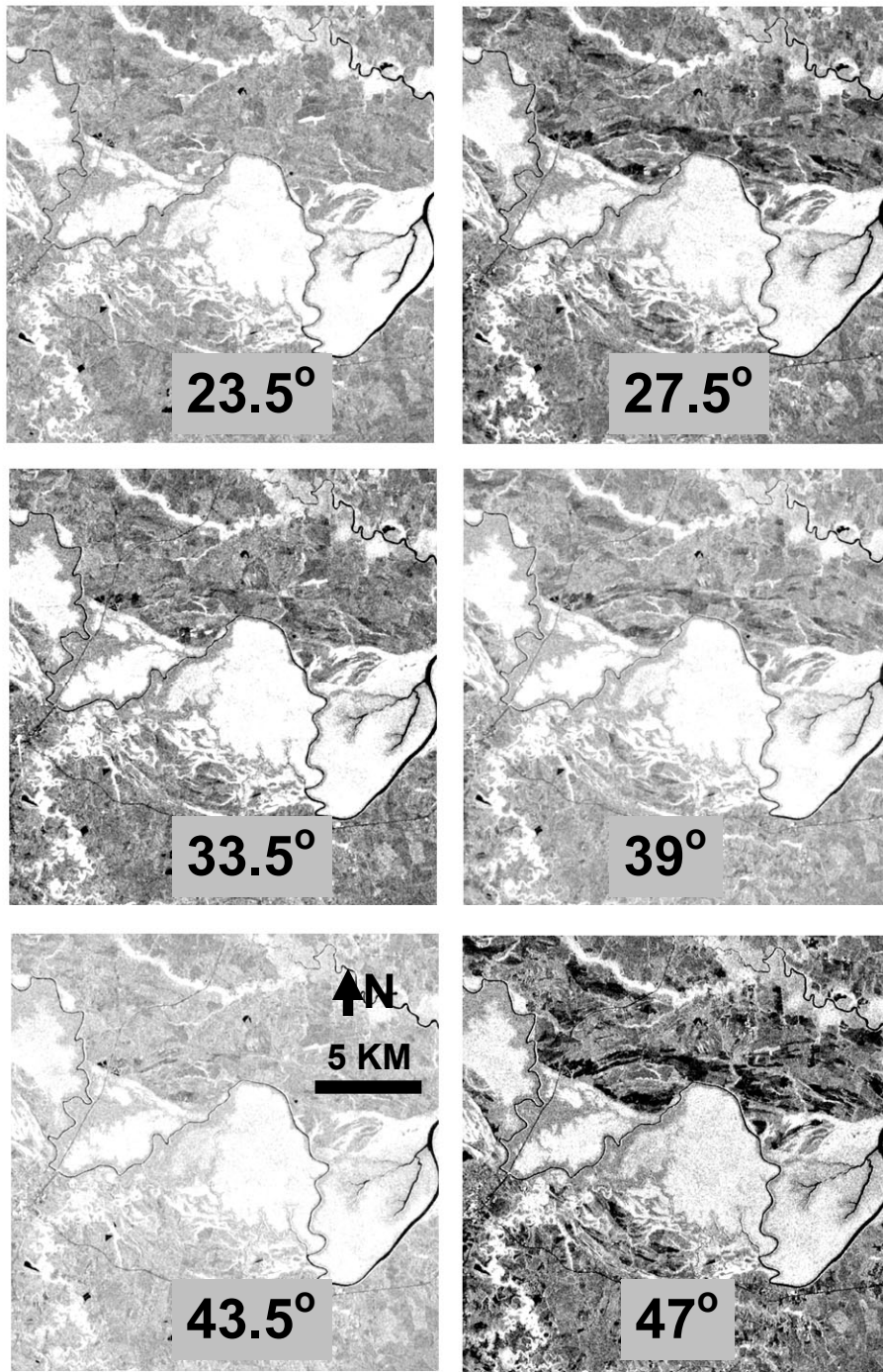
Figure 5.4: A portion of the leaf-off Radarsat images in order of increasing incidence angle. All images are from May or June of 2000 and were collected during a period of similar river discharge.

The leaf-on images had incidence angles ranging from 20° to 46° and the leaf-off images had incidence angles between 20° and 49° (Table 5.1). Although incidence angle varies

Date	Mode	Incidence Angle Range	Average	Discharge (cms)	Season
12/6/2000	S1	20° - 27°	23.5^o	107	leaf-off
12/23/2000	S2	24° - 31°	27.5^o	57	leaf-off
12/16/2000	S3	30° - 37°	33.5^o	59	leaf-off
12/9/2000	S5	36° - 42°	39°	169	leaf-off
12/2/2000	S6	41° - 46°	43.5^o	58	leaf-off
12/19/2000	S7	20° - 27°	23.5^o	86	leaf-off
6/21/2000	S1	24° - 31°	27.5^o	256	leaf-on
5/21/2000	S2	30° - 37°	33.5^o	113	leaf-on
6/7/2000	S3	36° - 42°	39°	170	leaf-on
5/31/2000	S5	41° - 46°	43.5^o	136	leaf-on
6/17/2000	S6	45° - 49°	47°	97	leaf-on

Table 5.1: Dates, incidence angles, and stream discharge for Radarsat acquisition.

from near to far range (closer to further from the sensor), it should be noted that the portion of the Roanoke River floodplain examined in this study extends across nearly the entire range direction of the image. The average incidence angle for the entire image should therefore be similar to the average incidence angle for the test sites examined in this study.

Before analysis, all SAR data were radiometrically calibrated, resampled to 30 m, and georeferenced to UTM coordinates using ground control points from a Landsat Thematic Mapper (TM) image. Calibration was performed at the University of Maryland Appalachian Lab's Landscape Ecology Lab using calibration data provided by the Alaska SAR Facility (Philip Townsend, personal communication). The cumulative root mean

square error was < 15 meters and a second order polynomial transformation and nearest neighbor resampling was used.

Vegetation type was derived from a digital map of vegetation communities (Townsend and Walsh 2001) that used multi-temporal Landsat TM and ground data to identify vegetation. To isolate the effects of physiognomic differences among forests, five forest types were selected for analysis (open tupelo-cypress, tupelo-cypress, mixed deciduous bottomland hardwood, upland deciduous, and pine). The tupelo-cypress forests were separated from the other types of floodplain forest because they are structurally distinct. On average, the tupelo-cypress forest had a higher basal area (BA frequently > 50 m^2/ha), fewer small trees, and increased trunk buttressing as compared to the mixed deciduous bottomland hardwood forests (Townsend 2002). This variation may have caused the microwave energy to interact differently with these forests. Other forest types were separated due to more obvious differences, such as the decreased canopy closure and basal area of the open tupelo-cypress forests (compared to the tupelo-cypress forests) and the varying structure and needle leaves of the pine forests.

Forest patches were identified using the digital map of forest type and the patches were reduced in size to decrease the chance of mixing or incorrectly identifying forest types. The tupelo-cypress, bottomland hardwood, and pine forest patches were reduced by two pixels or 60 m while the open tupelo-cypress and upland deciduous forests were only reduced by one pixel or 30 m due to the smaller size of those patches.

The areal extent of flooding was estimated for all eleven dates of Radarsat data using DEM and river discharge based flood simulation models and thresholds of filtered

SAR backscatter coefficient for each date (Townsend and Foster 2003). Flooded and non-flooded areas on a particular date were verified with both the model and the SAR backscatter coefficient thresholds, and were only used when there was agreement between both sources.

Average backscatter coefficient for flooded and non-flooded areas was calculated for the open tupelo-cypress, tupelo-cypress, and mixed deciduous bottomland hardwood forests while average backscatter coefficient in non-flooded areas was assessed for the upland deciduous and pine forests.

5.4 Results

Under non-flooded conditions, > 1,000 samples (pixels) of SAR backscatter coefficient were averaged for all forest types (Table 5.2). Under flooded conditions, > 1,000 samples (pixels) of SAR backscatter coefficient were averaged for all forest types but the bottomland hardwood. Under non-flooded conditions, tupelo-cypress forests had the highest backscatter coefficient values, with a relatively large increase (> 3 dB) in backscatter coefficient during the leaf-off season compared to the leaf-on season (Figure 5.5). Non-flooded bottomland hardwood and upland deciduous forests behaved similarly during leaf-off and leaf-on conditions over all incidence angles, with bottomland hardwood forests having slightly higher average backscatter coefficient (0.3 dB greater leaf-on and 0.4 dB greater leaf-off) at all times and incidence angles. Average backscatter coefficient from pine forests was slightly higher (0.6 dB higher) during the

	Bottomland		Tupelo-Cypress		Opn Tupelo-Cypress		Upl Dec	Pine
	Flood	Nt Fld	Flood	Nt Fld	Flood	Nt Fld	Nt Fld	Nt Fld
12/2/2000	51	69660	44742	95731	1263	1688	1503	470185
12/6/2000	61	69650	35717	104756	1244	1707	1503	470185
12/9/2000	66	69645	45834	94639	1280	1671	1503	470185
12/16/2000	49	69662	42154	98319	1267	1684	1503	470185
12/19/2000	30	69681	23443	117030	1130	1821	1503	470185
12/23/2000	101	69610	79691	60782	1561	1390	1503	470185
5/21/2000	53	69658	72483	67990	1195	1756	1503	470185
5/31/2000	69	69642	44255	96218	1346	1605	1503	470185
6/7/2000	135	69576	63317	77156	1580	1371	1503	470185
6/17/2000	137	69574	32060	108413	1666	1285	1503	470185
6/21/2000	107	69604	58454	82019	1664	1287	1503	470185

Table 5.2: Number of pixels in each forest class under flooded and non-flooded (nt fld) conditions during Radarsat acquisition. The forest types included in the graph are: Bottomland Hardwood (bottomland), tupelo-cypress, open tupelo-cypress, upland deciduous (upl dec), and pine.

leaf-on season at all incidence angles except 33.5°. Although the slope is gradual, when flooded, the general trend of decreasing backscatter coefficient with increasing incidence angle was more evident during the leaf-off period. During the leaf-on period, 23.5° backscatter coefficient for all flooded forests decreased by about 3 dB compared to leaf-off, flooded conditions (Figure 5.5).

During the leaf-off period, the ability to detect flooding was fairly constant for both types of tupelo-cypress forest although flooding resulted in higher backscatter coefficient differences in the open tupelo-cypress forests than the denser tupelo-cypress forests (Figure 5.6). The difference between flooded and non-flooded areas was nearly 2 dB greater in the bottomland forest areas (compared to the open tupelo-cypress forests), with data collected at a 27.5° incidence angle having the greatest difference and 23.5° and 47° having the least difference.
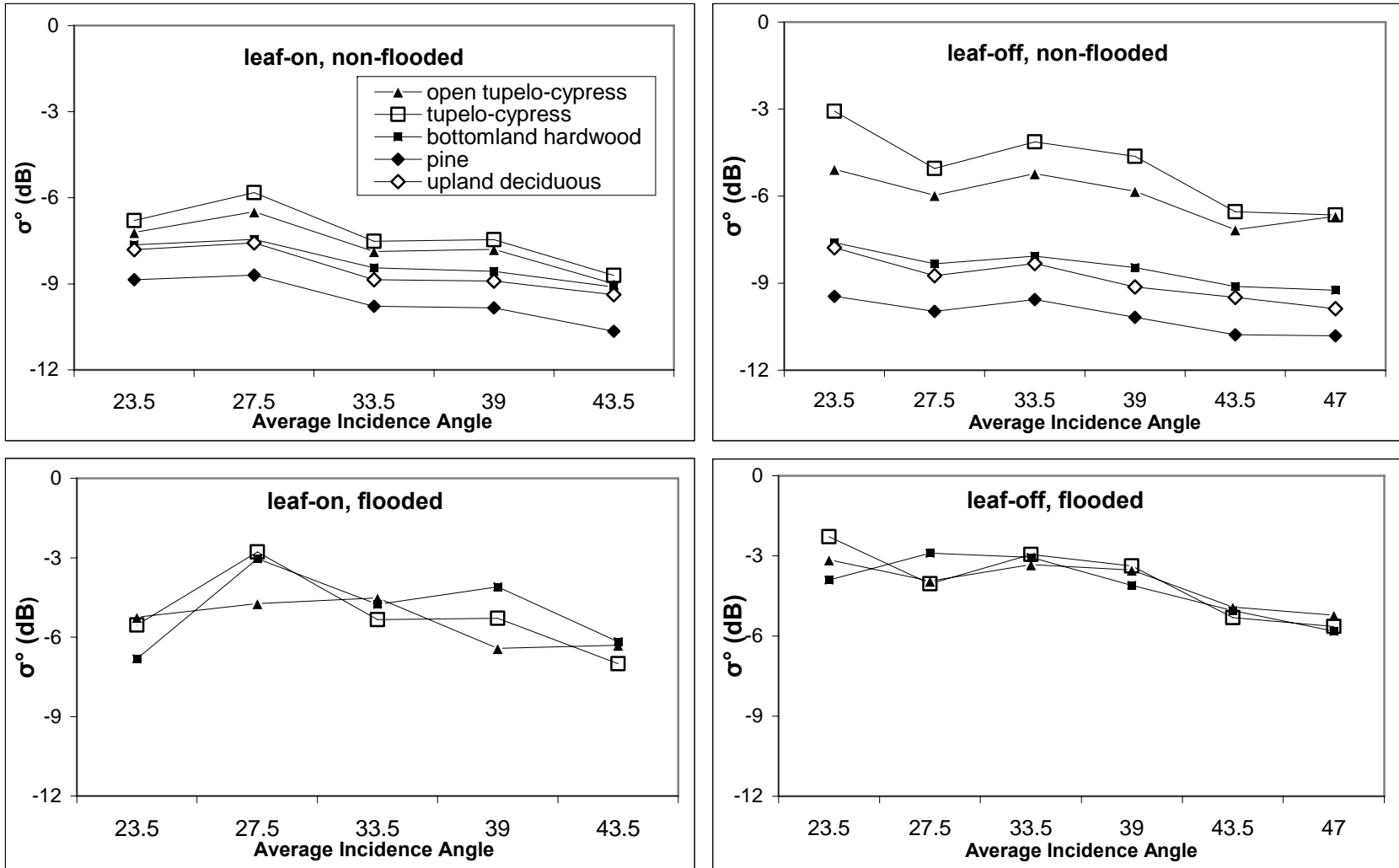
Figure 5.5: Backscatter coefficient (σ°) as a function of incidence angle for all forest types during: leaf-on non-flooded (top left), leaf-off non-flooded (top right), leaf-on flooded (bottom left), and leaf-off flooded (bottom right) conditions.

92
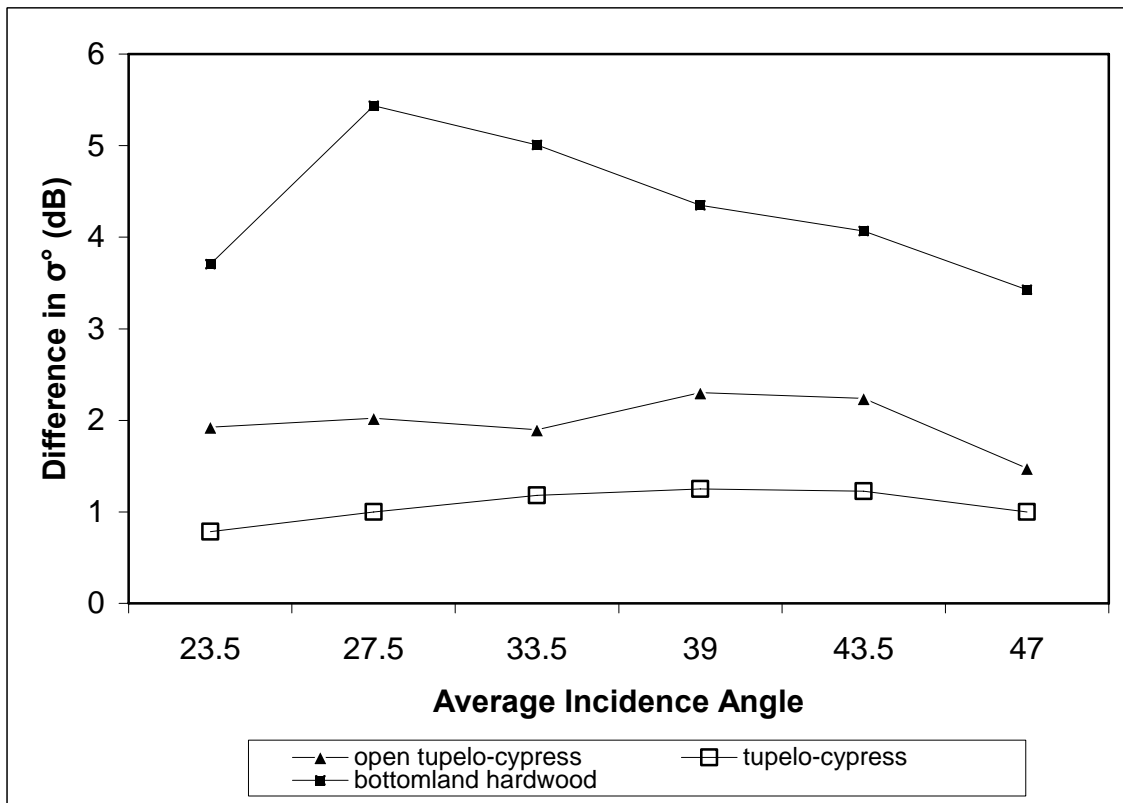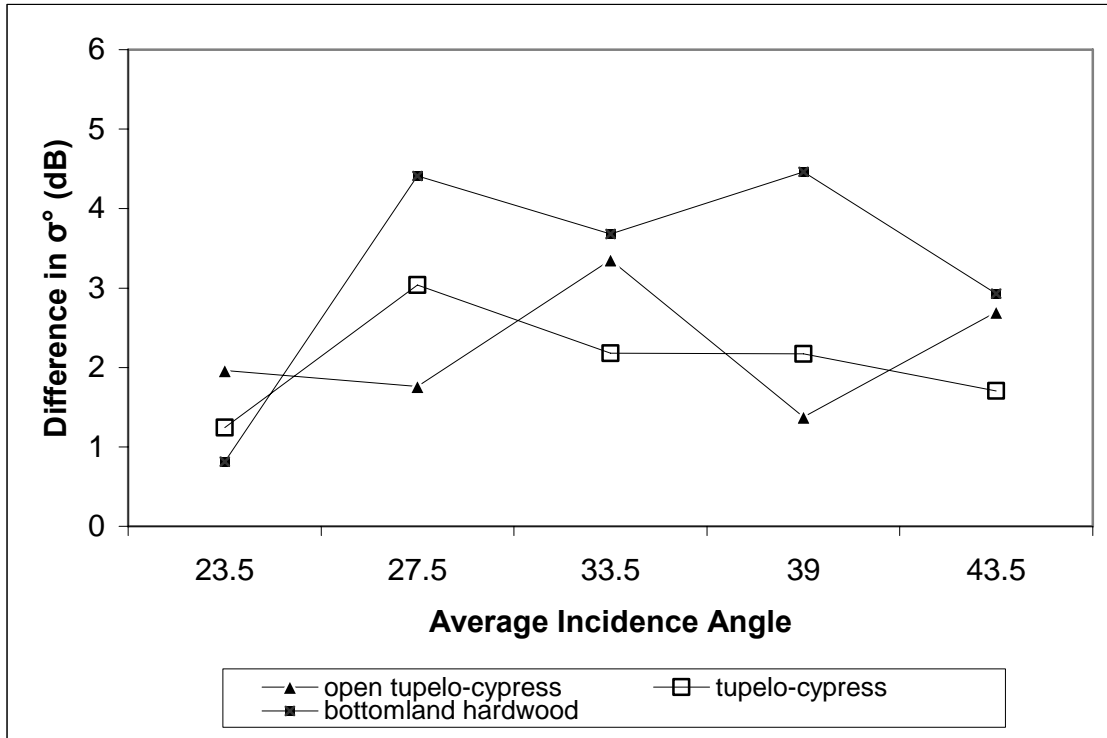
Figure 5.6: Difference in backscatter coefficient (σ°) between flooded and non-flooded forests for all forest types as a function of incidence angle during the leaf-on (top) and leaf-off (bottom) seasons.

The ability to detect flooding under leaf-on conditions varied much more according to incidence angle while forest type had a greater effect during the leaf-off season (Figure 5.6). Generally, an incidence angle of 23.5º provided the smallest difference in backscatter coefficient between flooded and non-flooded forests while the incidence angle that provided the largest difference in backscatter coefficient between flooded and non-flooded conditions varied with forest type. Based on past research, I hypothesized that the difference in backscatter coefficient between flooded and non-flooded conditions would always be larger during the leaf-off season but this was not always the case (Figure 5.6). The greater difference in backscatter coefficient between flooded and non-flooded areas during the leaf-on season (as compared to the leaf-off) was most noticeable in the tupelo-cypress forests.

Backscatter coefficient from the different floodplain forest types was averaged to illustrate general trends, regardless of forest type. Backscatter coefficient was found to generally decrease with incidence angle (Figure 5.7), but the distinction between flooded and non-flooded areas did not decline sharply with incidence angle, as expected (Figure 5.8). Although previous research has supported the use of smaller incidence angles to detect inundation in forests, data collected at the 23.5º incidence angle was found to be one of the least suited for this application (exhibited the smallest difference between flooded and non-flooded forests). Conversely, the ability to detect inundation under flooded forests is greater than expected for data with larger incidence angles (Figure 5.8). The ability to differentiate flooded and non-flooded forests was similar during the leaf-off and leaf-on seasons (Figure 5.8).
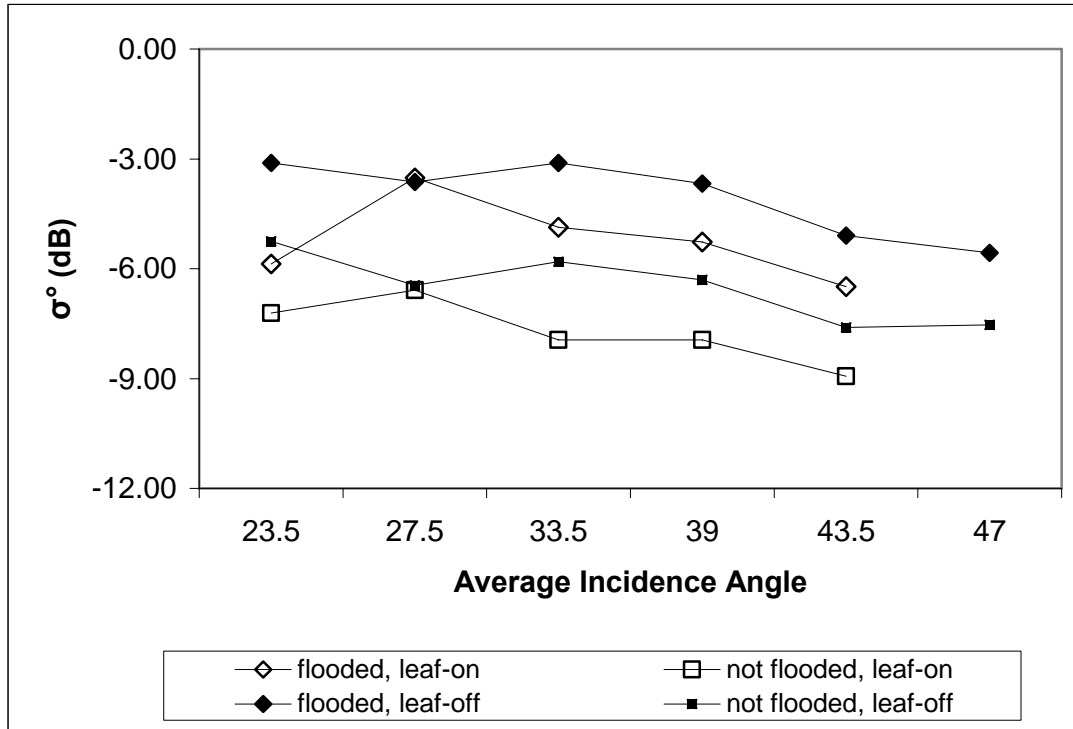
Figure 5.7: Backscatter coefficient (σ°; averaged for all forest types) as a function of incidence angle during the leaf-on and leaf-off seasons under flooded and non-flooded conditions.
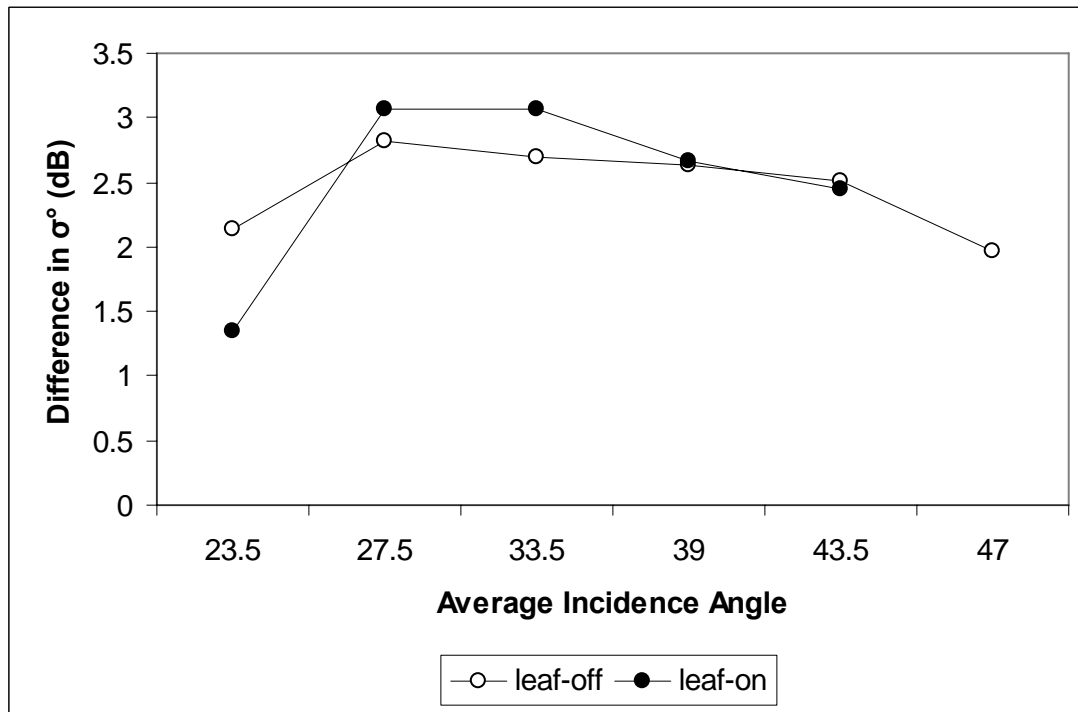
Figure 5.8: Difference in backscatter coefficient (σ°) between flooded and non-flooded areas as a function of incidence angle and averaged of all forest types.

5.5 Discussion

Averaging large samples (> 1,000 pixels) of backscatter coefficient increases the reliability of those averages by decreasing the influence of radar fading and other sources of noise. Therefore, the flooded bottomland hardwood category may have been more susceptible to noise than other forest types because it always had < 150 pixels per date. However, the angular signature of the flooded bottomland hardwood forest was very similar to that of the tupelo-cypress forests during the leaf-on season and both the tupelo-cypress and open tupelo-cypress forests during the leaf-off season, giving no indication of decreased reliability.

Previous research has suggested that flooding should be more detectable in forests using radar with smaller (steeper) incidence angles (Richards et al. 1987; Ford and Casey 1988; Hess et al. 1990; Wang et al.1995; Bourgeau-Chavez et al. 2001; Toyra et al. 2001). However, this research suggests that this is not the case (Figure 5.8). It was hypothesized that larger incidence angle data would encounter decreased transmissivity in the canopy layer and therefore be less sensitive to flooding on the ground. This decrease in transmissivity may have led to a general decline in backscatter coefficient with increasing incidence angle but it did not lead to a substantial decrease in sensitivity to flooding as predicted by previous studies (Richards et al. 1987; Ford and Casey 1988; Hess et al. 1990; Wang et al.1995; Bourgeau-Chavez et al. 2001; Toyra et al. 2001). In fact, C-HH SAR data collected at the smallest incidence angle considered by this study (average incidence angle 23.5°) was found to be one of the least effective for

distinguishing flooded forests (smallest difference in backscatter coefficient between flooded and non-flooded areas).

The relatively low ability of Radarsat SAR data collected at the 23.5^o incidence angle to distinguish between flooded and non-flooded areas occurs during both leaf-on and leaf-off conditions (Figure 5.8). It is hypothesized that during the leaf-on season, this was due to the orientation of canopy leaves. These leaves, which were at or above the size of the microwave wavelength, were primarily oriented parallel to the surface of the Earth. Therefore, energy transmitted at the smallest incidence angle (23.5^o) was most likely to encounter the front of leaves (the largest surface area of the leaf) while energy at larger incidence angles was more likely to encounter the narrow leaf sides and pass through the canopy via gaps between leaves. It is unknown why the ability of the smallest incidence angle (23.5^o) to detect flooding is much lower than that of the second smallest incidence angle (27.5^o) when considering the bottomland hardwood forests during the leaf-off season (Figure 5.6). However, it may have to do with the presence of ground cover which is absent from the tupelo-cypress and open tupelo-cypress forests. The largest incidence angle data, 47°, was only available during the leaf-off period; it also exhibited a drop in sensitivity similar to the smallest incidence angle data examined.

Although data collected at average incidence angles of 27.5^o and 33.5^o were found to provide the largest separation between flooded and non-flooded forests (Figure 5.8), this study demonstrated that larger incidence angles can be used to detect flooded forests. All of the larger incidence angles found a difference in backscatter coefficient > 1 dB (the relative Radarsat calibration error).

Although the ability of C-band SAR to detect flooding was thought to decrease substantially during the leaf-on season (Wang et al. 1995), these results support other work (Townsend and Walsh 1998) that concluded that flooding can be detected in forests during both the leaf-off and the leaf-on seasons. In fact, flooding was found to be slightly easier to detect during the leaf-on season at moderate incidence angles (average incidence angles of 27.5° and 33.5°), but the small (< 0.5 dB) difference may not be significant. Flooding was easier to detect during the leaf-off season at smaller incidence angles and the presence of the leaves had no impact at average incidence angles of 39° and 43.5°.

The differentiation of the angular signature of non-flooded open and regular tupelo-cypress forests from the other forest types was much greater during the leaf-off season (Figure 5.5). At this time of year, the open and regular tupelo-cypress forests are about 2.5 dB greater than the other forest types while during the leaf-on season they are only about 0.6 dB higher. This may have been due to the higher transmissivity of the canopy layer during the leaf-off season leading to the superior detection of soil moisture differences, higher soil moisture levels increasing backscatter coefficient (see section 5.2).Townsend (2002) also found distinctions between forest types to be influenced by differences in environmental conditions and Wang et al. (1998) noted that surface characteristics, like soil moisture, influenced backscatter coefficient from forests. This difference in soil moisture may also explain the slightly higher backscatter coefficient of the bottomland deciduous forests as compared to the upland deciduous forests under non-flooded conditions. It is notable that the pine forests, which are often found in drier areas (compared to deciduous forests) exhibited the lowest backscatter coefficient, but this

could only be attributable to lower soil moisture if transmission in the canopy and trunk layers was high enough.

During the leaf-off seasons, under non-flooded conditions, the angular backscatter coefficient signatures of open tupelo-cypress and tupelo-cypress converged at larger incidence angles (Figure 5.5). This may be due to the lower sensitivity of the microwave signal to soil moisture at larger incidence angles reported by Dobson et al. (1983). As expected, it appears that the ability of C-HH band SAR data to differentiate varying soil moisture levels is decreased during the leaf-on season due to the increased attenuation of the forest canopy.

Differences in the angular signature of diverse forest types are especially obvious under flooded conditions during the leaf-on season (Figure 5.5). The difference in backscatter coefficient response between the forest types may be due to variations in the canopy, made increasingly obvious by flooding. This assertion is supported by the distinction in angular signatures between the open and closed canopy tupelo-cypress forests and the greater similarity between the angular signatures of the closed canopy tupelo-cypress and the bottomland deciduous forests (also closed canopy) even though the closed canopy tupelo-cypress have buttressed trunks and therefore greater basal area than the bottomland hardwood forests (Townsend 2002). The increasing impact of forest characteristics on backscatter coefficient with the addition of inundation was also reported by Townsend (2002) who suggests that this may be due to the decrease in the impact of varying ground characteristics caused by flooding and/or the increase in interactions with the trunk and crown layer due to double-bounce and multi-path scattering.

It is hypothesized that the more obvious trend of decreasing backscatter coefficient with increasing incidence angle present in the flooded, leaf-off forests was due to the increasing impact of specular reflectance with increasing incidence angle that is lessened by greater canopy closure in the leaf-on data (Figure 5.5). The presence of the canopy may re-direct specular reflectance (from the inundated surface) back towards the sensor. A trend of increasing specular reflectance with lower canopy closer was reported by Rauste (1990). The trend is made even more distinct because the varying character of the ground layer among different forest types is eliminated by the presence of standing water.

The incidence angle most sensitive to flooding varied according to forest type, with the difference in angular signatures between flooded and non-flooded forests being much more consistent during the leaf-off season (Figure 5.6). This increasing variation in backscatter coefficient with incidence angle during the leaf-on season was likely due to the greater interaction of the radar signal with the trunk and canopy layers caused by the increase in canopy closure during the leaf-on season (Townsend 2002). This increased interaction may encourage the differentiation of forest types that vary not only in canopy closure but also in basal area and trunk shape. The greater ability to distinguish flooding in the deciduous bottomland forests may be due to the generally lower soil moisture found at these sites when they are not inundated. The difference in backscatter coefficient received from forests with drier soil versus inundation was greater than the difference in backscatter coefficient received from forests with moister soils versus inundation.

5.6 Summary and Conclusions

The backscatter coefficient from Radarsat C-HH SAR data varied as a function of incidence angle as well as vegetation structure, soil moisture and flooding. The simple model of radar backscatter coefficient presented in the background section of this chapter (Section 5.2), can be used to relate changes in total backscatter coefficient to *in situ* conditions. Backscatter coefficients from non-flooded and flooded forests decreased gradually with increasing incidence angle. It is hypothesized that this decrease was caused by lower transmissivity of the crown layer (τ_c), increased attenuation of energy from double-bounce (σ^o_d) and multi-path (σ^o_m) scattering, and possibly increased specular reflectance of the surface layer (σ^o_s) with increasing incidence angles.

In the absence of flooding, differences in soil moisture distinguished the different forest types. Forests with nearly saturated soils (tupelo-cypress) had a higher surface layer backscatter coefficient (σ^o_s), and therefore greater total backscatter coefficient than forests with drier soil. Forests with the lower soil moisture (upland deciduous and pine), had a lower surface layer backscatter coefficient (σ^o_s) and consequently lower total backscatter coefficient. This difference was more apparent during the leaf-off season, when the transmissivity of the crown layer (τ_c) was highest, allowing more energy to penetrate the canopy layer and interact with surface layer. The ability to distinguish differences in soil moisture appears to decrease slightly with increasing incidence angle with the sharpest declines at incidence angles greater than or equal to 47°.

Under flooded conditions, variations between forest types based on the surface layer were minimized and double-bounce (σ^o_d) and multi-path (σ^o_m) backscatter increased at all incidence angles, although most noticeably at 27.5^o and 33.5^o. During the

leaf-on season, canopy variations among the different forest types were enhanced by increased multi-path (σ^o_m) and double-bounce (σ^o_d) scattering (due to the flooding), leading to increased interactions at the canopy layer. This increased canopy scattering (σ^o_c) and decreased net surface scattering (σ^o_s). The variation in total backscatter coefficient due to differences in canopy closure was most obvious at incidence angles of 27.5^o and 39°. During the leaf-off period, variations in canopy closure were minimized due to the overall increase in canopy transmissivity (τ_c) caused by the absence of foliage.

Overall, flooding was easier to detect in the bottomland hardwood forests but the ability to detect flooding varied more with incidence angle during the leaf-on period and more with forest type during the leaf-off period. During the leaf-on period, canopy transmissitivy (τ_c) was primarily responsible for the variation in the ability to detect flooding with increasing incidence angle. It is hypothesized that during the leaf-off period, the surface backscatter coefficient (σ^o_s) (e.g., different levels of soil moisture) was more influential. The relatively large drop in the ability of the smallest incidence angle (23.5^o) to detect flooding may be due to the orientation of canopy leaves, parallel to the surface layer. This orientation may decrease canopy transmissivity (τ_c) at steep (small) incidence angles.

These results indicate that a wider variety of incidence angles and times of the year can be used when monitoring inundation under forest canopies using C-HH band SAR data. This increase in the range of acceptable data and hence frequency of possible data collection may be valuable for the study of highly dynamic events. These events include flooding brought on by tropical storms and other natural disasters and human actions, such as dam releases. The increased data availability has the potential to benefit a wide

variety of natural resource management issues. For example, although monthly monitoring of wetland hydropattern (which is possible when using only one incidence angle) is able to capture the general pattern of flooding in wetlands, higher temporal resolution could better define the length of flooding needed to develop commonly used indicators of wetland presence, such as hydric soils and hydrophytic vegetation. Although scientists agree that prolonged saturation of the upper substrate is necessary for the formation of wetlands, the threshold duration needed and the methods used to establish that threshold are in need of further research (National Research Council 1995). In addition to wetland delineation, the characterization of "normal" or average hydropattern could help to guide the management of existing and the establishment of new wetlands, since establishing natural hydrology is vital.

Although this study was conducted in the forests of northeastern North Carolina, it encourages the examination of multiple incidence angle data elsewhere, especially in other forest types and with other wavelengths and polarizations of SAR data. This is especially important since some earlier studies found that the increase in backscatter coefficient seen in flooded forests does not occur under certain limited circumstances, possibly due to very dense canopies and undergrowth (reduced transmission) or short, small diameter trees (reduced surface for double-bounce; Hess et al. 1990). The consideration of other wavelengths will increase the understanding of scattering and attenuation mechanisms from structures of varying sizes (e.g. leaves, trunks, and branches) while the consideration of other polarizations will increase the understanding of scattering and attenuation mechanisms due to the orientation of these structures.

Chapter 6: Assessment of C-band Synthetic Aperture Radar Data for Mapping Coastal Plain Forested Wetlands in the Mid-Atlantic Region, U.S.A.

6.1 Introduction

The biologic, aesthetic, and economic values of wetlands are now known to be disproportionate to the often small percentage of the landscape they occupy. Wetlands in the Chesapeake Bay Watershed are especially vital as they help maintain water quality and aquatic habitat in one of the nation's largest and most productive estuarine ecosystems (Tiner 1987; Chesapeake Bay Program 1998). Because of the high density of wetlands in the Mid-Atlantic Coastal Plain and the development that is a consequence of population increase, the U.S. Fish and Wildlife Service (FWS) has determined that this region is at high risk for wetland loss. Forested wetlands are especially vulnerable (U.S. Fish and Wildlife Service 2002) due to their inadequate legal protection and often ephemeral flooding or soil saturation, which makes them difficult to identify (Tiner and Burke 1996). Efforts are being made to conserve remaining forested wetlands and many policies have been adopted to support this goal.

A means of continuously monitoring forested wetlands is needed to understand landscape-scale wetland functions, to inform management, to regulate development, and to enforce legal codes. Mapping of the spatial extent, degree of inundation, and periodic variations (seasonal and inter-annual) in wetland hydrology would be a significant advance over current capabilities. Federal and State governments have sponsored wetland

mapping but many of the maps are out of date, especially in areas, such as the Mid-Atlantic, that are undergoing rapid development.

Field mapping and monitoring of forested wetlands is frequently undertaken for small areas, but this is too time consuming and costly at the broader scale required for regional ecosystem management and regulation. While aerial photography is used to map forested wetlands at broader scales, this method is often limited by cloud cover and the need to photograph forested wetlands in winter during the leaf-off period. Furthermore, aerial photograph acquisition and the necessary human interpretation are time consuming and expensive (Tiner 1999), especially since many forested wetlands are difficult to detect in aerial photographs.

Imaging radars, such as synthetic aperture radars (SARs), have the capability to detect the key hydrologic characteristics of wetlands (e.g., spatial patterns of flooding and variations in soil moisture). These systems can be used throughout the year owing to the ability of the instruments to collect images regardless of solar illumination and cloud cover. Therefore, the data collected by these systems are available at a greater temporal frequency (Morrissey et al. 1994; Hess et al. 1995; Wang et al. 1995; Townsend and Walsh 1998; Weiner et al. 2001; Townsend 2002; Kasischke et al. 2003). Most satellite-borne SAR sensors have a repeat-time of approximately one month, and can therefore provide information on seasonal as well as inter-annual variation in inundation, both important aspects of wetlands that cannot be obtained from aerial photography. Another difference is that radar data can be processed semi-automatically and does not require the same degree of expertise needed for aerial photograph interpretation. Nevertheless, SAR data is unlikely to replace aerial photograph interpretation since the spatial resolution of

available SAR instruments is typically about 25 m compared with the potential, sub-meter resolution of aerial photographs. As usual, the newer technology complements the existing methodology and does not replace it.

Although previous studies have demonstrated that C-band SAR data can detect relatively large areas of 100% inundation beneath the forest canopy, C-band SAR data has not been used to map lower amounts of flooding beneath the forest canopy in the smaller floodplains that are more typical of the Mid-Atlantic U.S. In addition, little is known about the ability of C-band SAR to distinguish the different amounts of flooding or levels of soil moisture below the forest canopy that are indicative of hydropattern. Finally, the availability of data and methods that determine the feasibility of forested wetland mapping in the Mid-Atlantic U.S. using C-band SAR has not been documented.

The goal of the research reported here was to investigate whether or not C-band SAR data can be effectively used to map and monitor forested wetlands. Maps created with multi-temporal ERS-1/2 and ENVISAT ASAR data were compared with direct observations of inundation and FWS National Wetland Inventory maps. The contribution of digital elevation data was also explored. The comparison was undertaken at the Patuxent Wildlife Research Center, Maryland, located on the upper Coastal Plain of the Mid-Atlantic, U.S.

6.2.1 Forested Wetlands in the Mid-Atlantic

By far the greatest area of wetlands in the Mid-Atlantic U.S. is found in the Coastal Plain and the majority of these are forested wetlands (Tiner and Burke 1996), which are amongst the most vulnerable to modification (U.S. Fish and Wildlife Service 2002). The importance of these ecosystems is underlined by the fact that they occur in a region that is densely populated and rapidly expanding, therefore increasing the need for wetland functions, such as removal of nutrients from runoff and flood control. Wetland hydroperiod (temporal variations in inundation and saturation) is the single most important factor in the formation and functioning of a wetland (see Chapters 2 and 3). Anticipated changes to the Mid-Atlantic climate (Mid-Atlantic Regional Assessment Team 2000) could further alter the water balance in this region's fresh water ecosystems, including wetlands (see Chapter 2).

6.2.2 Conventional Mapping of Forested Wetlands

Combinations of remotely sensed and field data have been used since the 1970's to map wetlands, and the techniques and quality of data have improved significantly over the past 3 decades. In the U.S. the majority of wetland maps are produced by government agencies, such as the FWS, National Oceanic and Atmospheric Administration (NOAA), and Environmental Protection Agency (EPA). The most comprehensive national mapping was undertaken through the FWS's National Wetlands Inventory (NWI). The NWI was established by Congressional mandate in 1974 (Tiner 1999) and produces wetland maps

using interpretation of mid- to high altitude aerial photographs combined with field verification and collateral data (Federal Geographic Data Committee 1994). The NWI maps usually err less by commission and more by omission; thus, if a wetland is indicated on a NWI map, there is a high probability that one exists or did at the time the photograph was taken (Tiner 1997). Using aerial photographs for wetland mapping requires dedicated teams of expert photointerpreters and is time consuming and relatively expensive (Lunetta and Balogh 1999). The majority of NWI maps for the Mid-Atlantic Coastal Plain were made using aerial photos that are at least 20 years old; therefore, they are frequently out of date in areas undergoing rapid changes in wetland extent, such as that caused by beaver activities, forestry, drainage for agriculture, and various forms of construction.

Owing to the cost and time necessary for mapping wetlands with aerial photography, new techniques are being developed by the FWS and others to update wetland maps (U.S. Fish and Wildlife Service 2002), including the use of satellite data. The advantages of using satellite data for wetland mapping include timeliness, digital format, lower costs, the ease with which it can be integrated with other types of digital geospatial data, and suitability for analysis using geographic information systems (Federal Geographic Data Committee 1992; Dobson et al. 1995;). Unfortunately, visible and near infrared satellite data alone have generally not produced adequate results without the use of additional aerial photography and ground data. Although mid-infrared data provide some increased sensitivity to spatial variations in site hydrology, these data have a relatively low signal to noise ratio (Neusch and Sties 1999). Although Landsat Thematic Mapper data are not used as a primary data source for wetland mapping, they

have proved suitable for updating wetland maps. For example, a technique known as cross-correlation analysis (CCA) uses multispectral satellite data to detect changes in land cover that have occurred since the wetland map was produced (Koeln and Bissonnette 1999). However, CCA is limited to detecting changes within existing mapped wetland polygons, and is therefore dependent on the existence of an accurate baseline map with low omission errors.

6.2.3 Mapping Forested Wetlands Using C-band SAR Data

When monitoring hydrology in forested ecosystems, imaging radars have certain advantages over sensors that operate in the visible and infrared portions of the electromagnetic spectrum (Smith 1997). For example, the scattering and reflection of microwave energy is sensitive to variations in soil moisture and the presence/absence of surface water and this energy is only partially attenuated by vegetation canopies (Townsend and Walsh 1998; Townsend 2002). To understand the ability of radar to detect variations in inundation and soil moisture beneath a forest canopy, as well as the limitations of using SAR, a simple model of backscatter can be employed (see Chapters 2 and 4).

While SARs with certain wavelengths and polarizations are preferable for mapping forested wetlands (see Chapter 2 and 4), data from these systems are not always available. Three spaceborne, C-band SAR systems were collecting imagery at the time of this study: ENVISAT ASAR (C-HH, C-VV, C-HV, and C-VH), Radarsat (C-HH), and ERS-2 (C-VV). The combination of ERS-1 (launched in 1991), ERS-2, and the newly launched ENVISAT satellite provide almost 15 years of continuous C-VV coverage

while RADARSAT (launched in 1995) and ENVISAT provide ten years of historic C-HH data. While these satellites do not automatically collect data over the entire globe, there is an ample supply of historic C-band data for the Mid-Atlantic U.S. Coastal Plain. These sensors continue to collect data and archival scenes can be ordered from the European Space Agency (ESA), the Canadian Space Agency, and the Alaska SAR Facility.

6.3 Methods

The goal of this study was to determine whether or not C-band SAR data could be used to map forested wetlands in the Mid-Atlantic U.S. and whether optical data could improve this ability. To achieve this goal, wetland maps produced from combinations of Landsat Enhanced Thematic Mapper Plus (ETM+), ERS-2, and ASAR SAR data were analyzed. Field data were collected in both uplands and wetlands from the spring of 2003 through the winter of 2004 to judge the accuracy of the wetland maps. The most important of these environmental measurements was percent area flooded, which has a strong effect on the level of backscatter within an image (see Chapter 4). Percent time flooded was compared to the forested wetland maps created in this study, as the more time an area is flooded, the more likely it is to be considered a wetland. Soil moisture measurements were also collected because wet soils can have higher backscatter relative to dry soils. Forest stand characteristics were measured to determine the potential for applying the methods developed under this study to other regions.

6.3.1 Study Area

The research was primarily conducted in the Patuxent Wildlife Research Center (see Chapter 3), but included parts of the U.S. Department of Agriculture's Beltsville Agricultural Research Center, and Fort Meade, M.D. This study focused on upland and wetland areas primarily surrounding the Patuxent River and but also near the Middle Patuxent River, which both drain into the Chesapeake Bay.

The Patuxent River has a well-developed floodplain with numerous wetlands. Other wetlands occur outside the floodplain in depressions and other topographic settings that result in accumulation of water. The braided channels of the Patuxent River are surrounded by levees that gradually decrease in elevation into backwater areas towards the uplands on either side of the floodplain. Much of the floodplain is inundated for only part of the year and the backwater areas can remain flooded for much of the year. The timing of inundation is controlled by annual variations in evapotranspiration, precipitation, and the amount of water coming from upstream dams (see Chapter 3).

6.3.2 Field Observations

Measurements of percent area inundated, soil moisture, basal area and percent tree canopy closure were made in twenty-four 200 x 200 m (4 ha) plots. Eight plots each were located in upland forests, wetland forests (usually backwater areas), and forests of intermediate hydrology (usually found on or adjacent to levees surrounding the stream). Using aerial photographs, the FWS NWI maps, and field reconnaissance, the plots were located in areas of relatively homogeneous forest type and cover and hydrology. Plot

corner locations were measured using a differentially-corrected global positioning system (GPS) and entered into a geographic information system (GIS) for to select the satellite data for each plot. Hydrologic data (inundation and soil moisture) were collected approximately once per month during the spring 2003 through the winter of 2004. For the collection of percent inundation, the 4 ha plots were divided into 64 equal sub-sections of 25 x 25 m and percent inundation was visually estimated in each. For comparison to the satellite data, average inundation was calculated for 1 ha sub-plots (4 per plot). Soil moisture, as volumetric water content, was measured at eight locations distributed evenly within each plot using a time-domain reflectometer (Hydrosense ® meter, Campbell Scientific, Inc.). Five measurements were taken at each location, one at the center and one at a random distance in the four cardinal directions. These 40 measurements were then averaged for comparison to the SAR data. Relative basal area of canopy trees was collected from the 24 plots using a 2 m prism and the Bitterlich method (Shiver and Borders 1996). Basal area was observed in nine areas, spread evenly throughout each plot and averaged for the entire plot. Percept canopy cover was measured at multiple times throughout the year (more frequently during the spring and fall) using digital hemispherical photos of the canopy. These measurements were collected at two backwater, two levee, and two upland sites. Photographs were taken at eight locations, spread evenly throughout each plot. Photos were standardized by tripod height and orientation, and analyzed with HemiView software (Vieglais and Rich 1997). All of the *in situ* measurements made during this study were selected because of their influence on the model of radar backscatter coefficient discussed in Chapter 4.

6.3.3 Remote Sensing Data and Analyses

Although the primary goal of this study was to evaluate the use of C-band SAR

data for the mapping of forested wetlands, part of this study evaluated whether Landsat

ETM+ combined with SAR data improved forested wetland classification. First, the

contribution of optical data to the mapping of forested wetlands was gauged by using it in

combination with the SAR data. Then the abilities of various types of C-band SAR data

under both leaf-on and leaf-off conditions were tested (Table 6.1). The relative merits of

C-HH SAR data and C-VV SAR data for mapping flooded forests were analyzed to test

the finding of previous studies (Townsend 2002; see Chapter 4) that C-HH is superior.

The ability of C-HH data during the leaf-off and leaf-on seasons and the ability of C-VV

during the leaf-off period to map forested wetlands were also evaluated.

SAR Data	Acquisition Dates	Lf-Off	Lf-On	C-HH	C-VV
C-HH ASAR	10/2/03, 10/28/03, 11/6/03, 12/2/03, 3/25/04, 4/20/04, & 4/29/04	X	X	X	
C-VV ASAR	10/2/03, 10/28/03, 11/6/03, 12/2/03, 3/25/04, 4/20/04, & 4/29/04	X	X		X
Leaf-Off ASAR	11/6/03, 12/2/03, 3/25/03, 4/20/04			X	
Leaf-On ASAR	7/15/03, 8/19/03, 10/2/03, 4/29/04, 5/25/04, & 6/3/04			X	
ERS	2/20/97, 3/22/95, 3/27/97, 3/28/98, & 11/27/97	X			X

Table 6.1: Summary of spaceborne SAR data used to map forested wetlands.

ERS (C-VV) and ENVISAT ASAR (C-HH and C-VV) images collected at an

average incidence angle of ~23° were obtained from ESA. The ASAR images were

collected approximately once per month between July 2003 and June 2004. The ERS

images were collected between 1995 and 1998 and selected based on conditions at the

time the scene was collected (only data acquired when the deciduous trees were leafless, on rain-free days with above freezing temperatures were chosen).

The precision corrected data (PRI) calibrated by ESA were further calibrated and coregistered (BEST software, European Space Agency ASAR Science Team 2004). The resultant data were georeferenced to UTM coordinates using a second-order polynomial transformation with nearest-neighbor resampling. The ASAR data were also delivered in PRI format but were geocoded by ESA. The georegisteration was later modified in the image headers to ensure spatial agreement among the data. This was necessary because the supplier's geocoding of the images was not sufficiently accurate for the spatial resolution of this study. The SAR intensity values were converted to dB and an iterative filtering approach was applied to the data to reduce the speckle.

The reduction of speckle is very important to the processing of radar data because it interferes with classification techniques and other algorithms developed for remotely sensed data. A combination of median and enhanced lee filters with kernel sizes of 3 and 5 pixels were used to smooth areas of the image that were similar while attempting to preserve the edges between areas. These filters alter pixel values to remove high frequency noise (speckle), but they attempt to retain high frequency features that are often at edges. The use of small kernel sizes also helped preserve edges. Pixel size was then resampled to 30 m, and a mask based on the Mid-Atlantic Regional Earth Science Applications Center (RESAC) tree canopy cover map (Goetz et al. 2000) was applied to remove all areas with less than 45% tree canopy cover.

Multispectral Landsat ETM+ data from March 2000 were pre-processed by the Mid-Atlantic RESAC (Goetz et al. 2000). Six visible, near-infrared and mid-infrared

114

bands and six tasseled cap (Kauth and Thomas 1976) transforms were used in combination with multi-temporal ENVISAT ASAR data and a USGS 1/3 arc second NED DEM (U.S. Geological Survey 2004) in a decision tree analysis (See5 software, Rulequest Research 2004) to distinguish upland from wetland forests. The decision tree did not find the multispectral or the transformed (tasseled cap) bands to be useful in improving the discrimination of upland forest from wetland forest, and these data were therefore eliminated from further study.

Multi-temporal SAR data were used to create maps of forested wetlands and a map of forested wetland hydroperiod. The first step to producing these maps was to use a principal components analysis (PCA) of the multi-temporal SAR data (Bourgeau-Chavez et al. 2005). PCA further reduces image speckle and isolates the sources of temporal variation between SAR images. PCA reduces temporal autocorrelation and presents information from multiple scenes in one or more principal components, the first containing the dominant temporal trend. Due to the high sensitivity of the scattering of microwave energy to the presence/absence of surface water, the first principal component (PC1) represented variations in image intensity associated with differences in hydrology. PC1 explained the majority of variation found in the multi-temporal data (~95% for all multi-temporal ASAR groups and 87% for the multi-temporal ERS group).

PC1 was used to create two types of maps, a binary map (forested wetland and other) using a threshold value of PC1 and a multi-class map using several thresholds of the PC1 values. To create the binary maps, the first principal component, the USGS DEM, and the forest mask were classified using a decision tree (Environment for Visualizing Images [ENVI], Research Systems, Inc.). Pixels were classified as wetland if

they were in forested areas, on slopes of less than 15 degrees, and if their backscatter coefficient was greater than a value determined by inspection of the SAR and field data. Binary classifications were made using C-HH ASAR data, C-VV ASAR data, leaf-on C-HH ASAR data, leaf-off C-HH ASAR data, and leaf-off C-VV ERS data (Table 6.1). The leaf-on/leaf-off distinction was made using field measurements of percent canopy closure, with visible sky measurements of > 30% being considered leaf-off and measurements < 15% being considered leaf-on. The chosen backscatter boundary values between upland forest and wetland forest were -5 dB, -5 dB, -7 dB, -3.5 dB, and -5 dB for the C-HH ASAR (leaf-off and leaf-on), C-VV ASAR (leaf-off and leaf-on), leaf-on C-HH ASAR, leaf-off C-HH ASAR, and leaf-off C-VV ERS data, respectively. To create the multi-class map, the first principal component from a PCA using C-HH ASAR was used in an unsupervised ISODATA (Duda and Hart 1973) classification and resultant classes were later re-grouped and color-coded to better represent variations in PC1 intensity.

The areas determined to be forested wetland by the SAR classification were compared to areas that were inundated 0%, 5%, 15% and 25% of the time as determined by field observations. A difference matrix was created to compare the classification results with the NWI map.

6.4 Results

Relative basal area within the study plots ranged from 28 to 44 m^2 ha^{-1} (average 35 m^2 ha^{-1}) (Table 6.2). The upland sites had a slightly lower basal area than the levee and backwater sites, possibly due to the use of these areas for agriculture in the recent past.

116

Percent visible sky (the complement of canopy closure) varied between 9% during the leaf-on season to 44% during the leaf-off season (Figure 6.1). A 1999 Forest Inventory and Analysis Program study of Maryland found average basal area to be approximately 23 m^2 ha^{-1} (Forest Inventory and Analysis Program 1999). Therefore the transmittance of radar energy through an average forest would be expected to be greater or equal to that at the Patuxent study site (Wang et al. 1995; see Chapter 4).

		Inundation	Soil Moisture	Tree Height	Basal Area
		%	(% vwc)	(m)	(m2/ha)
Backwater	Average	26	59	28	38
	SD	7	5	2	3
Levee	Average	8	47	28	38
	SD	5	9	2	4
Upland	Average	0	24	26	32
	SD	0	4	1	4

Table 6.2: Average and standard deviation (SD) percent area inundated, soil moisture (% volumetric water content), tree height, and relative basal area for the backwater, levee, and upland field plots at PWRC.

All groups of multi-temporal SAR data used in the binary classification of forested wetlands agreed best with the areas that were flooded on average for the longest period of time according to the field data (25%) and least with areas flooded for the shortest period of time (5%) (Table 6.3). Presumably, this is because areas that were flooded for the longest period had an increased probability of being imaged by the SAR while flooded. Of the five categories of SAR data, the leaf-off C-HH ASAR, the combination of leaf-off and leaf-on C-HH ASAR, and the C-VV ERS classifications had > 90% agreement with the field measurements of percent inundation. As expected, the C-VV ASAR and the leaf-on ASAR had the lowest agreement.
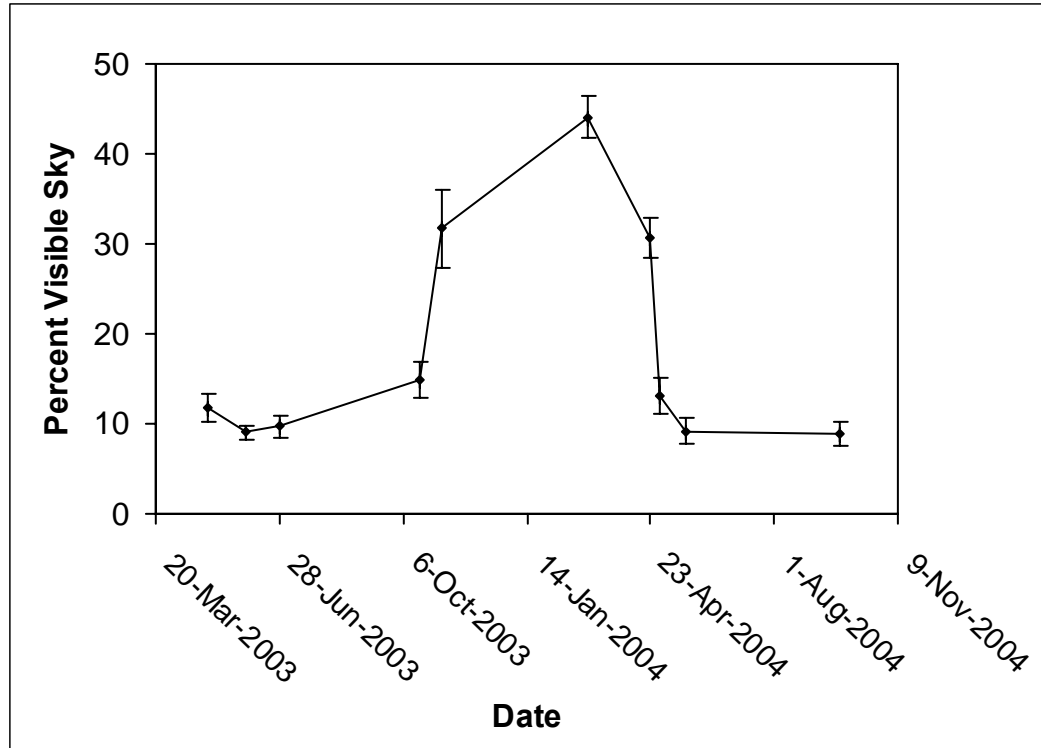
Figure 6.1: Average percent visible sky over ground plots at the PWRC. Temporal variation is due to the deciduous nature of the forest. The error bars on the chart represent one standard deviation.

The comparison of the NWI and the SAR binary classifications (Figure 6.2) agreed with the comparisons of the binary maps with measurement of *in situ* flooding. The difference matrix (Table 6.4) confirmed that the leaf-off C-HH ASAR, the C-HH ASAR (leaf-off and leaf-on), and the ERS (leaf-off, C-VV) performed best, with approximately 90% agreement of wetlands and uplands between the binary classifications and the NWI palustrine forested wetland map. The classifications using the leaf-on ASAR and the C-VV data agreed with the NWI forested wetlands map 89% and 88% of the time, respectively. In the approximately 10% of the area that was in disagreement, the binary SAR classification was consistently more conservative, finding a smaller forested wetland area than the NWI. The ASAR C-VV and the leaf-on C-HH ASAR were found to be most conservative. However, since these classifications were based on a threshold

118

of the first principal component, its inclusiveness can be adjusted to any arbitrary level,

although at the price of increases in the number of false positives (upland areas that are

classified as wetland).

	Wetland Areas (25% Inundation)		
	Correct	Incorrect	Percent
Leaf-off ASAR	263	11	95.99%
C-HH ASAR	264	10	96.35%
C-VV ASAR	173	101	63.14%
ERS	249	25	90.88%
Leaf-on ASAR	239	35	87.23%

	Wetland Areas (5% Inundation)		
	Correct	Incorrect	Percent
Leaf-off ASAR	771	96	88.93%
C-HH ASAR	725	142	83.62%
C-VV ASAR	381	486	43.94%
ERS	765	102	88.24%
Leaf-on ASAR	686	181	79.12%

	Wetland Areas (15% Inundation)		
	Correct	Incorrect	Percent
Leaf-off ASAR	422	21	95.26%
C-HH ASAR	413	30	93.23%
C-VV ASAR	230	213	51.92%
ERS	414	29	93.45%
Leaf-on ASAR	391	52	88.26%

	Upland Areas (False Positives)		
	Correct	Incorrect	Percent
Leaf-off ASAR	389	0	100.00%
C-HH ASAR	389	0	100.00%
C-VV ASAR	387	2	99.49%
ERS	389	0	100.00%
Leaf-on ASAR	389	0	100.00%

Table 6.3: Validation of binary forested wetland maps at the PWRC study site using observations of inundation in field plots. Correspondence between the binary classification and the plot inundation data is expressed in number of pixels correctly and incorrectly classified and percentage agreement. Comparisons are shown for four thresholds of inundation, 25%, 15%, 5% and 0% of the time. Upland areas with 0% inundation were compared to areas not classified as wetland by the binary maps.

Since the majority of the wetlands found in the study area were classified by the

NWI as palustrine, forested, broad-leaved deciduous, temporarily flooded (PFO1A) or

seasonally flooded (PFO1C), these classes were further analyzed. Of these forested

wetland classes, the one with the longer hydroperiod, (PFO1C) was more often identified

as forested wetland by the SAR classification. The classifications using C-HH ASAR

(leaf-off and leaf-on), C-VV ASAR (leaf-off and leaf-on), leaf-on ASAR, leaf-off ASAR, and leaf-off ERS data were 12%, 4%, 16%, 7%, and 2% more likely to recognize the seasonally flooded areas as wetland than the temporarily flooded areas.
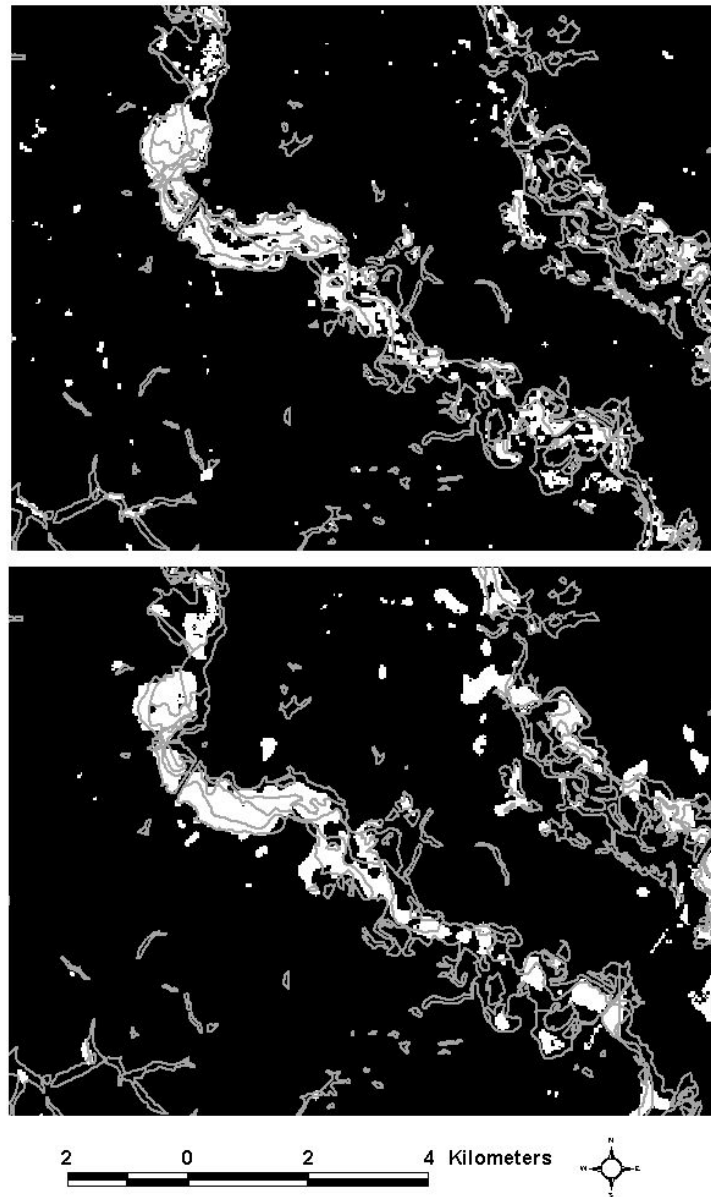
Figure 6.2: Binary forested wetland maps created using multi-temporal SAR data (white areas are forested wetland and black areas are not). Top: ASAR C-HH, bottom: ERS C-VV. NWI palustrine forested wetland boundaries are outlined in gray.

	PFO1 +	PFO1 -	PFO1C +	PFO1C -	PFO1A +	PFO1A -
ASAR C-HH +	6%	2%	1%	6%	4%	4%
ASAR C-HH -	8%	---	1%	---	5%	---
ASAR C-VV +	3%	1%	1%	3%	2%	2%
ASAR C-VV -	11%	---	2%	---	7%	---
ASAR Leaf-off +	7%	3%	1%	8%	5%	4%
ASAR Leaf-off -	7%	---	1%	---	5%	---
ASAR Leaf-on +	4%	2%	1%	5%	3%	4%
ASAR Leaf-on -	9%	---	1%	---	6%	---
ERS +	6%	2%	1%	7%	4%	4%
ERS -	8%	---	1%	---	5%	---

Table 6.4: Comparison of map results with the NWI. A difference matrix (values are percent of total area) between the NWI (top) and the binary map from different types of SAR data (left). Marginal labels: ++ indicates positive agreement (they both denote wetland), -- indicates negative agreement (they both denote upland), and +- indicates that either the NWI or the classification show wetlands where the other did not. The categories of NWI wetlands used were: All palustrine, broad-leaved deciduous forested wetlands (PFO1), palustrine, broad-leaved deciduous forested seasonally (PFO1C) flooded wetlands and palustrine, broad-leaved deciduous forested temporarily (PFO1A) flooded wetlands.

The multi-class forested wetland map, representing relative hydroperiod, was visually compared to the NWI and to *in situ* measurements of percent time flooded. Areas identified as being flooded with greater frequency by the multi-class map followed the NWI boundaries of PFO1C between the seasonally flooded wetlands and the upland edge of the floodplain. The NWI maps cannot be assumed to be completely correct, so the maps were checked in the field. The maps often followed precisely the subtle borders between the backwater areas and the areas of higher topography surrounding the river. Generally it can be seen that the higher elevation areas adjacent to the river were less likely to be flooded than the backwater areas with lower elevations adjacent to the terrace on either side of the floodplain (Figure 6.3). Field observations indicated that the multi-class map, based on the first principal component, was strongly related to wetland hydrology (Figure 6.4). All of the backwater and the upland field plots were correctly identified by the classification.
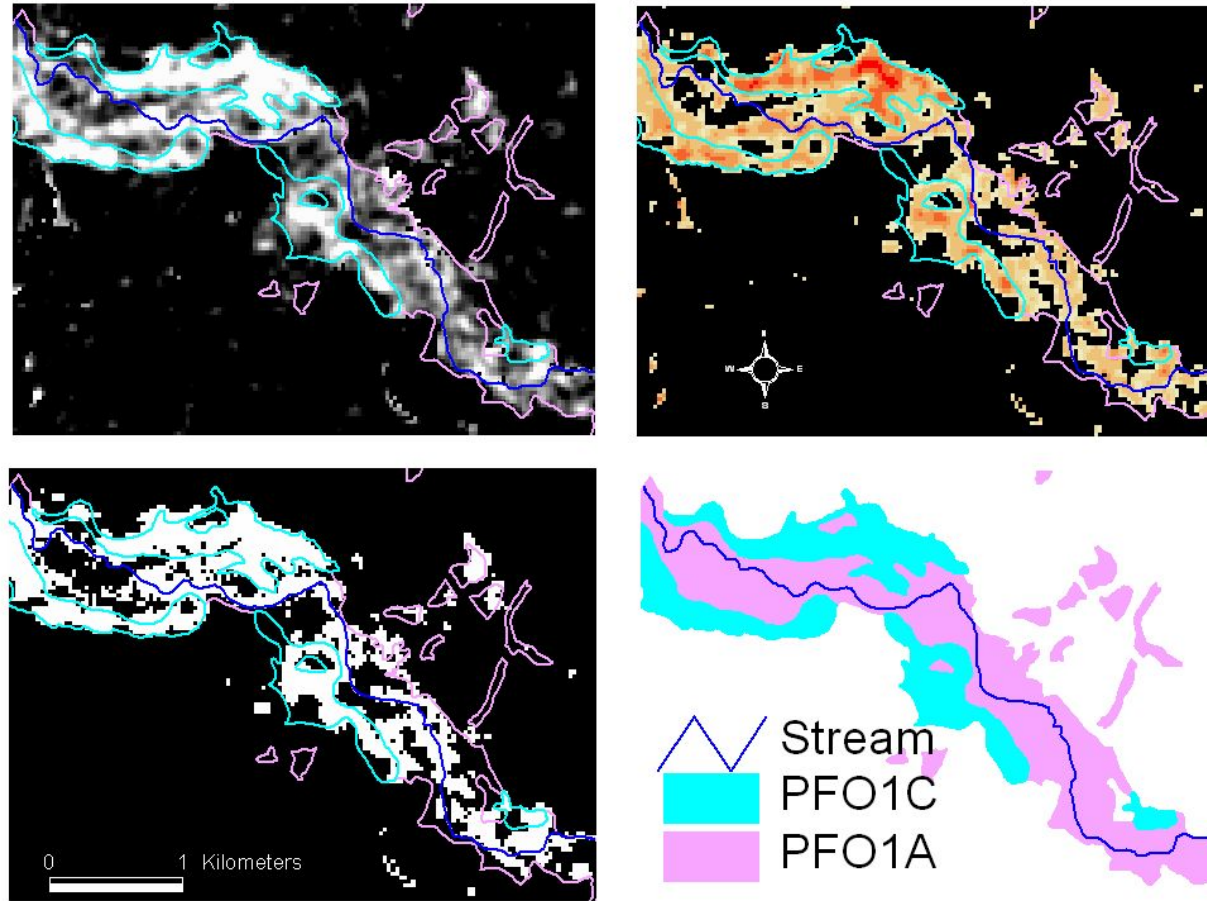
Figure 6.3: Multi-temporal ASAR wetland maps. PC1 (top, left), the binary forested wetland map (bottom, left), and the multi-class forested wetland map (top, right) over-laid with the NWI boundaries for palustrine, broad-leaved deciduous, forest with either seasonally (PFO1C – flooded longer) or temporarily (PFO1A – flooded shorter) flooded wetlands and the boundaries of the Patuxent River. Both types of wetland polygons are shown alone at the bottom right.

122
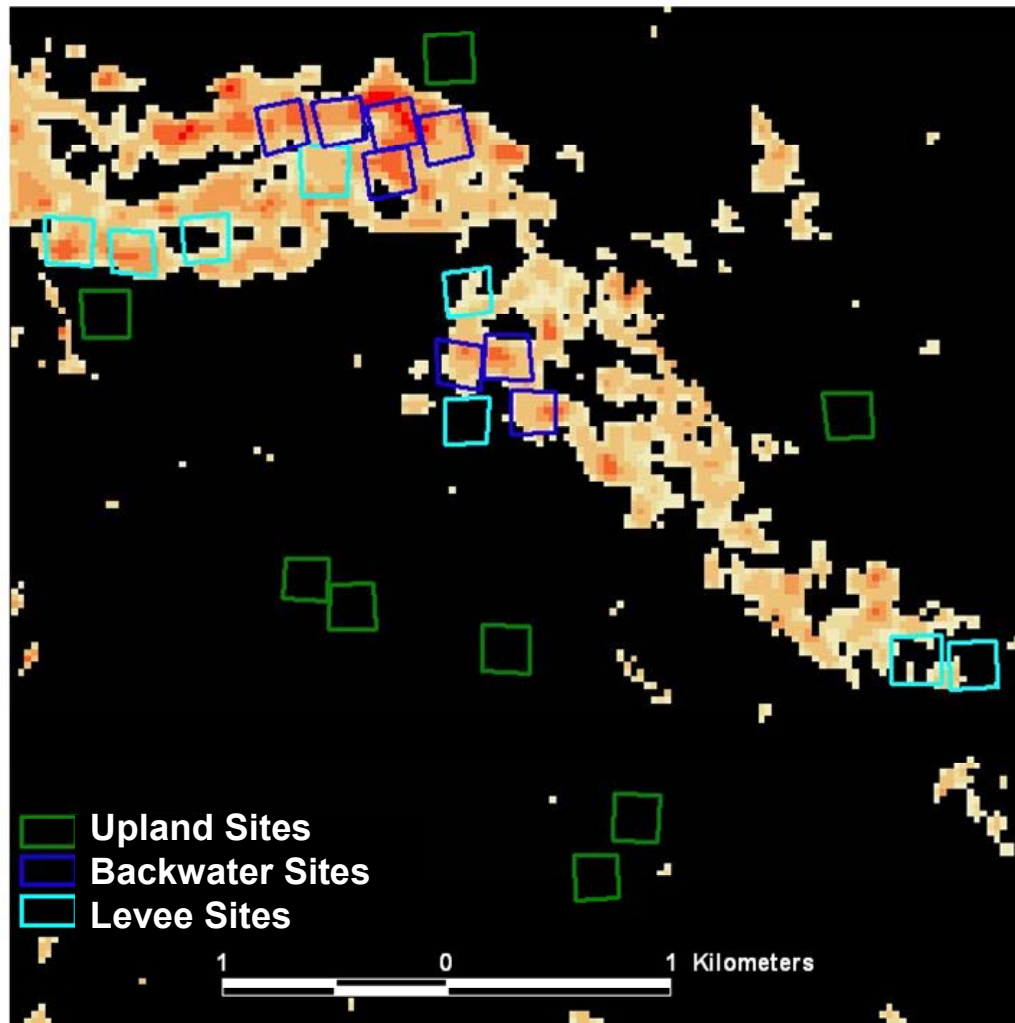
Figure 6.4: Multi-temporal SAR map of wetlands at the Patuxent Wildlife Research Center study site in Laurel, Maryland produced using the first principal component of multi-temporal C-HH ASAR data. Map colors indicate intensity of backscatter coefficient which is correlated with flooding (tan, less flooding to red, increased flooding and black, upland). Ground plot locations show upland sites in green, backwater sites in blue, and levee sites in cyan.

Variations within the backwater and levee plots agreed with differences observed in

the field. For example, the levee plots ranged from drier to wetter; the wettest of these

plots had frequencies of inundation very similar to the backwater sites and the driest of

the plots were almost as dry as the upland sites. When comparing field data to the multi-

class map it was found that wettest of the levee sites (average inundation 20.0%), had a much higher PC1 value than the driest of the levee sites (average percent inundation 1.4%).

6.5 Discussion

With both the binary and the multi-temporal maps, the use of a forest mask (derived from optical data) was an important step to the mapping of forested wetlands because it removed land cover types (such as urban areas containing buildings) that could be confused with wetlands. By removing areas of strong backscatter that were not wetlands, the mask increased the capability of radar backscatter to identify greater flooding and soil moisture. In addition to the forest mask, the DEM further reduced anthropogenic causes of increased backscatter and improved wetland mapping by removing areas where wetlands were unlikely to occur (areas where the slope > 15%). Addition of optical data to the classification did not improve the identification of forested wetlands although optical data have been shown to improve the mapping of multiple wetland types (Lozano-Garcia and Hoffer 1993; Kasischke 1997; Kushwaha et al. 2000).

As expected, the C-HH and leaf-off SAR data used to create binary maps of forested wetlands agreed the most with *in situ* data and the NWI (Chapter 4). However, the C-VV SAR data, especially the ERS C-VV SAR and the leaf-on ASAR data produced maps that were more accurate than expected from previous studies (Wang 1995; Kasischke 1997; Bourgeau-Chavez et al. 2001). In addition, the decreased correlation of the leaf-on ASAR to validation data may not have been entirely due to the attenuation and scattering of the microwave energy by the canopy leaves since there is

124

also less inundation during the times of the year when trees have leaves because of the

increased evapotranspiration (Mitsch and Gosselink 2000).

The more conservative nature of the SAR forested wetland maps as compared to the

NWI maps may have partly been caused by real differences in the location of wetlands at

the time the NWI aerial photographs were acquired and the date of the radar data. There

also could have been some misinterpretation of the aerial photographs and other errors in

preparation of the NWI wetland maps. Wetlands may have been lost to development and

alteration of hydrology during the approximately 20 years between the collection of the

aerial photographs and the radar images. Additionally, the entire floodplain is classified

as wetland according to NWI, even areas of higher elevation without flooding and with

relatively low soil moisture. This may be due to the minimum mapping unit of the NWI

map (1 – 3 acres) or to classification of all floodplain areas as wetlands based on potential

hydrology due to location in the floodplain. Thus the field data collected in the study

provide the most accurate means of assessment of the radar-derived maps.

It is possible that the lower levels of differentiation using both types of C-VV SAR

data between wetlands that are flooded more and less may have been due to the greater

effect of soil moisture and decreased effect of inundation with this polarization. The field

data showed that although the areas classified as having shorter hydroperiods by the NWI

had less flooding (spatially and temporally), these areas often continued to have soil

moisture levels that were higher than the surrounding upland areas. Although average soil

moisture throughout the year in the upland sites was 24%, the wetland sites maintained a

relatively stable 59% soil moisture year round, due mainly to the presence of ground

water near the soil surface (Table 6.2). Kasischke et al. (2003) showed that in non-

wooded wetlands, variations in microwave backscatter were positively correlated with soil moisture. Even in wooded wetlands, the results suggest that the higher backscatter values in wetlands that were not flooded were the result of higher backscatter from wet soils. Furthermore, Wang et al. (1998) showed that soil moisture content and other ground layer characteristics can increase C-HH band backscatter in forests.

The multi-temporal SAR backscatter map detected areas that were most likely to be flooded or have saturated soils, and therefore areas that were most likely to exhibit wetland characteristics such as hydrophytic vegetation and hydric soils (National Research Council 1995; Tiner 1999; Mitsch and Gosselink 2000). Although this map was created from multi-temporal data that did not cover the entire year, differences in backscatter did represent the amount of time these areas were inundated; thus SAR backscatter can be used as a proxy for hydroperiod. Since the varying levels of hydroperiod are not quantitatively defined, this map depicts relative hydroperiod. Further studies are needed to determine whether these relative values could be assigned more quantitative meaning. It is possible that further work with this type of information could better define the period of flooding and soil saturation (hydroperiod) that is necessary to the formation of longer-term wetland characteristics such as hydric soils and vegetation. In this way, maps of hydroperiod developed with multi-temporal SAR data could improve the delineation of wetlands.

While prolonged saturation of the upper substrate is necessary for the formation of wetlands, the threshold levels needed and the methods used to establish that threshold require further work (National Research Council 1995). A major technical challenge is the lack of reliable hydrologic data (National Research Council 1995). Such information

would be particularly helpful in areas where wetland delineation is difficult such as in floodplains where microtopography and young soils can complicate delineation (Lindbo 1997), or in areas that have undergone anthropogenic alteration (Janisch and Molstad 2004). Thus the type of information that multi-temporal SAR provides could assist in ecosystem management decisions.

Rather than the detailed mapping of vegetation types that optical data provide, SAR allows hydropattern, the principal functional characteristic of wetlands, to be mapped. Furthermore the capability of digital analysis allows SAR to be applied to areas that may be undergoing rapid change, providing the important capability of change detection and more detailed studies of hydropattern. Such targeted mapping was recently called for by the FWS (U.S. Fish and Wildlife Service 2002). When attempting to illustrate average hydropattern it is important to collect imagery during times of representative hydrology. With archival radar data, wetland hydrology change detection becomes possible. Maps based on multi-temporal SAR are easily updateable, require fewer resources than conventional mapping methods and can detect spatial gradations in time flooded.

6.6 Conclusions

This study demonstrates that C-band SAR data can map wetlands in deciduous forests in the Coastal Plain of the Chesapeake Bay Watershed. Although similar methods have been used to monitor hydrology in herbaceous wetlands (Bourgaeu-Chavez 2005), the application of these methods to forested wetlands was not thought to be possible (Wang et al. 1995; Kasischke 1997) until a more recent study by Townsend and Walsh (1998). However, this latter study was conducted in an area with large expanses of

flooded forest that undergo close to 100% inundation during portions of the year. This present study found that wetlands can be identified in much smaller floodplain systems that experience a lower range of percent inundation than has been achieved previously.

Although conducted in the Mid-Atlantic U.S., the methods used in this study have wide potential application. All of the data used in this study are or will shortly be available throughout the U.S., and much of it is available in other locations. Although the RESAC tree cover map is not available for the entire U.S., similar maps of forest cover are. Topographic relief can inhibit the use of the method, but DEMs may be used to correct for this effect (Kasischke et al. 1997). SAR data are well calibrated, enabling the creation of forested wetland maps using data from multiple paths and/or rows.

Chapter 7: Summary and Conclusions

7.0 Summary of Results

The goals of this study were to advance the understanding of how variations in climate influence the hydrologic condition of forested wetlands in the Coastal Plain of Maryland and to improve the capability to map and monitor these ecosystems through the use of spaceborne imaging radars.

First, this research explored the link between climate and wetland hydrology near the Patuxent River, Maryland using a conceptual water budget model. The model was developed and verified using detailed, multi-temporal measurements of flooding, and commonly available hydrometeorologic variables (stream discharge, precipitation, and temperature as a proxy for evapotranspiration). Climate variables (precipitation and temperature) and stream discharge, which is largely determined by climate, were found to be highly correlated with inundation at the study site. However, this relationship was modified in some areas by the presence of a dirt road.

After the relationship between climate and wetland hydrology was analyzed, the study investigated the ability of ENVISAT ASAR, C-band synthetic aperture radar (SAR) data to monitor different levels of wetland inundation and soil moisture in and near the floodplain of the Patuxent River. Previous studies (Townsend and Walsh 1998; Townsend 2000; Costa 2004) were conducted at broad spatial scales in large floodplain ecosystems, such as the Amazon in South America or the Roanoke River in the southeastern U. S. Previous studies indirectly estimated areal extent of flooding. In this

study, direct measurements of inundation and soil moisture were made in smaller wetlands (more typical of Mid-Atlantic forested wetlands). Significant differences in C-band backscatter coefficient existed between forested areas of varying hydrology (inundation and soil moisture) throughout the year. These differences in backscatter coefficient were significantly correlated with variations in inundation and soil moisture, even when percent area inundated was much lower than 100%. My results demonstrated that C-band data can be used to detect varying levels of inundation in forested wetlands, even at relatively low levels of percent inundation, instead of simply mapping flooded versus non-flooded areas. In addition, my study established that C-band SAR data are sensitive to variations in soil moisture below the forest canopy.

The ability of C-band SAR data to monitor forested wetland hydrology was found to be limited by polarization (HH versus VV), vegetation phenology, and incidence angle. Although recent studies have found that C-HH data can be used to accurately monitor wetland inundation in temperate forests (Townsend and Walsh 1998; Townsend 2000), and that C-VV data have some limited potential to map forested wetland flooding during the leaf-off season (Kasischke et al. 1997; Townsend 2000), this study was the first to directly compare the abilities of C-HH and C-VV data to monitor forested wetland hydrology throughout the year. C-HH backscatter coefficients were found to be better correlated with hydrology (inundation and soil moisture) than C-VV backscatter coefficients at all times of the year. The correlation of C-HH backscatter coefficients with hydrology (inundation and soil moisture) was always stronger during the leaf-off relative to the leaf-on season. Correlation of C-VV backscatter coefficients with inundation was

strongest during the leaf-off season but C-VV backscatter coefficients were better correlated with soil moisture during the leaf-on season.

The impact of incidence angle on the ability of C-band SAR data to monitor forested wetland hydrology was explored using Radarsat C-HH data collected over the Roanoke River floodplain during the leaf-off and leaf-on seasons. Although it is known that incidence angle can have a large effect on the ability of C-band SAR data to monitor flooding, direct studies of this effect, especially those including several different incidence angles, are very limited. This study found that the difference in backscatter coefficients between flooded and non-flooded areas does not sharply decline with increasing incidence angle, as predicted. In addition, although data with the smallest incidence angle (average incidence angle of 23.5°) were predicted to be best able to differentiate between flooded and non-flooded sites, they were actually least able to do so.

Finally, the accuracy of forested wetland maps produced using multi-temporal C-HH and C-VV SAR data was investigated. Maps, produced using both polarizations of SAR data, were found to have relatively high accuracy levels. This study was the first step towards exploring the ability of C-band SAR to aid in the regional mapping of forested wetlands.

7.1 Review of Hypotheses

To meet this study's first goal (to advance the understanding of how climate influences forested wetland hydrology), two sets of hypotheses were developed. The first

set of hypotheses guided research to define the sensitivity of C-band SAR microwave

energy to forested wetland hydrology, while the second set explored limitations on using

C-band SAR data to monitor forested wetland hydrology.

Hypothesis A1: In the Coastal Plain of Maryland, variations in precipitation,

 evapotranspiration, and stream discharge cause predictable changes in forested

wetland hydropattern that can be measured using SAR data.

Hypothesis A1a: Changing levels of inundation will affect the radar backscatter

signature in forested wetlands, with increases in backscatter when forests are

inundated and decreases in backscatter when they are not.

Hypothesis A1b: Radar backscatter will be positively related to soil moisture, with

higher soil moisture resulting in higher radar backscatter.

Significant linear correlations were found between inundation and stream

discharge (partial r^2 as high as 0.94, $p = <0.0001$), precipitation (partial r^2 as high as

0.58, $p = .0004$), and/or evapotranspiration (as indicated by temperature) (partial r^2 as

high as 0.70, $p = 0.0001$) in the study plots with increases in stream discharge and

precipitation increasing inundation and increases in temperature decreasing inundation.

Correlations (r^2) of models regressing inundation against discharge, precipitation, and

temperature for the individual plots varied from an r^2 of 0.41 to 0.92, with all but two

greater than or equal to 0.65 ($p < 0.05$). These correlations support the hypothesis that climate influences the hydrologic condition of Mid-Atlantic Coastal Plain wetlands. The majority of time hydrology was monitored at the field site was during 2003, an usually wet year. For that reason, the relationship between inundation and hydrology could differ during periods of average or lower than average precipitation. Even though most of the study site was relatively undisturbed, the relationship between inundation and stream discharge was found to be modified in one area by a road. The plots separated from the stream by a dirt road were not significantly correlated ($p < 0.05$) with stream discharge. Due to the relatively natural condition of the study site, the modification of the relationship between climate and hydropattern is likely to be more pronounced at other, more urban locations. These results partially support hypothesis A1.

Significant differences in C-HH and C-VV backscatter coefficients (ANOVA, F = 166.4, $p < 0.0001$; Tukey's studentized range [HSD] test, $p < 0.05$) were found between areas with higher levels of inundation and soil moisture (backwater wetlands) and areas with lower levels of inundation and soil moisture (uplands) during the entire year. Higher levels of inundation and soil moisture were correlated (C-HH leaf-off $r^2 = 0.47$, leaf-on $r^2 = 0.31$; C-VV leaf-off $r^2 = 0.26$, leaf-on $r^2 = 0.13$; all significant at $p < 0.0001$ level) with increases in radar backscatter coefficient when considering all plot locations. Higher levels of inundation were correlated with increases in backscatter coefficient (C-HH leaf-off $r^2 = 0.34$, leaf-on $r^2 = 0.25$, both significant at $p = < 0.0001$ level; C-VV leaf-off $r^2 = 0.11$, significant at $p = 0.0024$ level, leaf-on $r^2 = 0.06$, significant at $p = 0.0071$ level), when only backwater and levee plots were considered. Higher levels of soil moisture were correlated with increases in backscatter coefficient (C-HH leaf-off $r^2 = 0.58$, leaf-on

$r^2 = 0.24$; C-VV leaf-off $r^2 = 0.55$, leaf-on $r^2 = 0.36$; C-HH leaf-on significant at $p = 0.0004$ level and all others significant at the $p = < 0.0001$ level), when considering all plot locations. A positive linear relationship was found between backscatter coefficient and inundation, as well as backscatter coefficient and soil moisture. These findings partially support hypothesis A1 and support hypotheses A1a and A1b.

The following set of hypotheses were designed to test the limitations of using C-band SAR data to monitor forested wetland hydrology.

Hypothesis B1: Differences in the character of the SAR sensor (system parameters) will influence the ability of spaceborne SARs to monitor hydrologic conditions in forested wetlands.

Hypothesis B1a: At smaller incidence angles, microwave energy from C-band SARs will be more sensitive to inundation under forest canopies than at larger incidence angles.

Hypothesis B1b: Relative to C-VV, microwave energy from C-HH SARs will be more sensitive to hydrologic variations under tree canopies.

Hypothesis B2: Variations in plant phenology will influence the ability of spaceborne SAR data to monitor the hydrologic condition of forested wetlands

Hypothesis B2a: Microwave energy from C-HH and C-VV SARs will be more sensitive to changes in hydrology during times of low canopy closure.

Hypothesis B2b: Because of its greater ability to penetrate the forest canopy, microwave energy from C-HH SARs will be sensitive to variations in hydrology over a longer time period than microwave energy from C-VV SARs.

C-band SAR data collected at smaller incidence angles were found to be less able to detect variations in hydrology than C-band SAR data collected at larger incidence angles. There was a difference of 3.1 dB between average backscatter coefficients in inundated and non-inundated sites using C-HH data with an average incidence angle of 27.5^o during the leaf-on season and 2.8 dB during the leaf-off season. There was only a difference of 1.3 dB in average backscatter coefficient using C-HH data with an average incidence angle of 23.5^o during the leaf-on season and 2.1 dB during the leaf-off season. C-band SAR data collected at larger incidence angles were better able to differentiate between flooded and non-flooded areas than had been predicted based on the findings of previous studies. This analysis did not support hypothesis B1a since data collected at smaller incidence angles were actually less able to detect differences in inundation. However, it did partially support hypothesis B1 since incidence angle did affect the ability of C-band SAR data to detect differences in flooding.

Backscatter coefficients from C-HH SAR data were found to be better correlated with hydrology (inundation and soil moisture) than backscatter coefficients from C-VV data, at all times of the year. When regressed against inundation and soil moisture, C-HH

135

backscatter coefficients had an r^2 0.21 higher than C-VV backscatter coefficients during the leaf-off season and an r^2 0.18 higher during the leaf-on season. Backscatter coefficients from C-HH SAR data were found to be better correlated with inundation than backscatter coefficients from C-VV data at all times of the year. When regressed against inundation, C-HH backscatter coefficients had an r^2 0.23 greater than C-VV backscatter coefficients during the leaf-off season and an r^2 0.25 greater during the leaf-on season. Backscatter coefficients from C-HH SAR data were also found to be better correlated with soil moisture than backscatter coefficients from C-VV SAR data at all times of the year. When regressed against soil moisture, C-HH backscatter coefficients had an r^2 0.34 higher than C-VV backscatter coefficients during the leaf-off season and an r^2 0.19 greater during the leaf-on season. This analysis partly supports hypothesis B1 and supports hypotheses B1b and B2b.

The ability of C-band SAR data to detect variations in hydrology was better during the leaf-off period than the leaf-on period. Backscatter coefficients from both polarizations of C-band data were found to be better correlated with hydrology (inundation and soil moisture) during the leaf-off season (relative to the leaf-on season). C-HH backscatter coefficients had an r^2 0.16 higher during the leaf-off season relative to the leaf-on season and C-VV backscatter coefficients had an r^2 0.13 higher during the leaf-off season relative to the leaf-on season. Backscatter coefficients from both polarizations of C-band data were found to be better correlated with inundation during the leaf-off season (relative to the leaf-on season). When regressed with inundation, C-HH backscatter coefficients had an r^2 0.09 higher during the leaf-off season relative to the leaf-on season and C-VV backscatter coefficients had an r^2 0.05 higher during the leaf-off

season relative to the leaf-on season. Backscatter coefficients from C-HH data were found to be better correlated with soil moisture during the leaf-off season (relative to the leaf-on season). C-HH backscatter coefficients had an r^2 0.03 higher during the leaf-off season relative to the leaf-on season when regressed against soil moisture. Surprisingly, backscatter coefficients from C-VV data were found to be better correlated with soil moisture during the leaf-on season (relative to the leaf-off season). When regressed against soil moisture, C-VV backscatter coefficients had an r^2 0.12 higher during the leaf-on season relative to the leaf-off season. These analyses partly support hypothesis B1, support hypothesis B2, and mostly support hypothesis B2a

To meet the second goal of improved forested wetland mapping and monitoring, one hypothesis was developed.

Hypothesis C1: At intermediate spatial scales (30m), image processing approaches that use C-band SAR data are better able to differentiate forested wetlands from forested uplands than approaches that use optical data.

It was found that Landsat ETM+ did not improve the discrimination of forested wetlands from forested uplands. This is not surprising, as many of the intermediate scale mapping initiatives that identify forested wetlands do so with additional ancillary data (Dobson et al. 1995; personal communication Dmitry Varlyguin, 2004). The forested wetland maps produced using SAR data had relatively high accuracy levels. For example, wetland maps produced using C-HH ASAR data agreed with areas that were identified using *in situ* data as being flooded 25% of the time, 96% of the time during the leaf-off

season and 87% of the time during the leaf-on season. The same maps agreed with areas that were identified using *in situ* data as being flooded 5% of the time, 89% during the leaf-off season and 79% during the leaf-on season. These results support hypothesis C1.

7.2 Conclusions and Implications

C-band backscatter coefficient varied as a function of ground conditions (primarily canopy closure, inundation, and soil moisture) and sensor characteristics (incidence angle and polarization). The simple model of total backscatter coefficient presented in Chapters 4 and 5 can be used to summarize how these varying properties affected total backscatter coefficient and/or to explain how they control the ability of C-band SAR data to detect changes in hydrology caused by climate change, human impact, or other avenues of hydrologic alteration. Increasing canopy closure decreases the transmissivity of the canopy layer (τ_c) and increases backscatter from the crown layer (σ^o_c). When the transmissivity of the crown layer (σ^o_c) decreases, less energy is able to penetrate the canopy layer and interact with the surface layer (σ^o_s) where variations in hydrology largely determine the amount of backscatter coefficient contributed to total backscatter coefficient (σ^o) from the surface layer. When the entire year was considered, canopy closure was found to be better correlated with backscatter coefficient than inundation, although it was found to be less correlated with total backscatter coefficient (σ^o) than either soil moisture or inundation and soil moisture combined. As previous literature has shown (Wang et al. 1995), the influence of canopy closure on the ability of C-band SAR data to detect changes in forested wetland hydropattern (inundation and soil moisture)

was considerable. Although the correlation of total backscatter coefficient with inundation and soil moisture was greater than the correlation between total backscatter coefficient and canopy closure, it would be difficult to differentiate between the influences of hydrology and canopy closure without detailed ground measurements. In the absence of such data, the influence of canopy closure on total backscatter coefficient should be controlled for by limiting the analysis to either the leaf-on or the leaf-off season. The results from both seasons can later be related to one another to gain an annual perspective on hydrologic fluctuations.

Inundation and soil moisture are both positively related to total backscatter coefficient (σ^o) and they both act at the surface layer (σ^o_s), but the mechanisms controlling their relationship with total backscatter coefficient differ. The presence of inundation at the surface layer eliminates the surface backscatter coefficient (σ^o_s) by causing specular reflectance of incoming energy (all microwave energy is reflected away from the sensor). However, tree trunks can provide a surface for the reflection of that energy and in this way redirect energy back towards the sensor as double-bounce backscatter (σ^o_d). In addition, the trunk and/or canopy layers can serve to redirect energy towards the sensor as multi-path scattering (σ^o_m). In this way, inundation can greatly increase total backscatter coefficient (σ^o) by increasing double-bounce (σ^o_d) and multi-path scattering (σ^o_m). Increases in soil moisture in non-inundated areas can also increase multi-path scattering (σ^o_m), and greater soil moisture can increase the surface backscatter coefficient (σ^o_s) by increasing the dielectric constant of the soil (see Chapter 2).

My research found the influence of soil moisture on backscatter coefficient to be greater than that of inundation. However, the collinearity of inundation and soil moisture

139

makes the separation of their influences on backscatter coefficient (Chapter 4) difficult. The elimination of upland sites from the analysis of the relationship between inundation and backscatter coefficient removed a large degree of the influence of soil moisture from that analysis. However, although the influence of inundation was removed from a portion of the analysis that examined the influence of soil moisture on backscatter coefficient, it was not removed from the regression analyses (soil moisture regressed against backscatter coefficient; Table 4.6) because there were very few times in which levee or backwater sites were not inundated. For this reason, the influence of soil moisture on total backscatter coefficient (σ^o) may be exaggerated relative to the influence of inundation. This should be kept in mind when interpreting the analyses of inundation and soil moisture. This study demonstrated the ability of 1) C-HH SAR data to differentiate areas of varying hydropattern (inundation and soil moisture) during the leaf-off and the leaf-on seasons; 2) the ability of C-VV SAR to detect hydropattern during the leaf-off season; and 3) the ability of C-HH SAR to detect relatively small variations in inundation during the leaf-off season.

Some additional generalization can be made concerning the analyses of inundation and soil moisture that may benefit similar studies. The regression analyses of inundation and soil moisture found that the influence of polarization on the ability to detect hydropattern was greater than the influence of season. When monitoring hydrology in forested wetlands, leaf-on C-HH data were better correlated with hydropattern than leaf-off C-VV data. C-VV SAR data appear to be more sensitive to variations in soil moisture than to variations in inundation. An example of the result of this increased sensitivity to soil moisture can be seen in Chapter 6. Note the floodplain on the map created using ERS

data (C-VV) as compared to the floodplain on the map created using ASAR C-HH data (Figure 6.2). The ERS data identified the entire floodplain as forested wetland whereas the ASAR C-HH data did not. It is hypothesized that this is because the entire floodplain had much higher soil moisture values than the surrounding uplands (wetlands = 59%, levee = 47%, and uplands = 24% vwc), even though large portions of the floodplain were never inundated. The ASAR C-HH data, on the other hand, only identified a portion of the floodplain as wetland since C-HH data were more sensitive to inundation than C-VV data. In other words, the C-VV data differentiated forested wetland from non-forested wetland based on varying levels of soil moisture while the C-HH data did so based on inundation. It is likely that the C-HH data were generally more affected by inundation than soil moisture although the relative influence of inundation and soil moisture combined on C-HH data was greater than it was for the C-VV data.

The polarization of C-band SAR energy and the angle at which that energy intercepts the surface of the Earth (incidence angle) also influence the ability of C-Band SAR data to monitor variations in hydropattern. The polarization of C-band SAR data primarily influences the attenuation of that energy in the trunk layer (τ_c) although it can also influence the transmissivity of the crown layer (τ_t), depending on the size and orientation of branches and leaves (Townsend 2002). C-HH microwave energy is less attenuated by the trunk layer (τ_t) than C-VV, leaving more C-HH energy to be scattered at the surface layer (σ^o_s) (see Chapters 2 and 4). The influence of inundation and soil moisture on total backscatter coefficient should therefore be greater with C-HH than C-VV SAR data. This research supports previous studies (Hess et al. 1995; Wang et al. 1995), finding that C-HH SAR data were better correlated with inundation and soil

moisture than C-VV SAR data during the entire year. This study found that C-HH SAR data could monitor variations in hydropattern (inundation and soil moisture) throughout the year and could monitor changes in area inundated during the leaf-off season. On the other hand, this study supports the use of C-VV data to monitor changes in hydropattern (inundation and soil moisture) only during the leaf-off season.

The angle of incidence influences the attenuation of C-band microwave energy primarily in the canopy (τ_c) but also in the trunk layer (τ_t) as well as scattering at the surface layer (σ^o_s) (see Chapter 5). Previous studies considered smaller incidence angle SAR data superior to larger incidence angle SAR data (Richards et al. 1987; Ford and Casey 1988; Hess et al. 1990; Wang et al.1995; Bourgeau-Chavez et al. 2001; Toyra et al. 2001), but this research did not entirely support those findings. Although a gradual decrease in total C-HH backscatter coefficient (σ^o) was found with increasing incidence angle, the data collected at the smallest incidence angle considered (23.5^o) were least able to differentiate between flooded and non-flooded areas. C-HH SAR data with average incidence angles of 27.5^o and 33.5^o were best able to identify areas of flooding during both leaf-on and leaf-off seasons.

C-HH band ASAR data collected at an average incidence angle of 23° were able to detect variations in hydropattern (inundation and soil moisture) throughout the year and relatively small variations in flooding during the leaf-off season in a small Mid-Atlantic deciduous floodplain wetland. Based on the findings described in Chapter 5, the results described in Chapter 4 may be improved by collecting these data at slightly larger incidence angles (between 27.5^o and 33.5^o). However, that cannot be confirmed because although the influence of incidence angle on the ability of C-band SAR data to detect

flooding (Chapter 5) was investigated in an area of primarily deciduous forest, the tree species and morphology (primarily leaf size) varied considerably from the study area used for the rest of the research (Chapters 3, 4, and 6). Based on these findings, I would suggest that C-HH data with an incidence angle of 27.5^{o} be used for future studies of forested wetland hydrology. However, ideally the suitability of SAR data with different incidence angles should be investigated at the study site in question. This is especially important because my study did not investigate the influence of incidence angle on soil moisture.

Although forested wetlands comprise over half of the wetlands in the United States, these areas have been difficult to monitor with conventional ground-based and optical remote sensing methods, leading to a dearth of forested wetland hydrologic data. The ability of C-HH data to monitor wetland hydropattern (inundation and soil moisture) throughout the year is a significant improvement on current ground and optical-based techniques used to map forested wetlands and forested wetland hydrology. By linking climate and anthropogenic influence to hydropattern and demonstrating that C-band SAR data can detect these variations in hydropattern, this study established that C-band SAR data could be used to study variations in hydropattern caused by changes in climate or humans. The ten year historic record of C-HH band data should allow for the detection of changes in forested wetland hydropattern that have occurred over the past decade, including those caused by anthropogenic, natural (e.g. beavers and fluvial processes), and meteorological forces (e.g. periods of drought and flood). The ability of C-HH data to detect relatively small changes in percent area inundated during the leaf-off season could inform studies of wetland function linked directly to flooding, such as those concerning

the ability of wetlands to reduce flooding downstream or the suitability of certain wetlands as amphibian habitat. The capability of C-VV SAR data to detect changes in inundation and soil moisture during the leaf-off period, extends the capability of C-band SAR data to monitor forested wetland hydrology another 4 years (back to 1991). Although leaf-on hydrologic conditions can not be monitored with C-VV data, wetlands are most likely to be inundated during the leaf-off period when evapotranspiration is low and C-VV data can detect flooding during this crucial period.

The information provided by C-band SAR data has previously been unavailable at this spatial and temporal scale, is readily actionable, and can be used to make important ecosystem management decisions. This information can be used to help predict how hydrology will respond to climate change and anthropogenic influence, the impact of these changes on wetland function, and to judge the success of projects designed to create and improve wetlands. Multi-temporal C-band SAR data could be used to establish a baseline of normal forested wetland hydropattern that could be used as an index of forested wetland health. Doing so would allow broad-scale monitoring and assessment of these ecosystems as they are under increasing pressure from climate change and anthropogenic impacts. The characterization of "normal" hydropattern could also help to guide the establishment of new wetlands and determine the success of mitigation projects, since establishing natural hydrology is vital to the success of these projects. Forested wetlands have been the most difficult type of wetland to create, and incorrect hydrology is the most common reason these wetlands fail to function as intended (Hammer 1992; Konyha 1995). The lack of readily available hydrologic information is

often cited as a substantial limitation to the success of the creation and assessment of forested wetlands (Cole and Brooks 2000; Konyha 1995).

In addition, this study demonstrated the successful use of C-band SAR data to map wetlands in deciduous forests in the Chesapeake Bay Watershed. Forested wetlands, like all dynamic ecosystems, require an easily updateable monitoring system as well as synoptic inventories. This is especially vital in areas like the Mid-Atlantic Coastal Plain where population pressure on natural resources is severe and will continue to increase in the future. Multi-temporal C-band SAR data could be used to develop more realistic maps of forested wetlands since they could be represented as dynamic systems and the boundaries of flood extent could be observed during multiple times of the year and during years of varying climate. Maps based on multi-temporal SAR data are easily updateable and require fewer resources than conventional mapping methods.

C-band SAR data could be used to update regional mapping efforts, such as the National Wetland Inventory (NWI), in areas of rapid development. Although other techniques, such as cross-correlation, have been developed to update NWI maps, these techniques are dependent on accurate base maps and can not detect the addition of wetlands outside existing polygons. Maps created with SAR data could detect the addition of wetlands, which is especially necessary given the recent presidential mandate to move beyond the federal policy of "no net loss" and begin to increase the quantity and quality of U.S. wetlands. As part of this new policy, the federal government has set a goal to "restore, improve, and protect at least three million acres of wetlands over the next five years (Executive Office of the President Council on Environmental Quality 2005)." According to the Executive Office of the President Council on Environmental Quality

(2005), 328,000 acres of wetlands have already been restored or created since April 2004. The speed of digital analysis allows SAR technology to be applied to target areas that may be undergoing rapid change, providing change detection and more detailed studies of hydropattern. Such targeted mapping was recently called for by the U.S. Fish and Wildlife Service (FWS) (U.S. Fish and Wildlife Service 2002).

These types of maps would not replace, but could complement existing optical forested wetland maps. The use of radar and optical data together for forested wetland mapping is valuable since each is sensitive to distinct aspects of the wetland environment (Lyon and McCarthy 1995; Sahagian and Melack 1996; Ramsey et al. 1998; Kushwaha et al. 2000). Rather than detailed mapping of vegetation types, SAR data allows for the principal functional characteristic of wetlands to be monitored. This research supports the view that advances in identifying and monitoring forested wetlands will come from the joint application of multiple types of remotely sensed data (Wilen and Smith 1996).

Currently, one multiple incidence angle ($\sim15^{o} - 45^{o}$), dual-polarization sensor (ENVISAT ASAR, capable of collecting HH, VV, HV, and VH), one single incidence angle ($\sim23^{o}$) C-VV sensor (ERS-2), and one multiple incidence angle ($\sim20^{o} - 50^{o}$), C-HH sensor (Radarsat-1) are currently collecting satellite-borne C-band SAR data. Radarsat-2 is scheduled to be launched in 2006. It will collect similar data to Radarsat-1 plus it will collect C-band HH, VV, HV, and VH data at a finer spatial resolution than any other commercial SAR sensor. Both ERS-2 and Radarsat-1 have exceeded their design lifetimes (both being in orbit for about ten years) but continue to collect data. The combination of ASAR (launched in 2002) and Radarsat-2 should extend the C-band SAR

data record well into the future, adding to the historic record and increasing the ability to use C-band data to monitor long-term trends in wetland hydrology.

7.3 Future Research Directions

This dissertation lays the groundwork for research further exploring the abilities and restrictions of C-band SAR data, the maps created with these data, the impact of hydrology on wetland condition and function, and the linkage of wetland hydrology to climate change and anthropogenic impact.

The role of incidence angle should be further considered as it was found to have a large impact on the ability of SAR data to monitor forested wetland hydrology and the use of a greater range of incidence angles for this purpose could improve the temporal resolution of such studies. The influence of incidence angle on the ability of C-band SAR data to monitor forested wetland flooding should be investigated in other types of forests. This is especially important since several earlier studies found that the increase in backscatter seen in most flooded forests does not occur in some areas (Hess et al. 1990). In addition, the effect of different incidence angles on the ability of C-VV data to monitor inundation and the ability of C-HH and C-VV data to monitor soil moisture should be examined.

The launch of PALSAR by the Japan Aerospace Exploration Agency in 2006 will provide longer wavelength (L-band, 24 cm wavelength) data at multiple incidence angles. Although a similar sensor was flown aboard the JERS satellite, it only collected data at one incidence angle (39°) and that satellite has since ceased collecting data. The data collected by PALSAR (L-band) will allow the investigation of the influence of incidence

147

angle on the ability of L-band data to monitor inundation and soil moisture below the forest canopy. These longer wavelength data could help explain why there is a substantial decrease in the ability of C-band data to differentiate between flooded and non-flooded areas at an incidence angle of 23.5°.

Although this study demonstrated the ability of multi-temporal C-band SAR data to map forested wetlands in the Mid-Atlantic U.S., this technique needs to be tested over a broader area covering a wider variety of land cover and forested wetland types. This broader area should include more urban areas to test the ability of the forest mask to eliminate urban corner-reflectors, such as buildings, and to assess the impact of these corner-reflectors on the accuracy of the map when not eliminated. It should also include areas with different concentrations and distributions of wetlands. This is especially important since the ability of principal component analysis to map hydrology depends on the size of the area that experiences flooding and soil saturation and duration of flooding and soil saturation.

Additional field studies and analyses are needed to more quantitatively examine the relationship between different hydroperiods, as exhibited on the SAR-based maps, and duration of flooding and saturation in the field. When this is done, the relationship between different hydroperiods and field indicators of wetland presence (hydrophytic plants and hydric soils) or other indicators of wetland functioning (e.g. accumulation of organic matter or species composition) could be assessed. Such studies could better define the threshold circumstances necessary for wetland formation. Although all agree that prolonged saturation of the upper substrate is necessary for formation of wetlands, threshold circumstances needed to form wetlands and the methods used to establish that

threshold are in need of further research. Such information would aid in the delineation of wetlands in the field. In addition, information regarding hydroperiod could inform the study of numerous wetland functions. For example, information regarding hydroperiod could be linked to ground data to benefit the study of forested wetlands as habitat for various animal species, as a chemical, nutrient, and carbon transformer, or as a retention area for flood waters.

This study established the ability of C-band SAR data to monitor patterns of forested wetland inundation and soil moisture throughout the year. However, the period over which this study was conducted was abnormally wet, at least in 2003, and may not be representative of normal annual fluctuations in hydrology. Therefore, the extension of this research during a year of normal precipitation could be beneficial. In addition, the historic record of C-HH imagery and the hydrologic signature in these data should be explored, especially during drier years.

Finally, a study of hydropattern in two wetlands, one built or heavily impacted by society and one natural, could by undertaken using C-band SAR data. Such a study would be especially useful if it were conducted over multiple years with varying climate. Broader scale studies may be able to help determine whether the cumulative impact of society on wetland hydropattern is to increase flood variability due to "flashier" stream flow or to decrease variability due to the impact of roads and other barriers to flow.

Chapter 7: Citations

Baber, M. J., E. Fleishman, K. J. Babbitt and T. L. Tarr (2004). "The relationship between wetland hydroperiod and nestedness patterns in assemblages of larval amphibians and predatory macroinvertebrates." Oikos **107**(1)**:** 16-27.

Bedford, B. L. (1996). "The need to define hydrologic equivalence at the landscape scale for freshwater wetland mitigation." Ecological Applications **6**(1)**:** 57-68.

Blair, J. B., D. Rabine and M. Hofton (1999). "The Laser Vegetation Imaging Sensor (LVIS): A medium-altitude, digitization only, airborne laser altimeter for mapping vegetation and topography." ISPRS Photogrammetry and Remote Sensing **54:** 115-122.

Bolster, C. H. and J. E. Saiers (2002). "Development and evaluation of a mathematical model for surface-water flow within the Shark River Slough of the Florida Everglades." Journal of Hydrology **259:** 221-235.

Bourgeau-Chavez, L. L., E. S. Kasischke, S. M. Brunzell, J. P. Mudd, K. B. Smith and A. L. Frick (2001). "Analysis of space-borne SAR data for wetland mapping in Virginia riparian ecosystems." International Journal of Remote Sensing **22**(18)**:** 3665-3687.

Bourgeau-Chavez, L. L., K. B. Smith, S. M. Brunzell, E. S. Kasischke, E. A. Romanowicz and C. J. Richardson (2005). "Remote sensing of regional inundation patterns and hydroperiod in the greater Everglades using synthetic aperture radar." Wetlands **25**(1).

Bradley, C. (2002). "Simulation of the annual water table dynamics of a floodplain wetland, Narborough Bog, UK." Journal of Hydrology **261:** 150-172.

Brooks, R. T. (2004). "Weather-related effects on woodland vernal pool hydrology and hydroperiod." Wetlands **24**(1)**:** 104-114.

Burke, M. K., S. L. King, D. Gartner and M. H. Eisenbies (2003). "Vegetation, soil, and flooding relationships in a blackwater floodplain forest." Wetlands **23**(4)**:** 988-002.

Chesapeake Bay Program. (1998). Chesapeake Bay Program land cover, land use, and land practices technical requirements to address Chesapeake Bay agreement policy and restoration goal needs. Chesapeake Bay Program.

Cole, C. A. and R. P. Brooks (2000). "Patterns of wetland hydrology in the Ridge and Valley Province, Pennsylvania, USA." Wetlands **20**(3)**:** 438-447.

Conly, F. M. and G. Van der Kamp (2001). "Monitoring the hydrology of Canadian prairie wetlands to detect the effects of climate change and land use changes." Environmental Monitoring and Assessment **67**(1-2)**:** 195-215.

Costa, M. P. F. (2004). "Use of SAR satellites for mapping zonation of vegetation communities in the Amazon floodplain." International Journal of Remote Sensing **25**(10)**:** 1817-1835.

Cowardin, L. M., V. Carter, F. Golet and E. LaRoe. (1979). Classification of wetlands and deepwater habitats of the United States. U.S. Fish and Wildlife Service, Washington, D.C.

Cronk, J. K. and W. J. Mitsch (1994). "Periphyton Productivity on Artificial and Natural Surfaces in Constructed Fresh-Water Wetlands under Different Hydrologic Regimes." Aquatic Botany **48**(3-4)**:** 325-341.

Dahl, T. E. and C. E. Johnson. (1991). Wetlands: Status and trends in the conterminous United States mid-1970's to mid-1980's. First Update of the National Wetlands Status Report U.S. Department of the Interior, Fish and Wildlife Service, Washington, D.C.

Daubenmire, R. F. (1968). Plant Communities: A Textbook of Plant Synecology. New York, N.Y., Harper and Row.

Dobson, J. E., E. A. Bright, R. L. Ferguson, D. W. Field, L. L. Wood, K. D. Haddad, H. Iredale, J. R. Jensen, V. V. Klemas, R. J. Orth and J. P. Thomas. (1995). NOAA Coastal Change Analysis Program (C-CAP): Guidance for implementation. NMFS 123, National Oceanic and Atmospheric Administration, Seattle, WA.

Dobson, M. C., F. T. Ulaby, S. Moezzi and E. Roth (1983). A simulation study of the effects of land cover and crop type on sensing soil moisture with an orbital c-band radar. IEEE International Geosciences and Remote sensing Symposium (IGARSS '83), San Francisco, C.A.

Dobson, M. C., F. T. Ulaby, L. E. Pierce, T. L. Sharik, K. M. Bergen, J. Kellndorfer, J. R. Kendra, E. Li, Y. C. Lin, A. Nashashibi, K. Sarabandi and P. Siquei (1995). "Estimation of forest biophysical characteristics in Northern Michigan with SIR-C/X-S." IEEE Transactions on Geoscience and Remote Sensing **33**(4)**:** 877-895.

Dollar, E. S. J. (2002). "Fluvial geomorphology." Progress in Physical Geography **26**(1)**:** 123-143.

Drake, J. B., R. O. Dubayah, D. B. Clark, R. G. Knox, J. B. Blair, M. A. Hofton, R. L. Chazdon, J. F. Weishampel and S. D. Prince (2002). "Estimation of tropical forest structural characteristics using large-footprint lidar." <u>Remote Sensing of Environment</u> **79**(2-3)**:** 305-319.

Drexler, J. Z., R. L. Snyder, D. Spano and K. T. U. Paw (2004). "A review of models and micrometeorological methods used to estimate wetland evapotranspiration." <u>Hydrological Processes</u> **18**(11)**:** 2071-2101.

Dubayah, R., R. Knox, M. Hofton, J. B. Blair and J. Drake (2000). Land surface characterization using lidar remote sensing. <u>Spatial Information for Land Use Management</u>. M. Hill and R. Aspinall. Australia, Gordon & Breach Science Publishers**:** 25–38.

Dubois, P. C., J. Vanzyl and T. Engman (1995). "Measuring soil-moisture with imaging radars." <u>IEEE Transactions on Geoscience and Remote Sensing</u> **33**(4)**:** 915-926.

Duda, O. and P. E. Hart (1973). <u>Pattern Classification and Scene Analysis</u>. New York, NY, John Wiley and Sons, Inc.

Engheta, N. and C. Elachi (1982). "Radar scattering from a diffuse vegetation layer over a smooth surface." <u>IEEE Transactions on Geoscience and Remote Sensing</u> **20**(2)**:** 212-216.

Engman, E. T. (1996). "Remote sensing applications to hydrology: Future impact." <u>Hydrological Sciences Journal</u> **41**(4)**:** 637-647.

European Space Agency ASAR Science Team. (2004). ASAR Monthly Report: December 2004. Technical Report ENVI-CLVL-EOPG-TN-04-0009, European Space Agency.

Evans, D. L., J. J. Plaut and E. R. Stofan (1997). "Overview of the spaceborne imaging Radar-C/X-band synthetic aperture radar (SIR-C/X-SAR) missions." <u>Remote Sensing of Environment</u> **59**(2)**:** 135-140.

Executive Office of the President Council on Environmental Quality. (2005). Conserving America's Wetlands Implementing the President's Goal. Executive Office of the President of the United States of America, Washington, D.C.

Federal Geographic Data Committee. (1992). Application of satellite data for mapping and monitoring wetlands - facts finding report: technical report 1. Wetlands Subcommittee, Federal Geographic Data Committee., Washington, D.C.

Fisher, A. (2000). "Preliminary findings from the Mid-Atlantic Regional Assessment." <u>Climate Research</u> **14**(3)**:** 261-269.

Ford, J. P. and D. J. Casey (1988). "Shuttle radar mapping with diverse incidence angles in the rainforest of Borneo." <u>International Journal of Remote Sensing</u> **9**(5)**:** 927-943.

Forest Inventory and Analysis Program. 1999. Forest inventory data [Online]. Available by Producer http://www.fia.fs.fed.us/tools-data/.

Goetz, S. J., S. P. Prince, M. M. Thawley, A. J. Smith and R. Wright (2000). <u>The Mid-Atlantic Regional Earth Science Applications Center (RESAC): An overview</u>. ASPRS Annual Conference, Washington, D. C., American Society for Photogrammetry and Remote Sensing (ASPRS).

Grover, K., S. Quegan and C. D. Freitas (1999). "Quantitative estimation of tropical forest cover by SAR." <u>IEEE Transactions on Geoscience and Remote Sensing</u> **37**(1)**:** 479-490.

Hall, D. K. (1996). "Remote sensing applications to hydrology: Imaging radar." <u>Hydrological Sciences Journal</u> **41**(4)**:** 609-624.

Hammer, D. A. (1992). <u>Creating Freshwater Wetlands</u>. Boca Raton, F.L., Lewis Publishers.

Hess, L. L., J. M. Melack, S. Filoso and Y. Wang (1995). "Delineation of inundated area and vegetation along the Amazon floodplain with the SIR-C synthetic-aperture radar." <u>IEEE Transactions on Geoscience and Remote Sensing</u> **33**(4)**:** 896-904.

Hess, L. L., J. M. Melack and D. S. Simonett (1990). "Radar detection of flooding beneath the forest canopy: A review." <u>International Journal of Remote Sensing</u> **11**(7)**:** 1313-1325.

Hotchkiss, N. and R. Stewart. (1979). Vegetation and vertebrates of the Patuxent Wildlife Research Center: Outline of ecology and annotated lists. U.S. Department of Interior, Laurel, Maryland.

Hruby, T., W. E. Cesanek and K. E. Miller (1995). "Estimating relative wetland values for regional-planning." <u>Wetlands</u> **15**(2)**:** 93-107.

Hupp, C. R. (2000). "Hydrology, geomorphology and vegetation of Coastal Plain rivers in the south-eastern USA." <u>Hydrological Processes</u> **14**(16-17)**:** 2991-3010.

Imhoff, M., M. Story, C. Vermillion, F. Khan and F. Polcyn (1986). "Forest canopy characterization and vegetation penetration assessment with space-borne radar." <u>IEEE Transactions on Geoscience and Remote Sensing</u> **24**(4)**:** 535-542.

Imhoff, M. L., C. Vermillion, M. H. Story, A. M. Choudhury, A. Gafoor and F. Polcyn (1987). "Monsoon flood boundary delineation and damage assessment using space borne imaging radar and Landsat data." Photogrammetric Engineering and Remote Sensing **53**(4)**:** 405-413.

Jensen, J. R. (2000). Remote Sensing of the Environment: An Earth Resource Perspective. Upper Saddle River, N.J., Prentice-Hall, Inc.

Johnson, G. D., M. D. Strickland, J. P. Buyok, C. E. Derby and D. P. Young (1999). "Quantifying impacts to riparian wetlands associated with reduced flows along the Greybull River, Wyoming." Wetlands **19**(1)**:** 71-77.

Kadlec, J. A. (1993). "Effect of depth of flooding on summer water budgets for small diked marshes." Wetlands **13**(1)**:** 1-9.

Kasischke, E. S. and L. L. Bourgeau-Chavez (1997). "Monitoring south Florida wetlands using ERS-1 SAR imagery." Photogrammetric Engineering and Remote Sensing **63**(3)**:** 281-291.

Kasischke, E. S., J. M. Melack and M. C. Dobson (1997). "The use of imaging radars for ecological applications - A review." Remote Sensing of Environment **59**(2)**:** 141-156.

Kasischke, E. S., K. B. Smith, L. L. Bourgeau-Chavez, E. A. Romanowicz, S. Brunzell and C. J. Richardson (2003). "Effects of seasonal hydrologic patterns in south Florida wetlands on radar backscatter measured from ERS-2 SAR imagery." Remote Sensing of Environment **88**(4)**:** 423-441.

Kauth, R. J. and G. Thomas (1976). The tasselled cap - a graphic description of the spectral-temporal development of agricultural crops as seen by Landsat. Symposium on Machine Processing on Remotely-Sensed Data, Purdue University, West Lafeyette, IN.

Kirk, J. A., W. R. Wise and J. J. Delfino (2004). "Water budget and cost-effectiveness analysis of wetland restoration alternatives: a case study of Levy Prairie, Alachua County, Florida." Ecological Engineering **22**(1)**:** 43-60.

Koeln, G. and J. Bissonnette. (1999). Cross-correlation analysis: mapping land cover changes with a historic land cover database and a recent, single-date, multispectral image. Earth Satellite Corporation, Rockville, MD.

Konyha, K. D., D. T. Shaw and K. W. Weiler (1995). "Hydrologic design of a wetland - Advantages of continuous modeling." Ecological Engineering **4**(2)**:** 99-116.

Krasnostein, A. L. and C. E. Oldham (2004). "Predicting wetland water storage." Water Resources Research **40**(10).

Krohn, M. D., N. M. Milton and D. B. Segal (1983). "Seasat synthetic aperture radar (SAR) Response to lowland vegetation types in eastern Maryland and Virginia." Journal of Geophysical Research-Oceans and Atmospheres **88**(C3)**:** 1937-1952.

Kushwaha, S. P. S., R. S. Dwivedi and B. R. M. Rao (2000). "Evaluation of various digital image processing techniques for detection of coastal wetlands using ERS-1 SAR data." International Journal of Remote Sensing **21**(3)**:** 565-579.

Lent, R. M., P. K. Weiskel, F. P. Lyford and D. S. Armstrong (1997). "Hydrologic indices for non-tidal wetlands." Wetlands **17**(1)**:** 19-30.

Liao, C. M., J. W. Tsai and M. C. Lin (2001). "A simple modeling approach towards hydroperiod effects on fish dynamics in a northern Taiwan wetland ecosystem." Journal of Environmental Science and Health Part a-Toxic/Hazardous Substances & Environmental Engineering **36**(7)**:** 1205-1226.

Lindbo, D. L. (1997). Enticols-fluvents and fluvaquents: Problems recognizing aquic and hydric conditions in young, floodplain soils. Aquic Conditions and Hydric Soils: The Problem Soils M. J. Vepraskas and S. W. Sprecher. Madison, WI, Soil Science Society of America. Special Publication 50: 133-153.

Lozano-Garcia, D. F. and R. M. Hoffer (1993). "Synergistic Effects of Combined Landsat-TM and SIR-B Data for Forest Resources Assessment." International Journal of Remote Sensing **14**(14)**:** 2677-2694.

Lunetta, R. S. and M. E. Balogh (1999). "Application of multi-temporal Landsat 5 TM imagery for wetland identification." Photogrammetric Engineering and Remote Sensing **65**(11)**:** 1303-1310.

Lyon, J. and J. McCarthy (1995). Wetland and Environmental Applications of GIS. New York, N.Y., Lewis Publishers.

Magagi, R., M. Bernier and C. H. Ung (2002). "Quantitative analysis of RADARSAT SAR data over a sparse forest canopy." IEEE Transactions on Geoscience and Remote Sensing **40**(6)**:** 1301-1313.

Mather, J. R. (1978). The Climatic Water Budget in Environmental Analysis. Lexington, MA, Lexington Books.

Mendoza, G. F., T. S. Steenhuis, M. T. Walter and J. Y. Parlange (2003). "Estimating basin-wide hydraulic parameters of a semi-arid mountainous watershed by recession-flow analysis." Journal of Hydrology **279**(1-4)**:** 57-69.

Mertes, L. A. K., D. L. Daniel, J. M. Melack, B. Nelson, L. A. Martinelli and B. R. Forsberg (1995). "Spatial Patterns of Hydrology, Geomorphology, and Vegetation on the Floodplain of the Amazon River in Brazil from a Remote-Sensing Perspective." Geomorphology **13**(1-4)**:** 215-232.

Mid-Atlantic Regional Assessment Team. (2000). Preparing for a changing climate: The potential consequences of climate variability and change. U.S. Environmental Protection Agency and Pennsylvania State University.

Mitsch, W. J. and K. C. Ewel (1979). "Comparative biomass and growth of cypress in Florida wetlands." American Midland Naturalist **101**(2)**:** 417-426.

Mitsch, W. J. and J. G. Gosselink (2000). Wetlands. New York, N.Y., John Wiley & Sons, Inc.

Moore, M. V., M. L. Pace, J. R. Mather, P. S. Murdoch, R. W. Howarth, C. Y. Chen, P. A. Flebbe, C. L. Folt, H. F. Hemond and C. T. Driscoll (1997). "Potential effects of climate change on freshwater ecosystems of the New England/Mid-Atlantic region." Hydrological Processes **11**(8)**:** 925-947.

Morrissey, L. A., G. P. Livingston and S. L. Durden (1994). "Use of SAR in regional methane exchange studies." International Journal of Remote Sensing **15**(6)**:** 1337-1342.

Moustafa, M. Z. (1999). "Nutrient retention dynamics of the Everglades Nutrient Removal Project." Wetlands **19**(3)**:** 689-704.

Najjar, R. G., H. A. Walker, P. J. Anderson, E. J. Barron, R. J. Bord, J. R. Gibson, V. S. Kennedy, C. G. Knight, J. P. Megonigal, R. E. O'Connor, C. D. Polsky, N. P. Psuty, B. A. Richards, L. G. Sorenson, E. M. Steele and R. S. Swanson (2000). "The potential impacts of climate change on the mid-Atlantic coastal region." Climate Research **14**(3)**:** 219-233.

National Research Council Committee on the Characterization of Wetlands (1995). Wetlands: Characteristics and Boundaries. Washington, D.C., National Academy Press.

Neff, R., H. J. Chang, C. G. Knight, R. G. Najjar, B. Yarnal and H. A. Walker (2000). "Impact of climate variation and change on Mid-Atlantic region hydrology and water resources." Climate Research **14**(3)**:** 207-218.

Nestler, J. H. and K. S. Long (1997). "Development of hydrological indices to aid cumulative impact analysis of riverine wetlands." Regulated Rivers: Research & Management **13:** 317-334.

Neusch, T. and M. Sties (1999). "Application of the Dubois-model using experimental synthetic aperture radar data for the determination of soil moisture and surface roughness." Journal of Photogrammetry and Remote Sensing **54**(4)**:** 273-278.

Nichols, B. (2003). Changing Times. Chesapeake Futures: Choices for the 21st Century. D. F. Boesch and J. Geer. Edgewater, MD, Heritage Printing and Graphics. STAC publication number: 03-001: 31-45.

Oldak, A., T. J. Jackson, P. Starks and R. Elliott (2003). "Mapping near-surface soil moisture on regional scale using ERS-2 SAR data." International Journal of Remote Sensing **24**(22)**:** 4579-4598.

Ormsby, J. P., B. J. Blanchard and A. J. Blanchard (1985). "Detection of lowland flooding using active microwave systems." Photogrammetric Engineering and Remote Sensing **51**(3)**:** 317-328.

Penman, H. L. (1948). Natural evaporation from open water, bare soil, and grass. Proceedings of the Royal Society of London.

Polsky, C., J. Allard, N. Currit, R. Crane and B. Yarnal (2000). "The Mid-Atlantic region and its climate: past, present, and future." Climate Research **14**(3)**:** 161-173.

Poor, P. J. (1999). "The value of additional central flyway wetlands: The case of Nebraska's Rainwater Basin wetlands." Journal of Agricultural and Resource Economics **24**(1)**:** 253-265.

Pope, K. O., E. Rejmankova, J. F. Paris and R. Woodruff (1997). "Detecting seasonal flooding cycles in marshes of the Yucatan Peninsula with SIR-C polarimetric radar imagery." Remote Sensing of Environment **59**(2)**:** 157-166.

Price, J. S., B. A. Branfireun, J. M. Waddington and K. J. Devito (2005). "Advances in Canadian wetland hydrology, 1999-2003." Hydrological Processes **19**(1)**:** 201-214.

Pyke, C. R. (2004). "Simulating vernal pool hydrologic regimes for two locations in California, USA." Ecological Modeling **173**(2-3)**:** 109-127.

Ramsey, E. W., III, , S. C. Laine, G. A. Nelson, S. K. Sapkota, M. L. Strong, J. L. Wooderson, R. H. Day, R. E. Spell, D. K. Chappell, T. L. Stoute, R. G. Kirkman and M. A. Books (1998). Identifying wetland zonation and inundation extent by using satellite remote sensing and ground-based measurements. Vulnerability of coastal wetlands in the southeastern United States: Climate change research results, 1992-97. G. R. Guntenspergen and B. A. Vairin, U.S. Geological Survey, Biological Resources Division**:** 83-92.

Raney, K. (1998). Radar fundamentals: Technical perspective. Principles and Application of Imaging Radar. F. M. Henderson and A. J. Lewis. New York, NY, John Wiley and Sons, Inc. **2:** 9-130.

Rao, B. R. M., R. S. Dwivedi, S. P. S. Kushwaha, S. N. Bhattacharya, J. B. Anand and S. Dasgupta (1999). "Monitoring the spatial extent of coastal wetlands using ERS-1 SAR data." International Journal of Remote Sensing **20**(13)**:** 2509-2517.

Rauste, Y. (1990). "Incidence-angle dependence in forested and non-forested areas in Seasat SAR data." International Journal of Remote Sensing **11**(7)**:** 1267-1276.

Rich, P., J. Wood, D. Vieglais, K. Burek and N. Webb. (1999). Guide to HemiView: Software for the analysis of hemispherical photography. Delta-T Devices, Ltd., Cambridge, England.

Richards, J., G.-Q. Sun and D. Simonett (1987). "L-band radar backscatter modeling of forest stands." IEEE Transactions on Geoscience and Remote Sensing **25:** 487-498.

Richardson, C. J. (1994). "Ecological Functions and Human-Values in Wetlands - a Framework for Assessing Forestry Impacts." Wetlands **14**(1)**:** 1-9.

Richardson, C. J. and E. J. McCarthy (1994). "Effect of land-development and forest management on hydrologic response in southeastern coastal wetlands - A review." Wetlands **14**(1)**:** 56-71.

Roberts, J., B. Young and F. Martson. (2000). Estimating the water requirements for plants in floodplain wetlands: A guide. Occasional Paper 04/00. Land and Water Resources and Development Corporation, Canberra, Australia.

Rogers, C. E. and J. P. McCarty (2000). "Climate change and ecosystems of the Mid-Atlantic region." Climate Research **14**(3)**:** 235-244.

Rosenberry, D. O., D. I. Stannard, T. C. Winter and M. L. Martinez (2004). "Comparison of 13 equations for determining evapotranspiration from a prairie wetland, Cottonwood Lake Area, North Dakota, USA." Wetlands **24**(3)**:** 483-497.

Rulequest Research. (2004). Data mining tools See5 and C5.0 [Online]. Available by Rulequest Research http://www.rulequest.com/see5-info.html (posted November 2004; verified April).

Sahagian, D. and J. Melack. (1996). Global wetland distribution and functional characterization: Trace gases and the hydrologic cycle. The International Geosphere-Biosphere Programme, Santa Barbara, CA.

Sahebi, M. R., F. Bonn and Q. H. J. Gwyn (2003). "Estimation of the moisture content of bare soil from RADARSAT-1 SAR using simple empirical models." International Journal of Remote Sensing **24**(12)**:** 2575-2582.

Shiver, B. and B. Borders (1996). Sampling Techniques for Forest Resource Inventory. New York, N.Y., John Wiley & Sons, Inc.

Skaggs, R. W., D. Amatya, R. O. Evans and J. E. Parsons (1994). "Characterization and evaluation of proposed hydrologic criteria for wetlands." Journal of Soil and Water Conservation **49**(5)**:** 501-510.

Smith, L. C. (1997). "Satellite remote sensing of river inundation area, stage, and discharge: A review." Hydrological Processes **11**(10)**:** 1427-1439.

Stewart, L. K., P. F. Hudak and R. D. Doyle (1998). "Modeling hydrologic alterations to a developing wetland in an abandoned borrow pit." Journal of Environmental Management **53**(3)**:** 231-239.

Stewart, R. B. and W. R. Rouse (1976). "Simple method for determining evaporation from shallow lakes and ponds." Water Resources Research **12**(4)**:** 623-628.

Sun, G. and D. Simonett (1988). "Simulation of L-band HH microwave backscattering from coniferous forest stands: a comparison with SIR- B data." International Journal of Remote Sensing **9:** 907-925.

Survey, U. S. G. (2005). NWISWeb Data for the Nation [Online]. Available by U.S. Geological Survey http://waterdata.usgs.gov/nwis (posted; verified May 1, 2005).

Tiner, R. (1987). Mid-Atlantic wetlands - A disappearing natural treasure. U.S. Fish & Wildlife Service, Ecological Services, Northeast Region, Hadley, M.A.

Tiner, R. (1999). Wetland indicators: A guide to wetland identification, delineation, classification, and mapping. Washington, D.C., Lewis Publishers.

TIner, R. and D. Burke. (1996). Wetlands of Maryland. U.S. Fish & Wildlife Service, Ecological Services, Northeast Region, Hadley, M.A.

Townsend, P. A. (2000). "A quantitative fuzzy approach to assess mapped vegetation classifications for ecological applications." Remote Sensing of Environment **72**(3)**:** 253-267.

Townsend, P. A. (2001). "Mapping seasonal flooding in forested wetlands using multi-temporal Radarsat SAR." Photogrammetric Engineering and Remote Sensing **67**(7)**:** 857-864.

Townsend, P. A. (2002). "Relationships between forest structure and the detection of flood inundation in forested wetlands using C-band SAR." International Journal of Remote Sensing **23**(3)**:** 443-460.

Townsend, P. A. and J. R. Foster (2002). "A synthetic aperture radar-based model to assess historical changes in lowland floodplain hydroperiod." Water Resources Research **38**(7).

Townsend, P. A. and S. J. Walsh (1998). "Modeling floodplain inundation using an integrated GIS with radar and optical remote sensing." Geomorphology **21**(3-4)**:** 295-312.

Townsend, P. A. and S. J. Walsh (2001). "Remote sensing of forested wetlands: application of multitemporal and multispectral satellite imagery to determine plant community composition and structure in southeastern USA." Plant Ecology **157**(2)**:** 129-149A.

Toyra, J., A. Pietronira and L. Martz (2001). "Multisensor hydrologic assessment of a freshwater wetland." Remote Sensing of the Environment **75:** 162-173.

Trepel, M. and W. Kluge (2004). "WETTRANS: a flow-path-oriented decision-support system for the assessment of water and nitrogen exchange in riparian peatlands." Hydrological Processes **18:** 357-371.

U.S. Fish & Wildlife Service. (2002). National Wetlands Inventory: A strategy for the 21st century [Online]. Available by Department of the Interior http://www.nwi.fws.gov/Pubs_Reports/NWI121StatFNL.pdf (posted January 2002; verified July 20, 2005).

U.S. Geological Survey. (2002) USGS High Resolution Orthoimage, Washington, DC-VA-MD [Online]. Available by Producer http://seamless.usgs.gov/ (Accessed: March 27, 2003).

U.S. Geological Survey. (2004). National elevation dataset 1/3 arc second [Online]. Available by http://seamless.usgs.gov/website/seamless/products/3arc. asp#description (Accessed: October 28, 2004).

Ulaby, F. T., R. K. Moore and A. K. Fung (1982). Microwave Remote Sensing, Active and Passive: Volume II: Radar Remote Sensing and Surface Scattering and Emission Theory. Reading, M.A., Addison-Wesley Publishing Co.

Walton, R., R. S. Chapman and J. E. Davis (1996). "Development and application of the wetlands dynamic water budget model." Wetlands **16**(3)**:** 347-357.

Wang, C. Z., J. G. Qi, S. Moran and R. Marsett (2004). "Soil moisture estimation in a semiarid rangeland using ERS-2 and TM imagery." Remote Sensing of Environment **90**(2)**:** 178-189.

Wang, Y., J. L. Day and F. W. Davis (1998). "Sensitivity of modeled C- and L-band radar backscatter to ground surface parameters in loblolly pine forest." Remote Sensing of Environment **66**(3)**:** 331-342.

Wang, Y., L. L. Hess, S. Filoso and J. M. Melack (1995). "Understanding the radar backscattering from flooded and non-flooded Amazonian forests: Results from canopy backscatter modeling." Remote Sensing of Environment **54**(3)**:** 324-332.

Welsch, D. J., D. L. Smart, J. N. Boyer, P. Minkin, H. C. Smith and T. L. McCandless. (1995). Forested Wetlands: Functions, Benefits, and the Use of Best Management Practices. NA-PR-01-95, USDA Forest Service, Radnor, PA.

Whigham, D. F. (1996). Ecosystem functions and ecosystem values. Ecosystem Functions and Human Activities. R. D. Simpson and N. L. Christensen. New York, NY, International Thomson Publishing**:** 225-239.

Whitehead, J. C. and C. Y. Thompson (1993). "Environmental preservation demand - altruistic, bequest, and intrinsic motives." American Journal of Economics and Sociology **52**(1)**:** 19-30.

Wickel, A. J., T. J. Jackson and E. F. Wood (2001). "Multitemporal monitoring of soil moisture with Radarsat SAR during the 1997 Southern Great Plains hydrology experiment." International Journal of Remote Sensing **22**(8)**:** 1571-1583.

Wilen, B. O. and G. S. Smith (1996). Assessment of remote sensing/GIS technologies to improve National Wetlands Inventory maps. Sixth Biennial Forest Service Remote Sensing Applications Conference, Denver, CO.

Williams, T. (1996). "What good is a wetland?" Audobon **98:** 42-53.

Winter, T. C. and D. O. Rosenberry (1998). "Hydrology of prairie pothole wetlands during drought and deluge: A 17-year study of the Cottonwood Lake wetland complex in North Dakota in the perspective of longer term measured and proxy hydrological records." Climatic Change **40**(2)**:** 189-209.

Woodward, R. T. and Y. S. Wui (2001). "The economic value of wetland services: a meta-analysis." Ecological Economics **37**(2)**:** 257-270.

Zhang, L. and W. J. Mitsch (2005). "Modeling hydrological processes in created freshwater wetlands: An integrated system approach." Environmental Modeling & Software **20**(7)**:** 935-946.